

FINAL PROJECT

**SOIL EMBANKMENT STABILITY ANALYSIS WITH
GEOTEXTILE REINFORCEMENT**

**(A CASE STUDY AT EMBANKMENT STA 7+500 OF
CIBITUNG - CILINCING TOLL CONSTRUCTION
PROJECT)**

**Submitted to Universitas Islam Indonesia to Fulfil the Requirements to
Obtain Bachelor's Degree in Civil Engineering**



**ARIEF RENALDI WIWAHA
17511246**

**CIVIL ENGINEERING PROGRAM
FACULTY CIVIL ENGINEERING AND PLANNING
UNIVERSITAS ISLAM INDONESIA
2021**

FINAL PROJECT

**SOIL EMBANKMENT STABILITY ANALYSIS WITH
GEOTEXTILE REINFORCEMENT
(A CASE STUDY AT EMBANKMENT STA 7+500 OF
CIBITUNG - CILINCING TOLL CONSTRUCTION
PROJECT)**

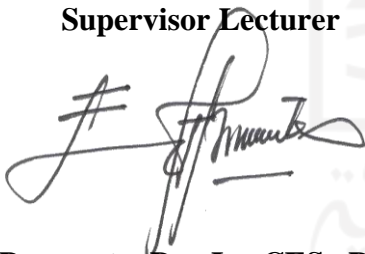
Arranged by

**Arief Renaldi Wiwaha
17511246**

Has been accepted as one of the requirements to obtain the Bachelor's
Degree of Civil Engineering

Examined on
By Board of Examiners

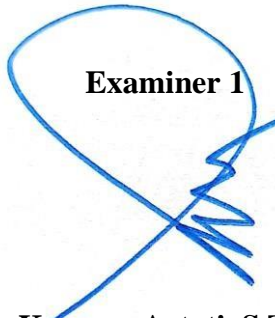
Supervisor Lecturer



Edy Purwanto, Dr., Ir., CES., DEA.

NIK:

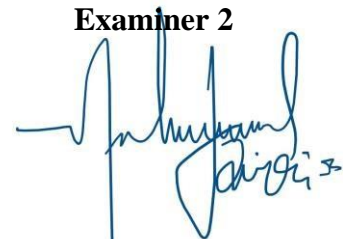
Examiner 1



Hanindya Kusuma Artati, S.T., M.T.

NIK:

Examiner 2



M. Rifqi Abdurrozak, S.T., M.Eng.

NIK:

Validate

Head of Civil Engineering Study Program



Dr. Ir. Sri Amini Yuni Astuti, M.T.

NIK:

PLAGIARISM FREE STATEMENT

The author declare that the Final Project compiled as a requirement for the completion of Bachelor's degree in the Civil Engineering Study Program, Faculty of Civil Engineering and Planning, Universitas Islam Indonesia is author's own work. As for certain parts in the writing of the Final Project which authors quoted from the work of others, has been written in source clearly in accordance with the norms, rules and ethics of writing scientific papers. If in the future when part or all of this Final Project is found or there is plagiarism in certain parts, the authors willing to accept sanctions according to the rules and applicable laws.

Yogyakarta, 24 February 2022

Who make the statement,



Arief Renaldi Wiwaha

17511246

PREFACE



Assalamu 'alaikum Wr.Wb

Alhamdulillah rabbil'alamiin, praise and gratitude to Allah SWT., for the presence of plenty of mercy and his grace, so that the authors can complete this Final Project properly. Sholawat and greetings are hopefully given to the Prophet Muhammad SAW, his family friends and the ummah until the end of yaumul.

This Final Project is one of the academic requirements in completing Bachelor Degree of Civil Engineering at the Civil Engineering Study Program, Faculty of Civil Engineering and Planning, Universitas Islam Indonesia. For the convenience during the preparation of this final project, the author would like to express his deepest gratitude to all those who have provided support and motivation for the completion of this final project especially as follows.

1. Mr. Edy Purwanto Dr, Ir., CES., DEA as the final project supervisor lecturer thank you for the guidance, advice and support given to the author during compiling the the final project.
2. Mrs. Hanindya Kusuma Artati, S.T., M.T. as Examiner 1 and Mr. Rifqi Abdurrozak, S.T., M.Eng. as examiner 2.
3. Mrs. Sri Amini Yuni Astuti, DR., IR., M.T., as Head of the Civil Engineering Undergraduate Study Program, Faculty of Civil Engineering and Planning, Universitas islam indonesia.
4. My beloved family especially my father and mother, Mr. Sarbidi and Mrs. Nurbaeti Arianti always gives support, motivation and advice in every prayer that never stops for me also my sister Rahma, Nayla and Hafsa who always inspires and motivate the author.
5. To all lecturers and academic section of the Department Civil Engineering Faculty of Civil Engineering and Planning, Universitas Islam Indonesia which has given knowledge and support during the course of the study.

6. My friends Tita, Bangkit, Thareq, and Alfian also all the parties who have given support until the completion of this Final Project.

The author is fully aware that this final project is still far from perfect, and hopefully this final project can gives many benefits for the authors and readers in general.

Wassalamu 'alaikum Wr.Wb

Yogyakarta, 24 February 2022



Arief Renaldi Wiwaha

17511246

الجمعة المباركة
الاستاذة الانيسة

TABLE OF CONTENTS

TITLE PAGE	i
VALIDATION SHEET	ii
PLAGIARISM FREE STATEMENT	iii
PREFACE	iv
TABLE OF CONTENTS	vi
TABLE LIST	ix
FIGURE LIST	x
APPENDIX LIST	xvi
NOTATIONS AND ABBREVIATION LIST	xvii
ABSTRACT	xix
CHAPTER I PRELIMINARY	1
1.1 Background	1
1.2 Problem Statement	3
1.3 Research Purposes	3
1.4 Benefits of Research	4
1.5 Research Limits	4
CHAPTER II BIBLIOGRAPHY	6
2.1 General Review	6
2.2 Slope Stability Analysis	7
2.3 Geotextile Reinforcement	8
2.3.1. Geotextile Function	8
2.3.2. Geotextile Behaviour	9
2.4 Effect of Earthquake Load on Embankment Stability	10
2.5 Previous Research	10
2.6 Comparison of Previous Research	13
CHAPTER III THEORITICAL BASIS	16
3.1 Soil Type and Classification	16
3.1.1 Soil Classification System	16
3.1.2 Grain Size and Grain Distribution	21
3.2 Soil Shear Strength Parameter	22
3.3 Slope Landslide	24

3.3.1	Causes of slope Landslide	24
3.3.2	Slope Landslide Prevention	25
3.4	Slope Embankment	26
3.4.1	Safety Factor	26
3.4.2	Slope Stability Analysis Method	27
3.5	Soil Consolidation	30
3.5.1	Consolidation Settlement	30
3.5.2	Consolidation Calculation Parameters	31
3.6	Geotextile Reinforcement	33
3.6.1	Geotextile for Embankment Reinforcement	33
3.6.2	Type of Geotextile	35
3.6.3	Geotextile Reinforcement Design	36
3.6.4	Stability Analysis of Embankment with Long Zone Geotextile Reinforcement	38
3.7	Plaxis Software	43
CHAPTER IV RESEARCH METHODS		45
4.1	Research Location	45
4.2	Data Used	46
4.2.1	Soil Parameter Data	46
4.2.2	Detailed Engineering Drawing	47
4.2.3	Geotextile Material Data	47
4.2.4	Load Data	48
4.3	Research Stages	50
4.4	Plaxis Program Analysis	51
4.4.1.	Plaxis Input	55
4.4.2.	Plaxis Calculation	61
4.4.3.	Plaxis Output	62
4.4.4.	Research Flowchart	62
CHAPTER V ANALYSIS AND DISCUSSION		64
5.1	General Review	64
5.1.1.	Analysis Data of Finite element method	65
5.2	Existing Embankment	68
5.2.1.	Analysis Using Plaxis Program	68

5.3	Fellenius Calculation Method	76
5.4	Calculation Analysis Embankment with Topography Variation	81
5.4.1.	Embankment With 1 Trap Variation	81
5.4.2.	Embankment with 2 Trap Variation	87
5.4.3.	Embankment with 3 Trap Variation	92
5.4.4.	Recapitulation of Safety Factor (SF) Results and Consolidation	97
5.5	Calculation of Geotextile Needs	98
5.5.1.	Geotextile Calculation Data	98
5.5.2.	External Stability	100
5.5.3.	Internal Stability	105
5.5.4.	Tensile Strength Check Between Geotextile - Soil	107
5.6	Calculation of Embankment Reinforced by 1 Layer Geotextile	108
5.6.1.	Existing embankment with Geotextile Reinforcement	108
5.6.2.	Embankment 1 Trap Variation with Geotextile Reinforcement	116
5.6.3.	Embankment 2 Trap Variation with Geotextile Reinforcement	123
5.6.4.	Embankment 3 Trap Variation with Geotextile Reinforcement	130
5.7	Recapitulation of Safety Factor (SF) and Consolidation	137
5.8	Discussion	138
5.8.1.	Results Analysis of Existing Embankment	138
5.8.2.	Results of Embankment Analysis with Topography Improvement	139
5.8.3.	Results of Embankment Analysis with Geotextile Reinforcement	139
CHAPTER VI CONCLUSION AND SUGGESTION		145
6.1	Conclusion	145
6.2	Suggestion	146
Bibliography		147
Appendix		150

TABLE LIST

Table 2.1	Comparison Between Previous Research and Research Conducted	13
Table 3.1	Soil Classification system based on the American Association of State Highway and Transportation Officials	18
Table 3.2	Soil classification system based on Unified (Unified Soil Classification)	20
Table 3.4	Slope Safety Factors for Slope Design According Sosrodarsono	26
Table 3.5	Relationship of Safety Factor Value with Landslide Intensity	27
Table 4.1	Soil Parameter Data	47
Table 4.2	Geotextile Woven UW-250 Parameter Data	48
Table 4.3	Traffic Load	49
Table 5.1	Soil Parameter Data	65
Table 5.2	Traffic Load Parameter Data	66
Table 5.3	Geotextile Woven UW 250 Parameter	67
Table 5.4	Existing Embankment Coordinates	69
Table 5.5	Calculation Recapitulation Using Fellenius Method	80
Table 5.6	Recapitulation Results of Safety Factor (SF) and Consolidation on Embankment	97
Table 5.7	Woven UW-250 Geotextiles Data	99
Table 5.8	Soil Bearing Capacity	99
Table 5.9	Recapitulation of Geotextile Length Requirement	105
Table 5.10	Input Coordinate of Existing Embankment with Geotextile Reinforcement	109
Table 5.12	Input Coordinate of Embankment 2 Trap Variation with Geotextile Reinforcement	123
Table 5.13	Input Coordinate of Embankment 3 Trap Variations with Geotextile Reinforcement	130
Table 5.14	Recapitulation of Safety Factor for Embankment with Geotextile Reinforcement	137
Table 5.15	Recapitulation of Safety Factor and Consolidation of Embankment	141

FIGURE LIST

Figure 1.1	Location of Cibitung – Cilincing Toll Road	2
Figure 1.2	Cross Section Geometry	2
Figure 2.1	Geotextile Stress-Strain Relationship, (a) Polypropylene and High-Density Polyethylene, (b) Polyester Materials	9
Figure 3.1	Grain size definitions by various particle-size classification schemes.	21
Figure 3.2	Mohr and Coloumb Failure Criteria	23
Figure 3.3	Slide Slope Failure	25
Figure 3.4	(a) Rotational slide and (b) Translational slide	25
Figure 3.5	Forces that Work on Slices	29
Figure 3.6	Compression Index, Cc	32
Figure 3.7	Woven Geotextiles	35
Figure 3.8	Woven Geotextiles	35
Figure 3.9	Embankment on Soft Soil	37
Figure 3.10	The Collapse Model of a Reinforced Embankment	38
Figure 3.11	The Soil Lateral Distributed Diagram	38
Figure 4.1	Toll Road Trace	45
Figure 4.2	Indonesia Earthquake Zoning Map	50
Figure 4.3	Create/Open Project Command Box	56
Figure 4.4	Project and Dimension Command	56
Figure 4.5	Dimension Tab	57
Figure 4.6	General Tab Command	59
Figure 4.7	Parameters Tab Command	59
Figure 4.8	Element from Generate Meshing	60
Figure 4.9	Initial Soil Stresses	60
Figure 4.10	Calculation Command	61
Figure 4.11	Determined the Point Curve	62
Figure 4.12	Research Steps	63
Figure 5.1	Graph of Acceleration and Time of the Whittier Narrows Earthquake	67
Figure 5.2	Existing Condition of Embankment	68
Figure 5.3	Modelling of Existing Embankment on Plaxis 8.6	69
Figure 5.4	Meshing on Existing Embankment	70

Figure 5.5	Initial Soil Stresses on Existing Embankments	70
Figure 5.6	Deformed Mesh of Existing Embankment Due to Traffic Load	71
Figure 5.7	Deformed Mesh of Existing Embankment Due to Traffic and Earthquake Load	71
Figure 5.8	Total Displacement of Existing Embankment Due to Traffic Load	72
Figure 5.9	Total Displacement of Existing Embankment Due to Traffic and Earthquake Load	72
Figure 5.10	Direction Movement of Embankment Due to Traffic Load	73
Figure 5.11	Direction Movement of Embankment Due to Traffic and Earthquake Load	73
Figure 5.12	Effective Stresses of Existing Slope Embankment Due to Traffic Load	74
Figure 5.13	Effective Stresses of Existing Embankment Due to Traffic and Earthquake Load	74
Figure 5.14	Potential Landslides of Embankment Due to Traffic Load	75
Figure 5.15	Potential Landslides of Embankment Due to Traffic Load and Earthquake Load	75
Figure 5.16	SF Curve of Existing Embankment	76
Figure 5.17	Stability Analysis of Sta. 7+500 with Fellenius Method	77
Figure 5.18	Embankment 1 Trap	81
Figure 5.19	Modelling 1 Trap Embankment	82
Figure 5.20	Deformed Mesh of Embankment Due to Traffic Load 1 Trap	82
Figure 5.21	Deformed Mesh of Embankment Due Traffic and Earthquake Load 1 Trap	83
Figure 5.22	Total Displacement of Embankment 1 Trap Due to Traffic Load	83
Figure 5.23	Total Displacement of Embankment 1 Trap Due to Traffic Load and Earthquake Load	84
Figure 5.24	Soil Movement of Embankment 1 Trap Due to Traffic Load	84
Figure 5.25	Soil Movement of Embankment 1 Trap Due to Traffic Load and Earthquake Load	85
Figure 5.26	Effective Stresses of Embankment 1 Trap Due to Traffic Load	85
Figure 5.27	Effective Stresses of Embankment 1 Trap Due to Traffic and Earthquake Load	85
Figure 5.28	Potential Landslides of Embankment 1 Trap Due to Traffic Load	86
Figure 5.29	Potential Landslides of Embankment 1 Trap Due to Traffic Load and Earthquake Load	86
Figure 5.30	SF Curve of Embankment 1 Trap	87
Figure 5.31	Embankment 2 Trap	87

Figure 5.32	Modelling of Embankment 2 Trap	87
Figure 5.33	Deformed Mesh of Embankment 2 Trap Due to Traffic Load	88
Figure 5.34	Deformed Mesh of Embankment 2 Trap Due to Traffic Load and Earthquake Load	88
Figure 5.35	Total Displacement of Embankment 2 Trap Due to Traffic Load	89
Figure 5.36	Total Displacement of Embankment 2 Trap Due to Traffic Load and Earthquake Load	89
Figure 5.37	Soil Movement Embankment 2 Trap Due to Traffic Load	90
Figure 5.38	Soil Movement Embankment 2 Trap Due to Traffic Load and Earthquake Load	90
Figure 5.39	Effective Stresses of Embankment 2 Trap Due to Traffic Load	91
Figure 5.40	Effective Stresses of Embankment 2 Trap Due to Traffic Load and Earthquake Load	91
Figure 5.42	Potential Landslides of Embankment 2 Trap Due to Traffic Load and Earthquake Load	92
Figure 5.43	SF Curve of Embankment 2 Trap	92
Figure 5.44	Embankment 3 Trap	92
Figure 5.45	Modelling of Embankment 3 Trap	93
Figure 5.46	Deformed Mesh of Embankment 3 Trap Due to Traffic Load	93
Figure 5.47	Deformed Mesh of Embankment with 3 Trap Due to Traffic and Earthquake Load	94
Figure 5.48	Total Displacement of Embankment 3 Trap Due to Traffic Load	94
Figure 5.49	Total Displacement of Embankment 3 Trap Due to Traffic and Earthquake Load	95
Figure 5.50	Soil Movement of Embankment 3 Trap Due to Traffic Load	95
Figure 5.51	Soil Movement of Embankment 3 Trap Due Traffic and Earthquake Load	95
Figure 5.52	Effective Stresses of Embankment 3 Trap Due to Traffic Load	96
Figure 5.53	Effective Stresses of Embankment 3 Trap Due to Traffic and Earthquake Load	96
Figure 5.54	Potential Landslides of Embankment 3 Trap Due to Traffic Load	96
Figure 5.55	Potential Landslides of Embankment 3 Trap Due to Traffic and Earthquake Load	97
Figure 5.56	Forces Acting on a Slope Embankment	100
Figure 5.57	Soil – Geotextile Friction Transfer	107
Figure 5.58	Modelling of Embankment Reinforced with Geotextile	109
Figure 5.59	Meshing of Existing Embankment with Geotextile Reinforcement	110

Figure 5.60	Initial Soil Stresses of Existing Embankment with Geotextile Reinforcement	110
Figure 5.61	Deformed Mesh on Existing Embankment with geotextile Reinforcement Due to Traffic Load	111
Figure 5.62	Deformed Mesh on Existing Embankment with Geotextile Reinforcement Due to Traffic and Earthquake Load	111
Figure 5.63	Total Displacement of Existing Embankment with Geotextile Reinforcement Due to Traffic Load	112
Figure 5.64	Total Displacement of Existing Embankment with Geotextile Reinforcement Due to Traffic and Earthquake Load	112
Figure 5.65	Soil Movement of Existing Embankment Due to Traffic Load	113
Figure 5.66	Soil Movement of Existing Embankment Due to Traffic and Earthquake Load	113
Figure 5.67	Effective Stresses of Existing Embankment with Geotextile Reinforcement Due to Traffic Load	114
Figure 5.68	Effective Stresses of Existing Embankment with Geotextile Reinforcement Due to Traffic and Earthquake Load	114
Figure 5.69	Potential Landslides of Existing Embankment Due to Traffic Load	115
Figure 5.70	Potential Landslides of Existing Embankment Due to Traffic and Earthquake Load	115
Figure 5.71	SF Curve of Existing Embankment with Reinforced Geotextile	116
Figure 5.72	Modelling of Embankment 1 Trap with Geotextile Reinforcement	117
Figure 5.73	Initial Soil Stresses of Embankment 1 Trap with Geotextile Reinforcement	117
Figure 5.74	Deformed Mesh of Embankment 1 Trap with Geotextile Reinforcement Due to Traffic Load	118
Figure 5.75	Deformed Mesh of Embankment 1 Trap with Geotextile Reinforcement Due to Traffic and Earthquake Load	118
Figure 5.76	Total Displacement of Embankment 1 Trap with Geotextile Reinforcement Due to Traffic Load	119
Figure 5.77	Total Displacement of Embankment 1 Trap with Geotextile Reinforcement Due to Traffic and Earthquake Load	119
Figure 5.78	Soil Movement of Embankment 1 Trap with Geotextile Reinforcement Due to Traffic Load	120
Figure 5.80	Effective Stresses of Embankment 1 Trap with Geotextile Reinforcement Due to Traffic Load	121
Figure 5.81	Effective Stresses of Embankment 1 Trap with Geotextile Reinforcement Due to Traffic and Earthquake Load	121

Figure 5.82	Potential Landslides of Embankment 1 Trap with Geotextile Reinforcement Due to Traffic Load	122
Figure 5.83	Potential Landslide of Embankment 1 Trap with Geotextile Reinforcement Due to Traffic and Earthquake Load	122
Figure 5.84	SF Curve of Embankment 1 Trap with Reinforced Geotextile	123
Figure 5.85	Modelling of Embankment 2 Trap with Geotextile Reinforcement	124
Figure 5.86	Initial Stresses of Embankment 2 Trap with Geotextile Reinforcement	124
Figure 5.87	Deformed Mesh of Embankment 2 Trap with Geotextile Reinforcement Due to Traffic Load	125
Figure 5.88	Deformed Mesh of Embankment 2 Trap with Geotextile Reinforcement Due to Traffic and Earthquake Load	125
Figure 5.89	Total Displacement of Embankment 2 Trap with Geotextile Reinforcement Due to Traffic Load	126
Figure 5.90	Total Displacement of Embankment 2 Trap with Geotextile Reinforcement Due to Traffic and Earthquake Load	126
Figure 5.91	Soil Movement of Embankment 2 Trap with Geotextile Reinforcement Due to Traffic Load	127
Figure 5.92	Soil Movement of Embankment 2 Trap with Geotextile Reinforcement Due to Traffic Load	127
Figure 5.93	Effective Stresses of Embankment 2 Trap with Geotextile Reinforcement Due to Traffic Load	128
Figure 5.94	Effective Stresses of Embankment 2 Trap with Geotextile Reinforcement Due to Traffic Load	128
Figure 5.95	Potential Landslide of Embankment 2 Trap with Geotextile Reinforcement Due to Traffic Load	129
Figure 5.96	Potential Landslide of Embankment 2 Trap with Geotextile Reinforcement Due to Traffic Load	129
Figure 5.97	SF Curve of Embankment 2 Trap with Reinforced Geotextile	130
Figure 5.98	Modelling of Embankment 3 Trap with Geotextile Reinforcement	131
Figure 5.99	Initial Stresses of Embankment 3 Trap with Geotextile Reinforcement	131
Figure 5.100	Deformed Mesh of Embankment 3 Trap with Geotextile Reinforcement Due to Traffic Load	132
Figure 5.101	Deformed Mesh of Embankment 3 Trap with Geotextile Reinforcement Due to Traffic and Earthquake Load	132
Figure 5.102	Total Displacement of Embankment 3 Trap with Geotextile Reinforcement Due to Traffic Load	133
Figure 5.103	Total Displacement of Embankment 3 Trap with Geotextile Reinforcement Due to Traffic and Earthquake Load	133

Figure 5.104 Soil Movement of Embankment 3 Trap with Geotextile Reinforcement Due to Traffic Load	134
Figure 5.105 Soil Movement of Embankment 3 Trap with Geotextile Reinforcement Due to Traffic and Earthquake Load	134
Figure 5.106 Effective Stresses of Embankment 3 Trap with Geotextile Reinforcement Due to Traffic Load	135
Figure 5.107 Effective Stresses of Embankment 3 Trap with Geotextile Reinforcement Due to Traffic and Earthquake Load	135
Figure 5.108 Potential Landslide of Embankment 3 Trap with Geotextile Reinforcement Due to Traffic Load	136
Figure 5.109 Potential Landslide of Embankment 3 Trap with Geotextile Reinforcement Due to Traffic and Earthquake Load	136
Figure 5.110 Curve of Embankment 3 Trap with Reinforced Geotextile	137
Figure 5.111 Comparison of Safety Factor with Variations of Trap without Geotextile Reinforcement	143
Figure 5.112 Comparison of Safety Factor with Variations of Trap with Geotextile Reinforcement	143
Figure 5.113 Comparison Consolidation of Embankment Improvement	144



APPENDIX LIST

Appendix 1.1 Cross Section	151
Appendix 1.2 Results Bor Log Test Data	152
Appendix 1.3 Data of Sub Soil Condition	153
Appendix 1.4 Data Specification of Geotextile Woven	154



NOTATIONS AND ABBREVIATION LIST

m	= Meters
mm	= Millimetre
Sta	= Station
Cu	= Undrained shear strength
τ	= Shear stresses (kN/m ²).
σ	= Normal stresses (kN/m ²).
γ	= Soil volume weight (kN/m ³)
γ_{sat}	= Saturated soil volume weight
SF	= Safety factor
Sc	= Consolidation settlement (m)
Cc	= Soil compression index
kN	= Kilo newton
Mpa	= Megapascal
%	= Percent
L	= Length of the geotextile
τ_f	= Soil shear strength
m ²	= Square metre
c	= Cohesion (kN/m ²)
ϕ	= Inner friction angle (°)
e	= Modulus young
k	= Permeability coefficient
g	= Shear modulus
σ	= Normal stresses
u	= Pore water pressure (kN/m ²)
R	= The radius of the landslide circle

n	= number of slices
W_i	= weight of the n-the soil slice
N_i	= the resultant of the effective normal force acting along the base of the slice
θ_i	= defined angle
a_i	= the length of the arch of the circle at the n-th intersection (m)
α	= shear angle
σ_v	= vertical soil pressure (kN/m ²)
σ_{ult}	= permit bearing strength (kN/m ²)
T_a	= allowable tensile strength
K_a	= active soil coefficient
σ_{hc}	= horizontal soil pressure (kN/m ²)
S_v	= vertical distance between geotextile layers (m).
T_{all}	= tensile strength of geotextile permit (kN/m ²).
H	= the thickness of the soil layer (m)
q	= load distribution (kN/m ²)
L_o	= geotextile overlapping length (m).

الجامعة الإسلامية
الاستدراكية

ABSTRACT

The construction project of Cibitung – Cilincing is part of the government's mandate to realize Medium Term Development Program (RPJMN), in order to support the national economic growth strategy which has significant role in supporting the effectiveness of distribution from surrounding industrial areas and increase accessibility and capacity of the traffic. In Cibitung – Cilincing there are many embankment slopes, especially embankment that carried out by the researcher at Sta. 7+500 which has height of 9m with 1V: 2H slope tilt. The purpose of this research is to obtain the safety factor (SF), and the consolidation value that occurs for one year.

Embankment stability analysis calculated using finite element method and Fellenius method will be used to find the safety factor (SF). This research uses model of existing embankment, embankment with topography improvement namely 1 trap embankment, 2 trap embankment and 3 trap embankment variations. The embankment with 1 layer geotextile UW-250 woven is to reinforced the embankment namely existing embankment with geotextile reinforcement, embankment 1 trap variation with geotextile reinforcement, embankment 2 trap variation with geotextile reinforcement and embankment 3 trap variation with geotextile reinforcement. In addition to analysing the safety factor, the value of consolidation that occurs on the embankment estimated for one year (365 days).

The results analysis safety factor of the existing embankment has a value 1,0306 and the analysis with Fellenius method has a value 1,0621 so, it can be concluded that the structure of the embankment is lower than the requirement needed (SF =1.5). For the modelling embankment with topography improvement namely, 1 trap has safety factor 1,0771 with consolidation settlement 0,27747m, modelling embankment 2 trap has safety factor 1,1147 with consolidation settlement 0,22237m, modelling embankment 3 trap has safety factor 1,1560 with consolidation settlement 0,17773m. For the modelling embankment with geotextile reinforcement namely, existing embankment with geotextile reinforcement has safety factor 1,3135 with consolidation settlement 0,13874m, 1 trap embankment with geotextile reinforcement has safety factor 1,4035 with consolidation settlement 0,11119m, 2 trap embankment with geotextile reinforcement has safety factor 1,6197 with consolidation settlement 0,09670m, 3 trap embankment with geotextile reinforcement has safety factor 1,8895 with consolidation settlement 0,08887m. So, the geotextile reinforcement has the great effect on the modelling in existing embankment and modelling embankment with topography improvement in resulting greater safety factor and has smallest consolidation settlement.

Keywords: Embankment, Safety Factor (SF), Consolidation Settlement, Geotextile, Plaxis 8.6.

CHAPTER I

PRELIMINARY

1.1 Background

Road transportation plays a very important role in the development of an area. In today's developed times, road transportation is needed as a connection between one region and another, serving activities in realizing high economic growth, even the progress and development of an area is influenced by its transportation system. The construction of the Cibitung to Cilincing toll roads is part of the government's mandate to realize the 2015-2019 Medium-Term Development Program (RPJMN), one of which is the provision of road infrastructure in order to support the national economic growth strategy. The Cibitung-Cilincing toll road section has a length of 34 km, connecting the JORR II section to the Cimanggis - Cibitung toll road and the JORR I east toll road.

In the Cibitung - Cilincing toll road construction project, there are various soil conditions. Cibitung Bekasi area has soft soil conditions. Soft soil has a low bearing capacity, low shear strength, high compressibility, and a large reduction, because the soil pores are filled with water. For this reason, the land needs to be repaired first by stabilizing or strengthening before it is used as a road structure above it so that the soil meets quality requirements, both physically and technically.

In the reality of the project, a more effective method is needed to improve and strengthen the poor soil types. One of the improvements that can be done is to provide improvements so that it can strengthen the soil. The current development of the construction industry has made it possible to make the elements of soil reinforcement construction with a fabrication system that makes implementation easy and fast. The use of synthetic materials in soil reinforcement can also be done later known as geosynthetics. Geosynthetics are generally distinguished based on the nature of materials, namely permeable, known as geotextile, and materials that are impermeable, namely geomembrane.

This issue encourages the compilers to conduct research with Finite element method with the aim of knowing how much influence the use of geotextiles has on the soil embankment, knowing how the stability condition of soil embankment with and without using a geotextile. The research location and cross-sectional geometry can be seen in Figure 1.1 and Figure 1.2 as follows.



Figure 1.1 Location of Cibitung – Cilincing Toll Road
Source: PT. CTP Tollways, (2020)

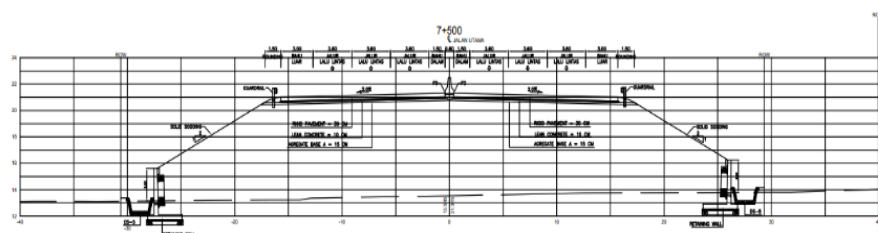


Figure 1.2 Cross Section Geometry
Source: PT. CTP Tollways, (2020)

1.2 Problem Statement

Many road constructions that are built in Indonesia, especially in the Cibitung - Cilincing toll road construction project, have a type of soil characterized by soft soil, how much use of geotextiles to solve road problems on soft soil. From the background explanation, the problem formulation is taken as follows:

1. How is the stability of the existing embankment at Sta.7+500 using Finite element method?
2. How is the stability of the embankment with topography improvement at Sta.7+500 using Finite element method?
3. How is the stability of the embankment with geotextile reinforcement at Sta.7+500 using Finite element method?
4. How is the soil consolidation settlement of the existing embankment at Sta. 7+500 using Finite element method?
5. How is the soil consolidation settlement of embankment with topography improvement at Sta. 7+500 using Finite element method?
6. How is the soil consolidation settlement of embankment with geotextile reinforcement at Sta.7+500 using Finite element method?

1.3 Research Purposes

The main purpose of this final project is to plan the development in Cibitung – Cilincing construction toll road. Thus, for the specific objectives of this planning are as follows:

1. Find out the safety factor (SF) of the existing embankments at Sta.7+500 using Finite element method.
2. Find out the safety factor (SF) of the embankment with topography improvement at Sta.7+500 using Finite element method.
3. Find out the safety factor (SF) of the embankment with geotextile reinforcement at Sta.7+500 using Finite element method.
4. Find out the soil consolidation settlements value that occurs on the existing embankment at Sta. 7+500 using Finite element method.

5. Find out the soil consolidation settlements value on the embankment with topography improvement using Finite element method.
6. Find out the soil consolidation settlements value on the embankment with geotextile reinforcement at Sta. 7+500 using Finite element method.

1.4 Benefits of Research

The benefits of this results analysis are as follows:

1. Diversification for further research in the field of geotechnics, especially the use of geotextiles for reinforcing embankment.
2. Provides an alternative method or geometric planning for the same soil type
3. Overcome problems that exist in the road embankment.
4. Apply and correlate the Plaxis program in geotechnical engineering to solve problems in slope stability analysis.

1.5 Research Limits

In order for research analysis to focus on problem formulation, it is necessary to provide limitations. The limitations of the research problem can be seen in the following description.

1. The research location is on an embankment in the Cibitung – Cilincing Toll Construction Project Section 1 Sta 7+500.
2. Soil data that used from Geotechnical Analysis Report of the Cibitung – Cilincing Toll Road Project Sta 7+500. (PT. Carina Griya Mandiri, 2017)
3. The height of the embankment soil is 9m with 1V: 2H slope tilt.
4. Geotextile Material data used in this research uses the product of PT. Teknindo Geosistem Unggul. The type of geotextile used in this research is woven geotextile UW-250. The allowable tensile strength of this type of geotextile is 52kN/m². (PT. Teknindo Geosistem 2020).
5. Strengthening only using 1 layer geotextile reinforcement.
6. Loading data input the traffic load. (SE PUPR 42/SE/M/2015).
7. Slope stability analysis using Finite element method.

8. Earthquake load is calculated according to the earthquake conditions in the Bekasi region. (SNI-1726, 2019).



CHAPTER II

BIBLIOGRAPHY

2.1 General Review

In this research, a literature review needed to be a reference source to be researched and provide knowledge about soil embankment stability analysis with geotextile strengthening. Literature review is taken from the results of research that has been done previously with each different variable. The reference can be literature review for the author in terms of research implementation.

Soil can be defined as a material consisting of all materials, organic and inorganic that are above a fixed stone. Soil consists of a mixture of solid grains in which there are cavities, these cavities are generally a mixture of water and air. Based on their origin, soils can be broadly classified into organic and inorganic soils. Organic soil is a mixture containing significant parts derived from chemical or physical weathering of rocks. Based on their origin, soils can be broadly classified into organic and inorganic soils. Organic soils are mixtures containing significant portions of weathering and plant debris and sometimes from the collection of skeletons and skins of small organisms. (Terzaghi & Ralph, 1987).

In general, soil can be consisted of 3 parts as follows:

1. Pores or empty spaces (voids), which are open spaces between soil grains of various sizes
2. Soil grains, which may be macroscopic or microscopic in size
3. Soil moisture, which will cause the soil to look wet, moist, or dry. the water in the pore may be present in sufficient quantity to fill the empty space or only partially. Physical and Geotechnical Characteristics of the soil, (Bowles, Joseph E., 1986)

2.2 Slope Stability Analysis

Slope is an oblique soil surface and forms a certain angle to the horizontal plane. If there two soil surfaces with different heights, there will be forces that work to push them, so that the soil with a higher position tends to move downward, causing landslides. However, landslides can be overcome if the soil strength parameters are sufficient (Surjandari, 2012).

Landslide is the results of an increase in the shear stress of a soil mass. The shear strength of a soil mass cannot withstand the working load (Azizah F. N., 2014). Problems with slope stability can be caused by various human activities or natural conditions. Unstable slopes can endanger the surrounding environment, therefore slope stability is needed.

One of the methods often used for slope stability analysis is the Fellenius method and Slices Method because it is easy to calculate and the required variables are not too complex, but there are several factors that are not taken into account in this method (Zakaria, 2009). Many slope analysis methods, the most frequently used is the equilibrium limit method, namely Fellenius method, the Bishop Simplified method, the Janbu Simplified method, the Spencer method and the Morgenstern and Price method (Simatupang, 2013).

2.3 Geotextile Reinforcement

Geotextiles are a group of geosynthetic materials that easily pass water. Geotextile is actually a material made of filter paper, wood planks, and bamboo fibres, as well as synthetic fibres that have a lot to do with soil works (Suryolelono K. B., 2000). Initially, the use of geotextiles to speed up consolidation time and as a substitute for sand as a drainage material (vertical sand drain) was widely used.

2.3.1. Geotextile Function

Research entitled Analysis of Embankment Behaviour with Geosynthetic Reinforcement Using Plaxis Software states that geosynthetics is used as reinforcement which is defined as soil retaining elements that are inserted into the soil mass to improve the mechanical behaviour of the soil (Ismanti, 2012). The use of geosynthetic materials is a mechanical method that is attempted to increase the safety factor of a structure.

There are five main functions of geosynthetics, namely separation, filter strengthening, drainage and barrier (John, 1987). Geosynthetics has six functions which are described as follows.

1. Filtration

Geosynthetic material that used to drain water into the drainage system and prevent soil particle migration through the filter.

2. Drainage

Geosynthetic material that used to drain water from the ground.

3. Separator

Geosynthetic material between two dissimilar soil materials to prevent material mixing.

4. Reinforcement

The tensile properties of geosynthetic materials used to withstand stress or deformation in the soil structure.

5. Barriers

Geosynthetic materials that used to prevent the movement of liquid or gas.

6. Protection

Geosynthetic material used as a layer that reduces local stress to prevent or reduce damage to the surface or layer.

In addition to technical functions, the use of geotextiles for soil reinforcement can reduce costs significantly and are more effective than conventional methods. The installation of a geosynthetic layer can reduce the number of stages of embankment, thereby shortening the embankment time.

2.3.2. Geotextile Behaviour

The relationship between stress and strain of geotextile materials is non-linear (Liu, 2007). Two different types of stress and strain relationships are shown in Figure 2.1 below. Most of the geotextile materials are made of polypropylene and high-density polyethylene which exhibit non-linear behaviour as shown in Figure 2.1 (a) with a decrease in tangent stiffness along the additional tensile strain. Figure 2.1 (b) shows the non-linear stress-hardening relationship for the type of material made of polyester, where the tangent stiffness initially decreases and then increases with the increasing tensile strain.

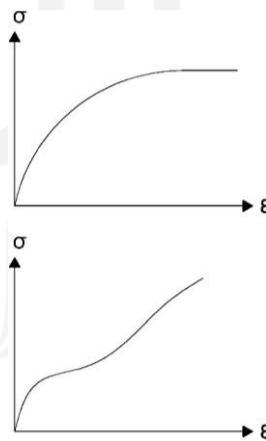


Figure 2.1 Geotextile Stress-Strain Relationship, (a) Polypropylene and High-Density Polyethylene, (b) Polyester Materials

(Source; Liu, H and Ling, H., 2007)

2.4 Effect of Earthquake Load on Embankment Stability

The effect of earthquake loads has an impact on slopes. If the soil layer that forms the slope with a certain depth has a weak layer, while underneath it is a hard layer (bed rock) the effect of the earthquake on the two different masses (soil and rock) will give different accelerations, so that the contact areas of the two layers become the unstable and weak part (Dayanum, 2012). In general, the effect of earthquake loads increases the deformation that has occurred on the slope.

The existence of an earthquake load on the embankment in the soft soil layer causes the following impacts:

1. The presence of soft soil will increase the surface acceleration,
2. Cyclic loads from an earthquake will reduce the undrained shear strength of soft clay soils,
3. The forces that occur on the embankment will increase.

2.5 Slope Stability Analysis Using Geotextile Reinforcement

Aisyah 2018, conducted this final project research is about stability analysis of road embankment using Fellenius method both manually and Geoslope program. There are several types of variation that made in road modelling with geotextile, including geotextile length, vertical distance between geotextile and slope angle. Each type of variation consists of three variations, such as variations in geotextile length are 10 m, 13 m and 15, variations in vertical distance between geotextile are 0.3 m, 0.4 m and 0.6 m and slope angle variations are 19°, 25° and 29°. Safety factor from analysis result without reinforcement with Fellenius method manually is 1.786, while using Geoslope without earthquake is 1.947 and with earthquake is 1.030. Safety factors from analysis result using reinforcement with Fellenius method manually on length variation with geotextile length of 10 m, 13 m and 15 m are 2.339, 2.347 and 2.375 while using Geoslope without earthquake 2.497, 2.855 and 2.947 and with earthquake 1.304, 1.422 and 1.488.

Abdul (2018) This final project research is about the analysis of slope stability with strengthening of geotextile, the analysis uses secondary data parameters taken from PT. Global Profex Synergi and simulated using Plaxis program version 8.2. Slope analysis in Plaxis version 8.2 made by 2D modelling. From the analysis of the Plaxis version 8.2 the safety factor of slopes without reinforcement is 1.345 due to own load, 1.353 due to load (own load) and vehicle load, 1.231 due to embankment load (own load), vehicle load and earthquake load and slope conditions were not safe so required reinforcement at the slope. After the geotextile reinforcement is 1.793 due to load of the embankment and 1.79 due to load of the pile and vehicle load and 1.789 due to vehicle load and earthquake load. This shows that the condition of the new geometry slope with the strengthening of the geotextile is safe for landslide because the value of safe numbers obtained is more than 1.5.

Kafilanda (2019) conducted a study on slope stability analysis using geotextiles with Geoslope program in a case study on Balikpapan – Samarinda Toll Road Sta.1+975. The purpose of this research is to determine the value of the safety factor on the slopes given with geotextile reinforcement. the conclusions obtained from this research include the safety factor (SF) from the results of the analysis Slope/W program $1,159 < 1,5$ and the safety factor (1.5) and the safety factor (SF) using Fellenius method and manual calculations on the existing condition of the embankment soil $0,95 < 1.5$ (unsafe) so it needs to be strengthened.

2.6 Slope Stability Analysis Without Geotextile Reinforcement

Sekarti (2018) conducted research on the analysis of embankment stability on the Semarang – Solo Toll Road, Salatiga – Kartasura Segment. The purpose of this research is to determine the safety factor (SF) of embankment slopes with trap variations based on slide analysis using Slope/W program, Fellenius, Janbu Simplified and Morgenstern Price methods. The results conducted from the research is that the embankment with trap variations without influence of earthquake loads using Fellenius, Janbu Simplified and Morgenstern Price methods has an increase in SF of 9,72%, 9,36% and 10,8%, respectively, while with the effects of earthquake loads is 1,86%, 1,94%, and 2%. The most critical results when compared to other equilibration methods is the Janbu Simplified method. Earthquake can affect the stability of the embankment significantly with an average of 44,4062% lowering the stability level of the embankment.

Hediyanto (2018) conducted research on slope stability analysis with cantilever and sheet pile reinforcement on the Code Riverbank. This research aims to determine the safety factor (SF) of the existing slope, cantilever reinforcement and sheet pile reinforcement using Geoslope/W program and to determine the movement of the soil in both variations of the reinforcement by comparison during an earthquake and without earthquake using Sigma/w program. Based on the results of the study, the safety factor (SF) of the existing slope due to its own weight is 1,118 due to earthquake of 0,565. The safety factor (SF) of the cantilever reinforcement due to its own weight is 2,639 and due to earthquake is 1,789.

2.7 Comparison of Previous Research

The research that has already carried out by other researcher can be used as reference material in the research being carried out, as a limitation of the research and as a research controller to keep it fit for its purpose. The comparison of previous research can be seen in Table 2.1 as follows.

Table 2.1 Comparison Between Previous Research and Research Conducted

Previous Research						Author
Researcher	Aisyah A. A. (2018)	Sekarti (2018)	Hediyanto (2018)	Abdul Hafiedz B. (2018)	Kafilanda (2019)	Arief (2021)
Research Title	Embankment Stability Analysis on Road Construction with Geotextile Reinforcement Using Fellenius Method on Solo – Kertasono Toll Road at Sta. 4+175.	Analysis of Embankment Stability on Semarang – Solo Road Segment Salatiga – Kartasura.	Slope Stability Analysis with Cantilever Wall Reinforcement and Sheetpile on the Code River Bank.	Slope Stability Analysis Using Geotextiles with Plaxis 8.2 Program (Case Study on the Semarang – Solo Toll Road.	Slope Stability Analysis using Geotextile with Geoslope Software	Soil Embankment Slope Stability Analysis with Geotextile Reinforcement (A Case Study at Cibitung – Cilincing Toll Construction Project).

Continuity of Table 2.1 Comparison Between Previous Research and Research Conducted

Research Purposes	Find the safety factor from the analysis using Fellenius in manual calculations and with the Geoslope program.	Find the results of safety factor (SF) for embankment with trap variations based on landslide analysis using Slope/W program.	Find the safety factor (SF) of the existing slope, cantilever reinforcement and sheet pile reinforcement using Geoslope/W program.	Find the value of slope safety without geotextile reinforcement and knowing the value of slope safety with geotextile reinforcement.	Find the value of the safety factor on the slope with geotextile reinforcement using Geoslope program.	Find the slope stability analysis with and without geotextile reinforcement using Plaxis program.
Research Method	Using Fellenius method both manually and Geoslope program. with several types of variations including geotextile length, vertical distance between geotextile and slope angle.	Analysis using direct soil testing in the laboratory and the result of safety factor uses Slope/W program.	Analysis using Geoslope program for slope stability with cantilever reinforcement and sheet pile.	Slope stability analysis uses secondary data parameters taken from PT. Global Profex Synergi and simulated using the Plaxis version 8.2.	Analysis using Geoslope program for slope stability and manual calculations.	Analysis using the Plaxis program for stability analysis and consolidation settlement.

Continuity of Table 2.1 Comparison Between Previous Research and Research Conducted

Results	Safety factors from analysis results using reinforcement with Fellenius method manually on vertical distance between geotextile variation with number of Sv 0.3 m, 0.4 m and 0.6 m are 2.646, 2,347 and 2.059, using Geoslope without earthquake 2.869, 2,855 and 2.758, while with earthquake 1.436, 1.422 and 1.405.	The results of the analysis of embankment with trap variations without the influence of earthquake loads using Fellenius, Janbu Simplified, and Morgenstern-Price method respectively is 9,72%, 9,36%, and 10,8% while 1,86%, 1,94% and 2% due to earthquake load.	The safety factor (SF) of the slope with Sheet Pile reinforcement due to its own weight is 2,726 and due to earthquake loads is 1,846.	The safety factor in the analysis results using the Slope/W program is reinforced with geotextiles is 1,789 due to own burden load, vehicle load and earthquake load.	From the analysis, after geotextile reinforcement is geotextile with variations in geotextile length per zone and added earthquake loads produces a safety factor value of 1,5 and for the safety factor value on slopes reinforced geotextiles without earthquake loads is 1,66.	The results analysis of the stability on the embankment with geotextile reinforcement conducted in greater safety factor than the embankments without geotextile reinforcement.
---------	--	--	--	---	---	---

CHAPTER III

THEORETICAL BASIS

3.1 Soil Type and Classification

Generally, most soil can be characterized as being made up of either or both of two distinctive types of grains. “Rounded” or “bulky” grains have a relatively small surface area with respect to their volume, similar to that of a sphere. These soil grains typically have little intergranular attraction (or bonds) and are therefore termed “cohesionless” referring to lack of tendency to “stick” together. Soil with these grain characteristics may also be called “granular.” This soil group includes sands and gravels. Clay particles are very different and are made of very thin plate-like grains, which generally have a very high surface to volume ratio. Because of this, the surface charges play a critical role in their intragranular attractive behaviour and are termed “cohesive.”

3.1.1 Soil Classification System

There are a number of different soil classification systems that have been devised by various groups, which vary in definition and categories of soil type. The Unified Soil Classification System (USCS; ASTM D2487), American Association of State Highway and Transportation Officials (AASHTO) system. The AASHTO classification designation categorizes soil types based on their usefulness in roadway construction application, as follows.

1. AASHTO System Classification

The AASHTO classification system is shown in table 3.1 developed in 1929 and underwent several revisions until 1945 which are used until now. This classification is based on the characteristics as follows.

a. Grain size, divided into gravel, sand, silt and clay.

1) Gravel

Part of the soil that passes the sieve with diameter of 75 mm and is held in a 2 mm diameter sieve.

2) Sand

Part of the soil that passes the sieve with a diameter of 2 mm and is held in a 0.0075 mm diameter sieve.

3) Silt & Clay

Part of the soil that passes the sieve with diameter of 0.0075 mm.

- b. Plasticity, the name silt soil is used when the finer parts of the soil have a plasticity index (IP) of 10 or less. Clay soil when it is finer parts of the soil have a plasticity index of 11 or more.

The AASTHO classification system is shown in Table 3.1 as follows.

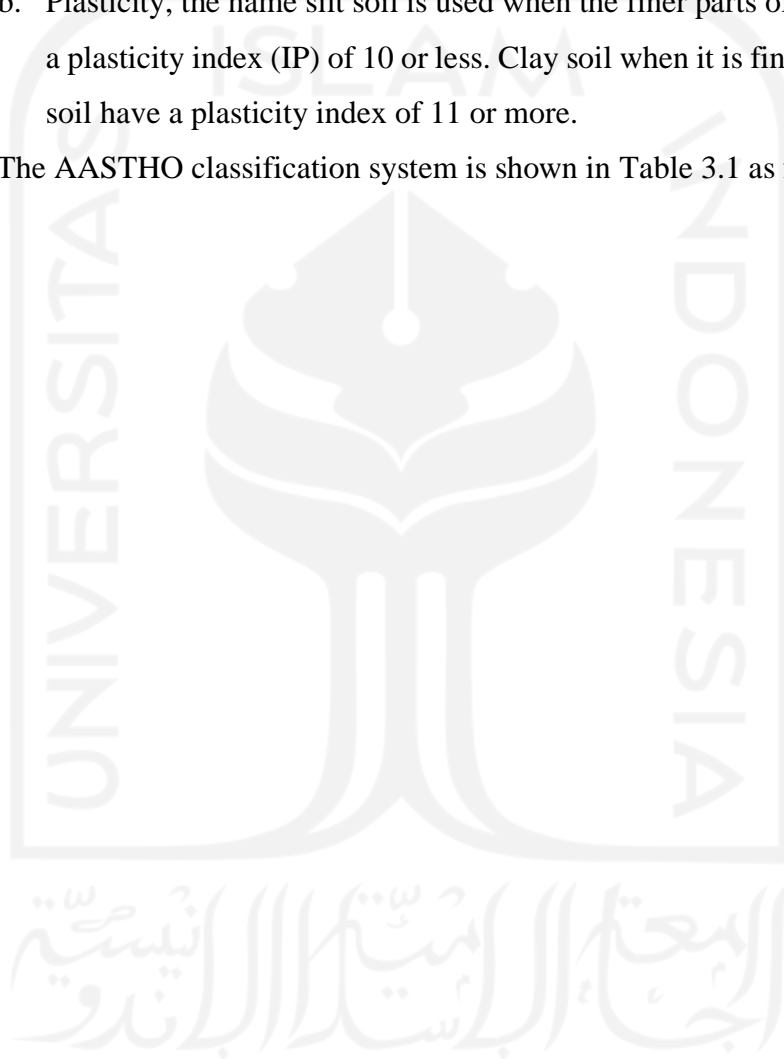


Table 3.1 Soil Classification system based on the American Association of State Highway and Transportation Officials

General Classification	Granular Material (<35% passes sieve no 200)				Soil - Soil Silt - Clay (>35% passes sieve no 200)			
	A-1	A-3	A-2		A-4	A-5	A-6	A-7
Group Classification	A-1-a A-1-b		A-2-4 A-2-5	A-2-6 A-2-7				A-7-5 A-7-6
Sieve Analysis (% Passes) 2.00 mm (no. 10) 0.425 mm (no. 40) 0.075 mm (no. 200)	50 maxes 30 max 50 max 15 max 25 max	51 min 10 max	35 max 35 max	35 max 35 max	3min	36min	36min	36min
The character of the fraction passed the filter no. 40 Liquid limit (LL) Plastic index (IP)	6 maxes	np	40 max 41 min 10 max 10 max	40 max 41 min 11 max 11 max	40 max 10 max	4 min 10 max	40 max 11 max	41 max 11 max
Group Index (GI)	0	0	0	4 max	6 max	12 max	16 max	20 max
Basic material types in general	Grave and rocks fraction	Fine sand	Silty gravel and sand		Silt Soil		Clay Soil	
General appraisal as subgrade	Very good to good				Moderate to bad			

Source: Das B.M. (1988)

2. Unified Soil System Classification

This system was introduced by Cassagrande in 1942, then refined again in 1952 in cooperation with the Unified States Bureau of Reclamation. Unified system divided soil into 2 groups, i.e., coarse grained soil and fine-grained soil.

- a. Coarse grained soil, is gravel and sand with less than 50% of the total weight of the soil sample passes through sieve no. 200. The symbol for this group is G (for gravel soil) and S (for sandy soil). In addition, the soil gradation is also stated with the symbols W (for well-grained soils) and P (for poorly grained soil).
- b. Fine grained soil, is the soil with weight more than 50% of the soil weight. Fine grained soil for example is the soil that passes through sieve No. 200, the symbol of this group is C (for inorganic clay, clay) and O (for organic silt), the plasticity stated in L (low plasticity) and H (high plasticity).

The USCS table can be seen in Table 3.2 as follows.

Table 3.2 Soil classification system based on Unified (Unified Soil Classification)

Main division		Group Symbol	Name Types	Classification Characteristics		
50% coarse-grained soil grains retained by sieve no.200 (0.075 mm)	50% gravel or from the coarse fraction held by sieve no 4 (4.75 mm)	GW	Well graded gravel and sand-gravel mixture, containing little or no fine grains	$CU = \frac{D_{60}}{D_{10}} > 4; CU = \frac{(D_{30})^2}{D_{10} \times D_{60}}$ between 1 and 3		
			GP		Poorly graded gravel and mixed sand gravel, containing little or no fine grains	Does not meet both criteria for GW
		Gravel contains a lot of fine grains	GM	Silty gravel, silt gravel mixture	Atterberg boundaries below line A or PI > 4 If the Atterberg boundary is in the shading region of the plasticity diagram, a double symbol is used	
			GC	Clay gravel mixture of silt sand gravel		Atterberg boundaries above line A or PI > 7
		sand more than 50% coarse fraction passes sieve No.4 (4.75 mm)	Clean sand (little or no fine grain)	SW	Well graded sand, gravel sand, containing little or no fine grains	$CU = \frac{D_{60}}{D_{10}} > 6; CU = \frac{(D_{30})^2}{D_{10} \times D_{60}}$ between 1 and 3
				SP	Poorly graded sand, gravel sand, little or no fine grains	
	Sand contains a lot of fine grains		SM	Silty sand, silt sand mixture	Atterberg boundaries are below line A or PI < 4	If the Atterberg boundary is in the shading region of the plasticity diagram, a double symbol is used
	Classification based on the percentage of fine grains less than 50% passes sieve no. 200 : GM, GP, SW, SP, more than 12% passes sieve no. 200 : GM, GC, SM, SC, 5%-12% passes sieve no. 200 : limits a classification that has a double symbol					

Source: Hardyatmo H.C. (2010)

3.1.2 Grain Size and Grain Distribution

At this point, one needs to clearly define a standard size to differentiate between coarse and fine-grain size. This has been done for a number of classification systems using a standard screen mesh with 200 openings per inch, referred to as a #200 sieve. The effective opening size of a #200 sieve is 0.075 mm. material able to pass through the #200 sieve is termed “fine-grained” while that retained on the sieve is termed “coarse-grained”. The following is Figure 3.1 can be seen as follows.

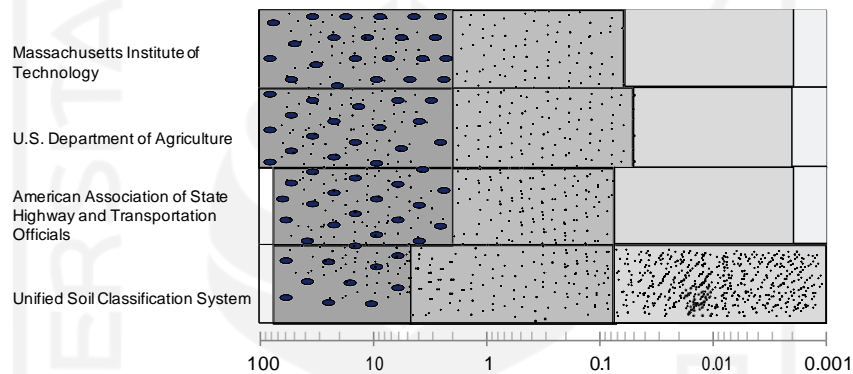


Figure 3.1 Grain size definitions by various particle-size classification schemes.

Coarse-grained soils will generally fall into one of three different gradation types. Figure 3.1 depicts a representation of the general shape or trends of well-graded, poorly graded, and gap-graded soils. Well-graded soils span a wide range of grain sizes and include representation of percentage from intermediate size between the maximum and minimum sizes. Well-graded soils are often preferred as they are relatively easy to handle, can compact well, and often provide desirable engineering properties. Poorly graded (or well-sorted, or uniform) soils have a concentration of a limited range of grain sizes. Gap-graded which refers to a soil with various grain size but with lacks representation of a range of intermediate sizes.

3.2 Soil Shear Strength Parameter

Soil shear strength is the ability of the soil to resist the shear stresses that occur when the soil is loaded. Soil shear failure can occur not because of the collapse of the soil grains. This happens because the relative motion between the soil grains.

Soil shear strength can be interpreted as the resistance force which done by the soil grains against pull or pressure. So, it can be interpreted that when the soil is subjected to loading it will be resisted by:

1. Friction between soil grains which is directly proportional to the normal stress on the shear plane, and
2. Soil cohesion which depends on the type of soil and its density, but does not depend on the normal stresses that occur in the shear plane.

The failure condition of a material can occurs due to a combination of critical conditions of normal stresses and shear stresses (Mohr 1910). Soil shear strength parameters are needed for analysis of soil bearing capacity, slope stability and thrust on retaining walls (Hardiyatmo, 2010). The functional relationship of the two stresses between the normal stresses and shear stresses in the failure plane can be expresses by the following Equation 3.1.

$$\tau = f(\sigma) \tag{3.1}$$

With:

- τ = Shear stresses (kN/m²)
 σ = Normal stresses (kN/m²).

In simple terms, the shear strength of soil can be divided into a value that depends on the shear resistance between the soil grains and the cohesion at the surface of the soil grains themselves. So, soil can be divided into cohesive soil and non-cohesive soil. Sandy soil which has a cohesive value (c) = 0 is an example of an incohesive soil, while clay soil is an example of a cohesive soil.

Coloumb (1776) defines the following Equation 3.2

$$\tau = c + \sigma \operatorname{tg} \varphi \quad (3.2)$$

With:

- τ = Soil shear strength (kN/m²)
- c = Soil cohesion (kN/m²)
- σ = Normal stress in failure plane (kN/m²)
- φ = Inner friction angle (°)

The shear strength of the soil can also be expressed in terms of the effective stresses σ_1' and σ_3' at the time of failure, σ_1' is the effective major stresses and σ_3' is the effective minor stresses. Mohr's circle in the form of a circle stress can be seen in Figure 3.2 as follows.

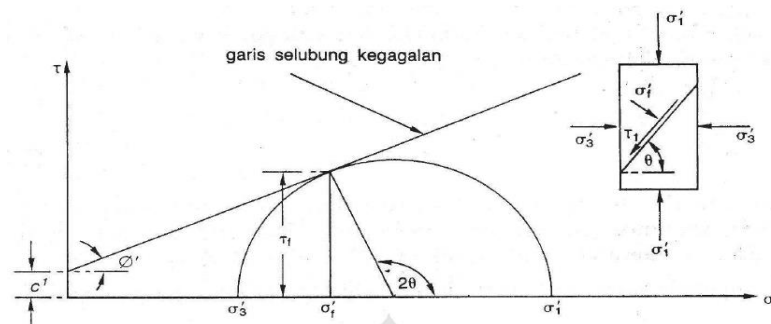


Figure 3.2 Mohr and Coloumb Failure Criteria

(Source: Hardyatmo, 2010)

From the Mohr circle in Figure 3.2 it can be seen as follows:

- c' = Cohesion (kN/m²)
- φ = Effective inner friction angel (°)
- σ_1' = Effective major stresses (kN/m²)
- σ_3' = Effective minor stresses (kN/m²)
- θ = Collapse angle (°)
- $\tau' f$ = Effective shear stress at the time of failure
- $\sigma' f$ = Normal effective stress at the time of failure

Terzaghi (1925) changed the Coloumb equation in the effective form because the soil is strongly influenced by pore water pressure which can be seen in Equations 3.3 and 3.4 below.

$$\tau = c' + (\sigma - u) \operatorname{tg} \varphi' \quad (3.3)$$

Since, $\sigma' = \sigma - u$, so

$$\tau = c' + \sigma' \operatorname{tg} \varphi' \quad (3.4)$$

With:

σ' = Effective normal stresses (kN/m²)

c' = Effective soil cohesion (kN/m²)

φ' = Soil inner friction angle (°)

u = Pore water pressure (kN/m²)

3.3 Slope Landslide

Difference in elevation on the ground surface, such as those occurring on slopes, can result in the movement of the soil mass from a plane with a high elevation to a plane with a lower elevation due to gravity, water, or earthquake forces which result in instability in the soil.

3.3.1 Causes of slope Landslide

Landslide can occur due to human activities or natural events. some of the causes of slope landslide as follows. Type of Slope Landslide

In Landslide Types and Processes (Cruden, 1996) classify slope failures into 5 categories, but in this study the landslides generated from the Slope/W software are rotational slide.

Geotextile have been increasingly applied as reinforcement in road embankment on soft soil. Slide (slip), a shift in the soil mass under the slope that occurs predominantly on the collapse surface or to a small area in shear strain. The movement is usually progressive from the local collapse area. There are two types of landslides, namely rotational slide and translational slide as shown in Figure 3.3

and Figure 3.4 Rotational slide has a circular arc-shaped slip plane, which is generally associated with homogeneous soil condition. Translational slides have a flat slip plane. This landslide is influenced by the presence of different shear strength in the adjacent soil layers. Translational soil tends to occur when the adjacent soil layers are located at a relatively shallow depth below the slope surface. The following Figure 3.3 and Figure 3.4 are slide collapse rotational slide and translational.



Figure 3.3 Slide Slope Failure
Source: Das B.M., (1985)



Figure 3.4 (a) Rotational slide and (b) Translational slide
Source: Das B.M., (1985)

3.3.2 Slope Landslide Prevention

It's very important to overcome slope failure, so that if it does not occur it can be prevented as early as possible before there are victims or losses, or if the landslide has occurred, it can be repaired and minimize the losses that occur again. Below is the method for dealing with landslides that can be done.

1. Soil terracing

Soil terraces are soil conservation structures that are mechanically made to reduce the tilt of the slope or reduce the length of the slope by digging and

filling the soil across the slope. Making terraces is useful for increasing the infiltration of water into the soil and reducing the amount of surface runoff, thereby minimizing the risk of erosion due to water. Below is the functions of soil terracing:

- a. maintain and increase slope stability,
- b. increase the absorption of rainwater into the soil,
- c. reduce the runoff or speed of water flow at ground level,
- d. facilitate maintenance or conservation of slopes,
- e. reduce the length of the slope or reduce the level of the slope,
- f. controlling the direction of the flow of water to a lower area so that it's concentrated in one place,
- g. accommodate and hold water on tilt land.

Terraces can be divided according to their shape, which are as follows.

3.4 Slope Embankment

3.4.1 Safety Factor

The landslide of a slope generally occurs through a certain plane called the slip surface. The safety factor has an important role in the analysis of the stability of the embankment, namely as a factor in reducing the risk of collapse to acceptable level. The comparison between the retaining forces to the forces that move the soil is called the safety factor.

The safety factor for unreinforced slopes according to (Sosrodarsono, 2003) can be seen in Table 3.4 as follows.

Table 3.4 Slope Safety Factors for Slope Design According Sosrodarsono

Safety Factor (SF)	Slope Condition
$SF < 1,00$	Slope in unstable condition
$1,00 < SF < 1,20$	Slope in doubtful stability
$1,30 < SF < 1,40$	Slope in good condition
$1,50 < SF < 1,70$	Slope in steady condition

Source: Sosrodarsono, et al (2003)

Table 3.5 Relationship of Safety Factor Value with Landslide Intensity

Safety Factor (SF)	Landslide Possibilities
SF < 1,07	Landslides occur regularly/frequently (unstable slope)
1,07 < SF < 1,25	Landslides has occurred (critical slope)
SF > 1,25	Landslides are rare (slope are relatively stable)

Source: Bowles, (1989)

The number of safety factors used in this research analysis is, good stability with a long-term time, namely for a safety factor of 1.3. The stability of a slope depends on the value of cohesion (c) and the angle of friction in the soil (ϕ). Soil with dry conditions generally have a high safety factor. On the other hand, the more saturated soil conditions generally the value of the safety factor is getting smaller. One of the causes of unstable slopes is the rising ground water level, thus increasing the degree of saturation and pore water pressure, thereby reducing the effective stress and shear strength of the soil.

3.4.2 Slope Stability Analysis Method

1. Embankment Stability Analysis with Fellenius Method

This method was invented by Fellenius in 1936. This method assumes that the horizontal force pushing the work plane from both directions is ignored, because it is assumed to have the same value. Below are the Figure 3.15 forces that acting on the landslide plane.

Fellenius express his method by stating the assumption that failure occurs through the rotation of a block of soil on a circular landslide surface with point O as the centre of rotation. This method also assumes that the normal force P acts in the middle of the slice. It is also assumed that the resultant forces between the slices at each slice are equal to zero, it can also be stated that the resultant forces between the slices are ignored.

In the Fellenius method, the values of W_n and P_n are assumed to be in the middle of the work plane. The following is Equation 3.5 to get the value of the safety factor using Fellenius method.

So, the total assumptions made by this method are:

- a. The position of the normal force P lies in the centre of the base of the slice:
n
- b. The resultant force between the slice is zero: $n - 1$

Total: $2n - 1$

With these assumptions, it is possible to test the moment balance equation for all slices at the centre of rotation and obtain a value of the safety factor. With this assumption, the balance of the vertical direction and the working forces is:

$$N_i + U_i = W_i \cos \theta_i$$

Or,

$$\begin{aligned} N_i &= W_i \cos \theta - U_i \\ &= W_i \cos \theta - u_i a_i \end{aligned} \quad (3.5)$$

The safety factor is defined as follows,

$$\begin{aligned} F &= \frac{\text{sum of the moments shear resistance along the sliding plane}}{\text{Sum of the moments mass of the mass landslide}} \\ &= \frac{\sum Mr}{\sum Md} \end{aligned}$$

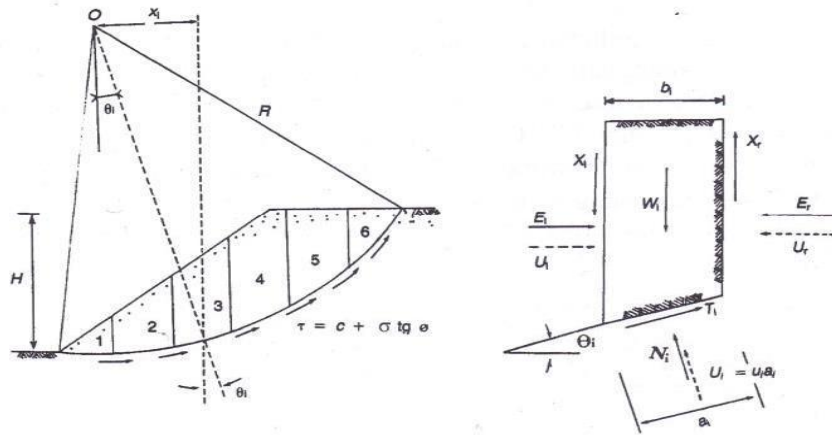


Figure 3.5 Forces that Work on Slices

Source: Hardiyatmo, (2010)

The moment arm of the weight of the soil mass per slice is $R \sin \theta$, then:

$$\Sigma M_d = R \Sigma_{n=1}^{i=n} W_i \sin \theta_i \quad (3.6)$$

With:

R = The radius of the landslide circle.

n = number of slices.

W_i = The weight of the soil mass of the n -th slice.

N_i = The resultant of the effective normal force acting along the base of the slice.

θ_i = Defined angle.

In the same way, the moment resists the soil from slide is:

$$\Sigma M_r = R \Sigma_{n=1}^{i=n} (ca_i + N_i \operatorname{tg} \varphi) \quad (3.7)$$

Then the equation for the safety factor become as follows:

$$F = \frac{\sum_{n=1}^{i=n} (ca_i + N_i \operatorname{tg} \varphi)}{\sum_{n=1}^{i=n} W_i \sin \theta_i} \quad (3.8)$$

If there is water on the slope, then the pore water pressure in the landslide area does not increase the moment due to the soil that will slide (Md), because the resultant force due to the pore water pressure at the centre of the circle.

$$F = \frac{\sum_{n=1}^{i=n} ca_i + (W_i \cos \theta_i - u_i a_i) \operatorname{tg} \varphi}{\sum_{n=1}^{i=n} W_i \sin \theta_i} \quad (3.9)$$

With:

F = Safety factor

C = Soil cohesion (kN/m²)

φ = Inner friction angle (°)

a_i = The length of the arc of the circle at the n-th intersection (m)

W_i = Weight of the n-th soil slice (kN)

u_i = Pore water pressure at slice-n

θ_i = Defined angle

If when there are forces other than the weight of the soil itself, such as building on a slope, then the effect off this load is calculated as Md.

3.5 Soil Consolidation

When a layer of soil is applied above it, the soil particles will experience an increase in stresses, resulting in a settlement in the soil. The decrease is caused by the deformation of the soil particles, the release of air from the pores, and others. One of the main problems in soft soil in a construction work is very large soil consolidation. The large consolidation settlement was caused by the consolidation decrease in the soil when the soil was loaded.

3.5.1 Consolidation Settlement

The addition of a load on a saturated soil layer causes the pore water pressure to increase and causes water to try to flow out of the soil pores so that its

volume will decrease. This soil consolidation is known as consolidation settlement. The amount of consolidation settlement for soft soil types is highly dependent on the geological history of the soil. Soil at a certain depth has experienced pre-consolidation effective stress, which is the largest effective stress.

The effective pre-consolidation stress can be less than or equal to the current effective overburden stress. Normally consolidated, the current effective overburden stress is the largest (maximum) stress experienced by the soil.

3.5.2 Consolidation Calculation Parameters

In calculating the amount of consolidation of a soil layer, several parameters are needed. The following are the parameters for calculating primary consolidation settlement as follows.

1. Soil compression index (C_c)

Terzaghi and Peck (1967) suggest the use of empirical equations to calculate the compression index in clays whose soil structure is undisturbed. Calculations are carried out using the following Equation 3.11.

$$C_c = 0,009 (LL - 10) \quad (3.11)$$

Where LL is the liquid limit. This equation is used for inorganic clays that have a low to moderate sensitivity with an error of 30% (this equation should not be used if the sensitivity is greater than 4). Terzaghi and Peck also proposed the same relationship with remolded clay as in Equation 3.12 and the graph of C_c compression index graph relationship can be seen in Figure 3.6 as follows.

$$C_c = 0,007 (LL - 100) \quad (3.12)$$

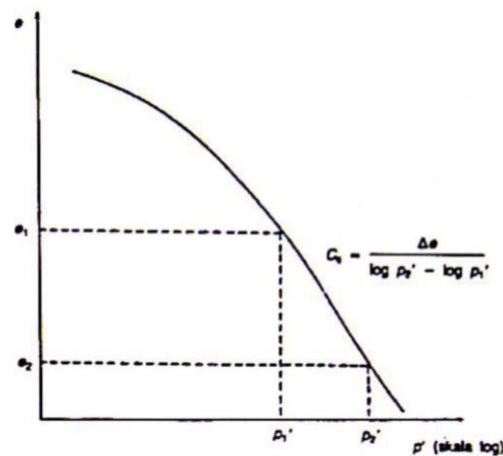


Figure 3.6 Compression Index, C_c

Source: Hardiyatmo, (2003)

Some C_c values based on soil properties at certain places given by Azzous (1976) can be seen in Equations 3.13 to 3.15 as follows.

$$C_c = 0,01 w_n \text{ (Chicago clay)} \quad (3.13)$$

$$C_c = 0,0046 (LL - 9) \text{ (Brasilia clay)} \quad (3.14)$$

$$C_c = 0,208e_o + 0,0083 \text{ (Chicago clay)} \quad (3.15)$$

Where w_n is the original water content in the field (%) and e_o is the void ratio.

2. Effective Overburden Stresses (P_o)

Effective overburden stress is the effective vertical stress of the original soil due to the load or soil layer above the original soil point under consideration (Winner, 2017). The effective overburden stress can be calculated by the following Equation 3.16 as follows.

$$P_o = \gamma' \times H \quad (3.16)$$

With:

P_o = Effective overburden stresses

γ' = Effective soil volume

H = The thickness of the soil layer

3. Distribution of Soil Stresses (Δp)

The addition of soil stress due to the influence of the load on the soil in terms of the midpoint of each layer of soil. The calculation of the addition of stress is defined as in Equation 3.17 as follows.

$$\Delta p = q \times l \quad (3.17)$$

With the value of q defined in Equation 3.18 below.

$$q = \gamma_{\text{embankment}} \times H \quad (3.18)$$

With:

Δp = Vertical stress change

q = Embankment load

H = The thickness of the soil layer

$\gamma_{\text{embankment}}$ = Volume weight of embankment

l = Influence factor

3.6 Geotextile Reinforcement

3.6.1 Geotextile for Embankment Reinforcement

Geotextiles have been widely used for subgrade reinforcement in road pavement structures. Geotextiles have also been frequently used for stabilization of road embankments that located on soft soil foundation. The important and beneficial effect of various use of geotextiles for reinforcing embankments is for the reinforcement that increase the subgrade bearing capacity of the soil and the main function as a separator between the soil.

Embankments built on soft soil have a tendency to move laterally, due to the result of horizontal soil pressure acting on the embankment. This horizontal stress creates shear stress at the base of embankment, which the soft foundation soil must withstand. If the foundation soil does not withstand this shear stress, the embankment may collapse. Therefore, at the base of the embankment a geotextile with high tensile strength can be installed which is useful to increase the stability value of the embankment.

According to the Federal High Way Administration (1998) in (Hardiyatmo, 2013) in its function as reinforcement, geotextiles provide a reinforcement effect through three possible mechanisms, as follows.

1. Lateral restraint on the road foundation layer and subgrade through friction and locking between aggregates. When the vehicle passing, wheel loads tend to shift the aggregate moving laterally. This movement is resisted by subgrade or geosynthetic friction. Geotextile which has high friction resistance can provide tensile resistance to the lateral motion of the aggregate. Soft subgrade is usually not resistant to lateral forces, so when the aggregate moves laterally it will form grooves or curvature on the top of the aggregate and subgrade.
2. Increase the bearing capacity of the soil, by forcing the collapsed plane to move outward, thereby increasing the shear resistance of the soil.
3. Membrane supports due to wheel loads. This membrane support increases the road bearing capacity, by the influence of the membrane tensile force in the geosynthetics by the influence of wheel loads.

If the subgrade is soft, when traffic loads act on it, the geotextile will deform significantly. This deformation causes the tensile strength to be mobilized. The greater the deformation, the greater the mobilized tensile resistance. This mobilized tensile force in the geotextile adds to the subgrade support by increasing the CBR, thereby reducing the required thickness of the base layer aggregate.

3.6.2 Type of Geotextile

Based on the method of manufacture, geotextiles are divided into two types, namely as follows

1. Woven Geotextile

Woven geotextiles are made by woven as seen in Figure 3.7, this type of geotextile has high tensile strength so that in its application in the field it is widely used as a reinforcement layer and as a separating layer.

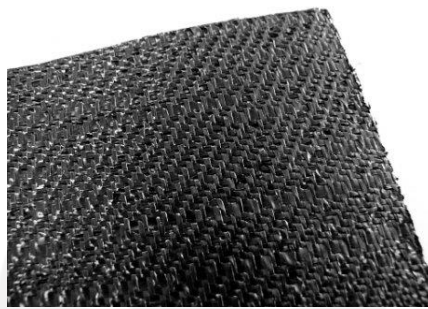


Figure 3.7 Woven Geotextiles

Source: Isparmo, (2010)

2. Non-Woven Geotextile

Non-woven geotextiles are not made by woven, but the fibre's formed to each other by binding or adhesives as shown in Figure 3.8 as follows.

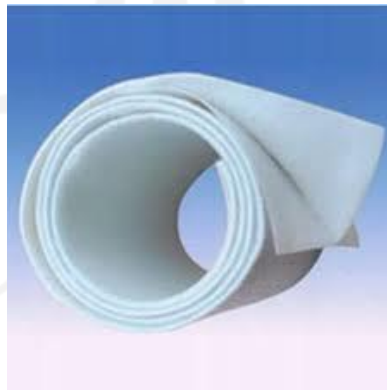


Figure 3.8 Woven Geotextiles

Source: Isparmo, (2010)

Based on Isparmo (2010) the function of geotextiles consists of a function as a geotechnical reinforcement material as follows.

1. As separator

Separator function is needed when placed between two different types of materials, to avoid contamination and mixed materials, that may occur between the materials.

2. As soil reinforcement

The function of geotextiles as soil reinforcement because, the soil has the strength to withstand compression, but can't withstand tension stress. Otherwise, geotextiles have the ability to withstand strong tension, so the function of geotextiles is met to reinforced the soft soil conditions.

3.6.3 Geotextile Reinforcement Design

The criteria for geotextile material that must be considered in the case of road construction are the optimum resistance of the geotextile to puncture, tensile strength and strain. The selected geotextile must have the following criteria:

1. a certain modulus or tensile strength adapted to subgrade conditions,
2. deformation characteristics due to the load required for the selected geotextile to mobilize its tensile strength.

The use of geotextiles for temporary and permanent roads must be considered the criteria for their durability. In the design, the stress that acts on the surface above the subgrade due to the aggregate own load and the traffic load must be less than the carrying capacity of the soil with a certain safety factor. When the implementation is done, the stress that occurs in the subgrade and geotextile can be greater than the service load. Therefore, the selection of a geotextile for road is usually based on the stresses it is expected to work on and is selected based on its resistance to the most critical conditions.

Geotextile installation on embankment must have the required safety factor value, for temporary or permanent embankment. The design of embankments is considered critical if:

1. a slope failure resulting in victim or significant residential damage,

2. there is a mobilized tensile force in the reinforcing reinforcement at the design age of the structure,
3. failure of the reinforcement causes the collapses of the structure.

Geotextile reinforcement can be installed in one or more layers depending on the magnitude of the shear force to be resisted, as in the Figure 3.9 as follows.

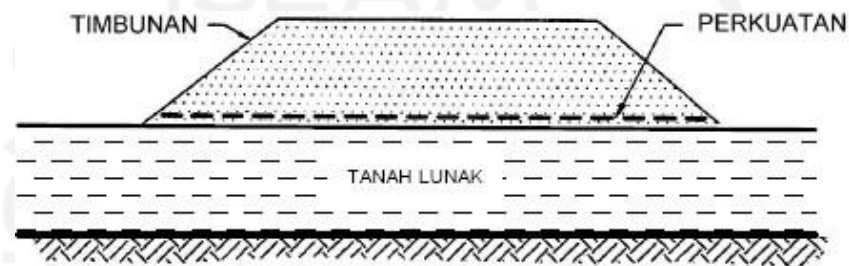


Figure 3.9 Embankment on Soft Soil

Source: Hardiyatmo, (2008)

Reinforced embankment planning is to prevent collapse. Figure 3.9 shows a model of failure that can occur in a reinforced embankment. The three possible collapses provide an indication of the type of stability analysis required. In addition, the reduction in embankment and the potential for creepage on the reinforcement should also be considered.

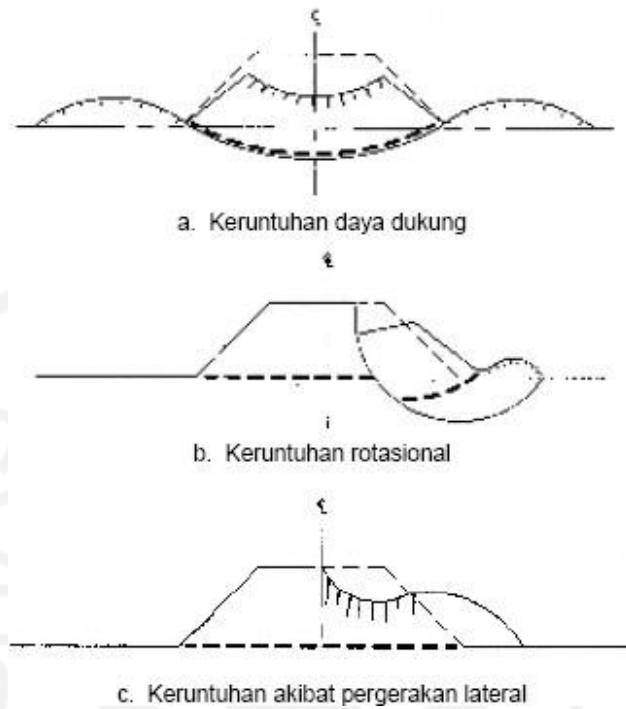


Figure 3.10 The Collapse Model of a Reinforced Embankment
Source: (Holtz, 1996)

3.6.4 Stability Analysis of Embankment with Geotextile Reinforcement

Analysis of forces acting for stability against internal forces used stress analysis such as the retaining wall using the classical theory of Rankine and Coulomb. The method used is two kinds, assuming the shape of the landslide is a triangle and a trapezoid which is still in the advanced research stage. The following is the figure of lateral distributed diagram can be seen in Figure 3.11 below.

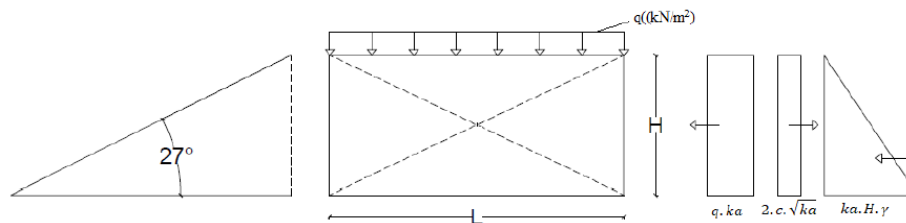


Figure 3.11 The Soil Lateral Distributed Diagram
Source: (Purwanto, 2012).

Construction stability analysis has 2 points of view, as follows.

1. Using the soil pressure coefficient idle, with the following Equation 3.19 as follows.

$$K_0 = 1 - \sin \varphi \quad (3.19)$$

With:

K_0 = coefficient of idle pressure,

φ = inner shear angle ($^\circ$).

2. Using the active soil pressure coefficient, with the following Equation 3.20 as follows.

$$K_a = \tan^2\left(45^\circ - \frac{\varphi}{2}\right) \quad (3.20)$$

With:

K_a = active soil coefficient,

φ = inner shear angle ($^\circ$).

In this research analysis, the active soil pressure coefficient is used using Equation 3.21 above. Furthermore, the calculation will be reviewed from the internal stability and external stability as follows.

1. Internal stability

Horizontal soil stress is soil stress caused by horizontal movement of the soil. The horizontal stress in this research is influenced by the stress due to the load acting on the embankment. In Figure 3.21 above is a description of the forces acting on the embankment, the following Equation 3.21 is to calculate horizontal soil pressure.

$$\sigma_{hc} = q \cdot K_a + K_a \cdot H_i \gamma \quad (3.21)$$

With:

σ_{hc} = horizontal soil pressure (kN/m^2),

q = distributed load (kN/m^2),

K_a = active soil coefficient,

H_i = height of the soil under review is calculated from the soil surface (m),

γ = the weight of the volume of the soil (kN/m^3).

Furthermore, calculating the vertical distance between geotextile layers (S_v) can be calculated using the following Equation 3.22.

$$S_v = \frac{T_{all}}{\sigma_{hc} \cdot SF} \quad (3.22)$$

With:

S_v = vertical distance between geotextile layers (m),

T_{all} = tensile strength of geotextile permit (kN/m),

σ_{hc} = horizontal soil pressure (kN/m^2),

SF = safety factor (used 1.5).

a. Overlapping Geotextile

Here is Equation 3.23 to calculate the overlapping geotextile.

$$L_o = \frac{\sigma_{hc} \times S_v \times SF}{2 \times Z_i \times \gamma_b \times \tan \varphi} \quad (3.23)$$

With:

L_o = geotextile overlapping length (m).

σ_{hc} = Ultimate stress (kN/m^2).

S_v = The distance of the reinforcement in vertical direction (m).

Z_i = The depth of the reinforcement bent into the soil (m).

SF = Safety factor.

γ_b = Volume weight of soil (kN/m^3).

φ = inner shear angle ($^\circ$).

b. Effective Length of Geotextile

The length of reinforcement behind the slip plane (L_{ef}) at the end of the geotextile can be seen in Equation 3.24 as follows.

$$L_{ef} = \frac{SF \times S_v \times K_a \times \gamma_b \times Z_i}{2 \times Z_i \times \gamma_b \times \tan \varphi} \geq 0,5 \quad (3.24)$$

With:

- L_{ef} = Effective length of geotextile (m).
- K_a = Coefficient of active soil.
- S_v = Vertical distance of reinforcement (m).
- Z_i = The depth of the reinforcement bent into the soil (m).
- γ_b = Volume weight of soil (kN/m^3).
- SF = Safety factor
- φ = inner shear angle ($^\circ$).

2. External stability

The external stability of the embankment review to 3 stabilities as follows.

a. Rolling stability

The safety factor due to rolling can be expressed in Equation 3.25 below.

$$SF = \frac{L^2 \cdot (\frac{1}{2} \cdot q + \frac{1}{2} \cdot \gamma_b \cdot H)}{\frac{1}{2} \cdot q \cdot k_a \cdot H^2 \cdot \gamma_b - c \cdot \sqrt{K_a} \cdot H^2} \quad (3.25)$$

With:

- SF = active soil coefficient.
- L = Geotextile length (m).
- H = Soil layer height (m).
- c = Cohesion (kN/m^2).
- γ_b = volume weight of soil (kN/m^3).
- q = Distributed load (kN/m^2).

b. Shear stability

The equation for calculating the safety factor due to shear stability can be seen in Equation 3.26 below.

$$SF = \frac{L \cdot (1 + \gamma b) \cdot \tan \varphi}{(q \cdot ka \cdot H + ka \cdot H^2 \cdot \gamma b - 2 \cdot c \cdot \sqrt{ka \cdot H})} \quad (3.26)$$

With:

SF = Safety factor

φ = Angle friction between soil and geotextile ($^{\circ}$).

L = Length of the geotextile (m).

H = Soil layer height (m).

γb = Volume weight of soil (kN/m^3).

Ka = Active soil coefficient.

C = Cohesion (kN/m^2).

q = Distributed load (kN/m^2).

c. Stability due to Eccentricity

The value of $1/6 L$ must be greater than the eccentricity value that stated as follows.

$$\frac{1}{6} \geq e$$

$$\frac{1}{6} \geq \frac{\frac{1}{2} \cdot 1 \cdot Ka \cdot H^2 + \frac{1}{6} \cdot Ka \cdot H^2 \cdot \gamma b - c \cdot \sqrt{Ka \cdot H^2}}{(q \cdot L + \gamma b \cdot H \cdot l)} \quad (3.27)$$

With:

e = soil eccentricity (m).

q = distributed load (kN/m^2).

Ka = Coefficient of active soil.

H = Height of soil layer (m)

c = Cohesion (kN/m^2)

- L = Geotextile length (m)
 γ_b = Volume weight of soil (kN/m³).

d. Stability due to bearing strength that occurs

The calculation due to the bearing strength of soil permits can be seen in the Equation 3.28 and Equation 3.29 below.

1) Ultimate bearing permit

$$\sigma_{ult} = c \cdot N_c + q \cdot N_q + 0.5 \cdot \gamma \cdot L \cdot N_\gamma \quad (3.28)$$

$$q_{ult} = c \cdot N_c + 0.5 \cdot L \cdot \gamma_b \cdot N_\gamma \quad (3.29)$$

With:

σ_{ult} : permit bearing strength (kN/m²),

c : soil cohesion (kN/m²),

N_c, N_q, N_γ : soil bearing capacity factor of Terzaghi

So that the stability of the embankment towards the bearing strength can be calculated using the following Equation 3.30.

$$SF = \frac{\sigma_{ult}}{q_{ult}} > 1.3 \quad (3.30)$$

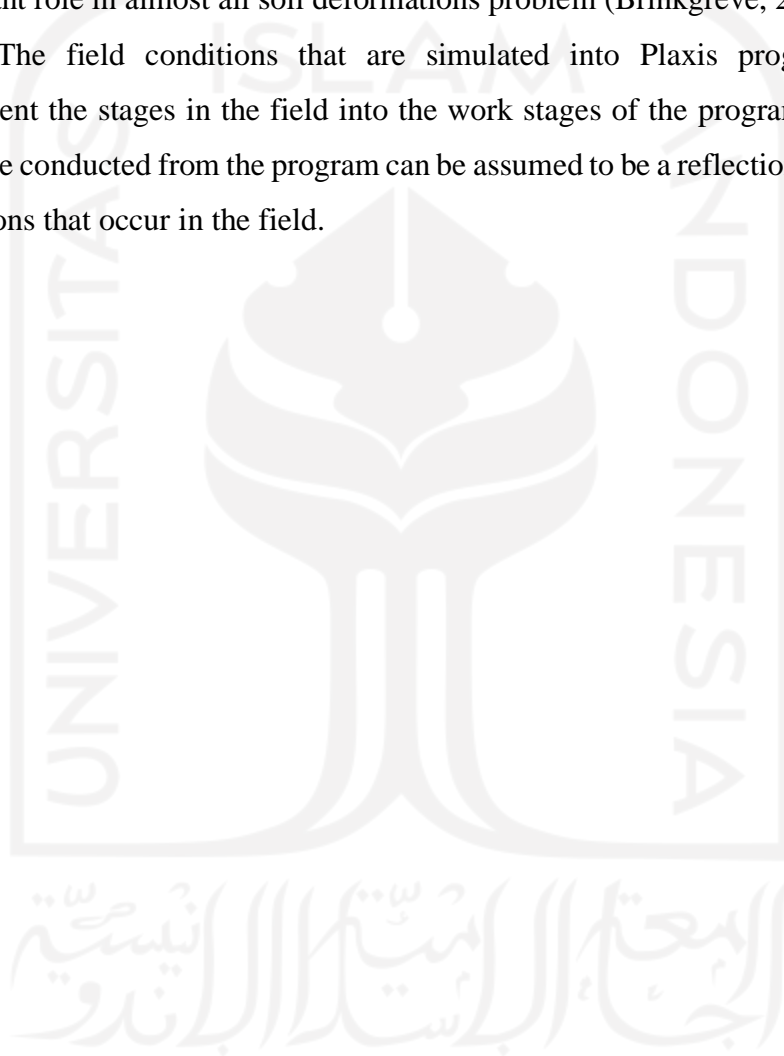
3.7 Plaxis Software

Plaxis is a software program that can be used to simplify geotechnical analysis. Plaxis program is designed based on two-dimensional finite element method which can be used specifically to analyse deformation and stability. The actual condition can be modelled in plane-strain or asymmetrically. This program implements a graphical interface model, also can create geometric and mesh models based on cross-section of the conditions to be analysed. This program consists of four sub-programs, namely input calculations, outputs, and curves.

The model that will be used in this research is Mohr-Coloumb model. This model is an elastic – plastic model consisting of five parameters, namely E and μ to design soil elasticity, ϕ and c to design soil plasticity, and as the angle of dilatation. The Mohr-Coloumb model is a “first order” approximation of soil or rock

behaviour. This model is recommended to be used in the initial analysis of the problems encountered. Each layer will be modelled with a constant average stiffness value. Because of the constant stiffness, calculations tend to be fast and an initial estimate of the deformation shape of the model can be obtained. Besides the five parameters of the model, the initial stress conditions of the soil play an important role in almost all soil deformations problem (Brinkgreve, 2007).

The field conditions that are simulated into Plaxis program aim to implement the stages in the field into the work stages of the program, so that the response conducted from the program can be assumed to be a reflection of the actual conditions that occur in the field.



CHAPTER IV

RESEARCH METHODS

4.1 Research Location

This research was conducted on the Cibitung – Cilincing Toll Road Section 1 at Station 7 + 500. The following Figure 4.1 is the Cibitung – Cilincing toll road trace.

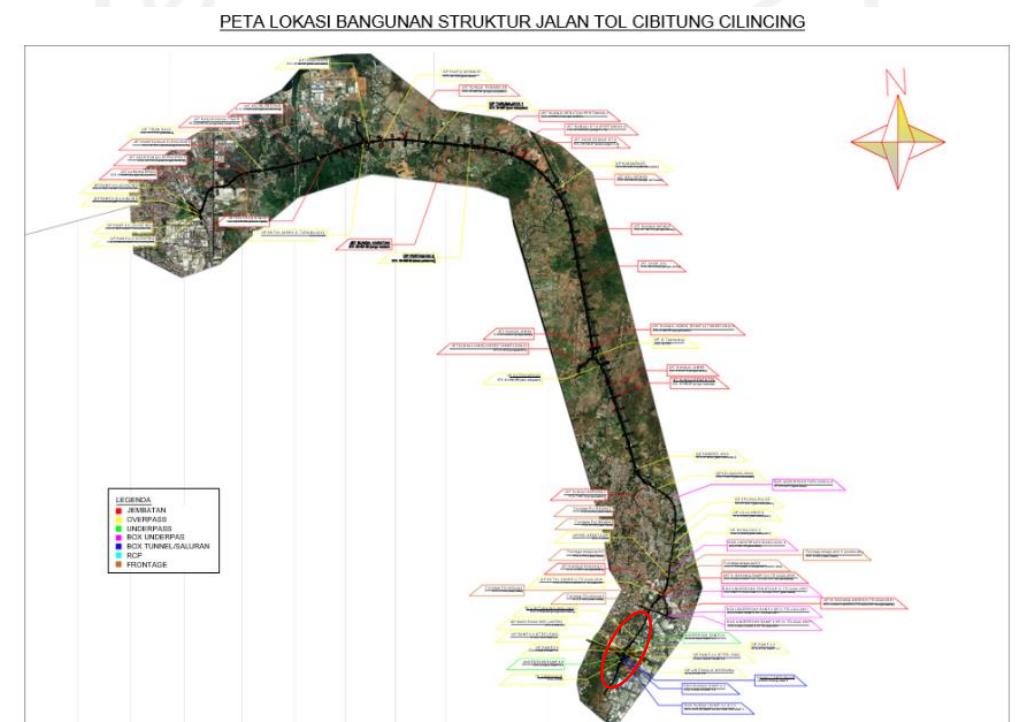


Figure 4.1 Toll Road Trace
Source: Waskita Karya (2020)

Figure 4.1 above represents the trace of the Cibitung – Cilincing Toll Road, starting from the Cibitung Intersection on the Jakarta - Cikampek Toll Road KM 25, heading north in the Babelan District and continue westward to meet the North Outer Ring at the Cilincing interchange. Which includes 4 sections, the first section is Cibitung IC - Telaga Asih IC along Sta 0+400 – 8+000 IC, while the research location is at the section 1 in IC Telaga Asih at Sta 7+500. With the characteristics

of the soil is silty clay which results in a relatively large reduction in the embankment when given load on it.

4.2 Data Used

There are several data used to complete the research, as follows.

4.2.1 Soil Parameter Data

Soil parameter data used are data related to physical properties and mechanical properties in subgrade. This data is conducted from secondary data. This data will be used as the main data for manual calculations and analysis using the Plaxis software. The secondary data include as follows:

1. Soil data: which includes: field test soil data and laboratory test soil data. Field test soil data is data from the results of the SPT (Standard Penetration Test) test in the form of tables and graphs. Laboratory test soil data, namely data from laboratory test which includes:
 - a. Soil volume weight (γ)
 - b. Cohesion (c), and
 - c. Inner friction angle (ϕ).
2. Soil layer data
3. Earthquake data
4. Slope embankment data.

In this analysis, soil parameter data from the Geotechnical Analysis Report of Cibitung – Cilincing Toll Road Project. The soil parameter data can be seen in Table 4.1 as follows.

Table 4.1 Soil Parameter Data

Name		Silty Clay	Silt	Silt	Clay Sand (Embankment)
Model	-	MC	MC	MC	MC
Type	-	UNDRAINED	UNDRAINED	UNDRAINED	UNDRAINED
γ unsat	kN/m ³	14	18	20	16
γ sat	kN/m ³	16	20	22	19
Kx	m/day	4,500E-03	4,300E-05	4,300E-05	0,1
Ky	m/day	4,500E-03	4,300E-05	4,300E-05	0,1
E	kN/m ³	4000	20000	24000	11000
ν	-	0,30	0,30	0,334	0,30
Cohesion (C)	kN/m ³	10,1043	79,37	85	10
Friction angle (ϕ)	°	8	30	30	25

(Source: PT. Carina Griya Mandiri, 2017)

4.2.2 Detailed Engineering Drawing

This research requires data engineering drawing in the form of a road plan as an input for the in the Plaxis software the detailed engineering drawing for cross section embankment can be seen in Appendix 1.1.

4.2.3 Geotextile Material Data

Geotextile Material data used in this research uses the product of PT. Teknindo Geosistem Unggul. The type of geotextile used in this research is woven geotextile UW-250. The geotextile value as input for the Plaxis software is in the form of value normal stiffness (EA) which can be calculated by Equation 4.1 as follows.

$$EA = \frac{Fg}{\Delta l/l} \quad 4.1$$

Description:

F_g : The allowable tensile strength of the geotextile kN/m^2 , and

Δ/l : Strain of the geotextile

The allowable tensile strength of this type of geotextile is 52kN/m^2 . Geotextile material can be seen as follows.

Table 4.2 Geotextile Woven UW-250 Parameter Data

Parameter	Notation	Value	Unit
Allowable tensile strength	TA	52	kN/m
Strain	E	20	%
Normal stiffness	EA	260	kN/m

Source: PT. Teknindo Geosistem (2020)

4.2.4 Load Data

The loads that work on this embankment are rigid pavement loads, traffic loads and earthquake loads.

1. Rigid pavement and traffic loads

The traffic load used for this stability analysis refers Traffic load guide for stability analysis (Pt T-10-2002-B) in SE PUPR. The road class on this toll road is arterial primary roads, so the traffic load is 15 kN/m^2 , and the rigid pavement is 10 kN/m^2 from secondary data.

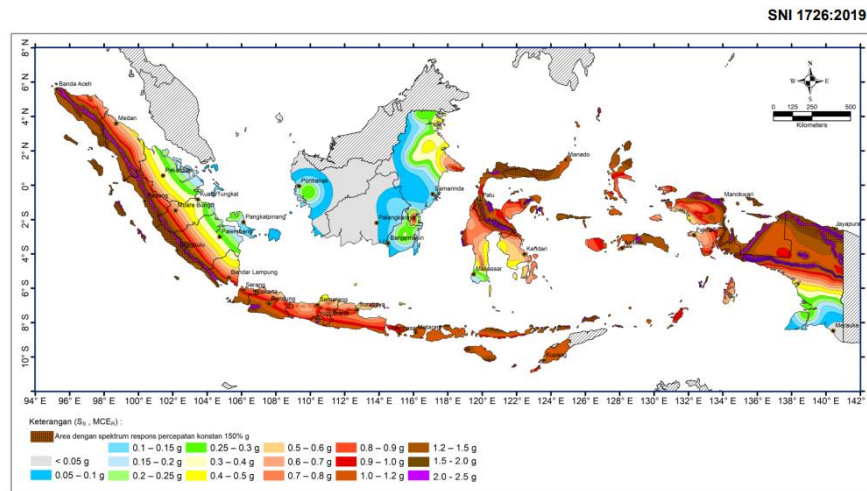
Table 4.3 Traffic Load

Function	System	LHR	Traffic Load (kN/m ²)
Primary	Artery	All	15
	Collector	>10000	15
		<10000	12
Secondary	Artery	>20000	15
		<20000	12
	Collector	>6000	12
		<6000	10
	Local	>500	10
		<500	10

Source: Ministry of Public Works and Public Housing (2009)

2. Earthquake Load

The earthquake load used in this analysis comes from Ministry of Public Works and Public Housing. The earthquake acceleration that is entered in the seismic load input program Plaxis is selected based on the earthquake zoning area of Bekasi which has as earthquake peak acceleration (PGA) of 0.3 - 0.4 g. Earthquake data that matches this value is earthquake data in the American Canyon area of California late 2014 which has an earthquake peak acceleration of 0,3938 g. Earthquake interval time used is 3,2 seconds assuming it has passed the peak. Zoning maps and graphs of the relationship between earthquake time can be seen in Figures 4.2 as follows.



Gambar 15 – Parameter gerak tanah S_a , gempa maksimum yang dipertimbangkan risiko-tertarget (MCE_a) wilayah Indonesia untuk spektrum respons 0,2-detik (redaman kritis 5%)

© BSN 2019

233 dari 238

"Hak cipta Badan Standardisasi Nasional, copy standar ini dibuat untuk Sub KT 91-01-S4 Bahan, Sain, Struktur & Konstruksi Bangunan, dan tidak untuk dikomersialkan"

Figure 4.2 Indonesia Earthquake Zoning Map

Source: (SNI-1726, 2019)

4.3 Research Stages

The research steps carried out in this Final Project can be seen in the following explanation.

1. Research preparation

Research preparation includes collecting data from the project construction. The data collection stage, where this stage includes the stage of collecting soil data (field and laboratory test data) needed for analysis purposes from the Geotechnical analysis report of the Cibitung – Cilincing Toll Road Project.

2. The data analysis and processing stage

At this stage, the data that has taken (field test data and laboratory data), is then processed with theory that applies as a correction (analysis with the

Plaxis software), then the follow-up can be determined from the results of the Plaxis software.

3. Discussion and conclusion

This stage will be written into a report which contains the results that have been obtained from the analysis stage, then a solution will be conducted from the problems that arise and conclusions are conducted based on the existing theory.

4.4 Modelling of the Embankment

4.4.1. Existing Embankment

The existing condition of the embankment and the existing soil type for each layer can be seen in Figure 4.3 as follows.

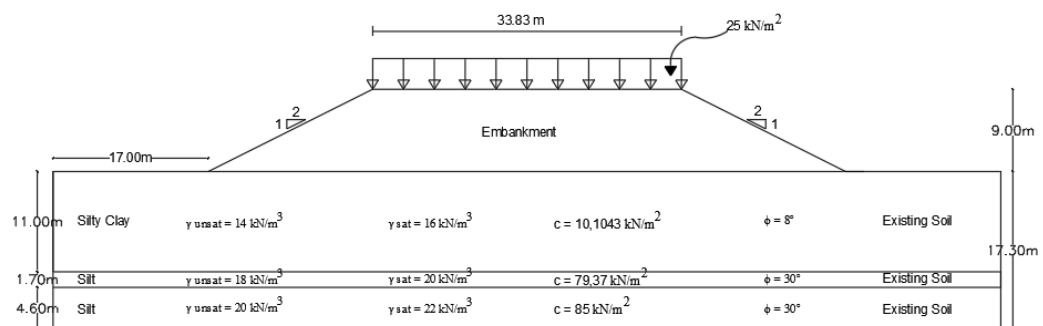


Figure 4.3 Existing Condition of Embankment

4.4.2. Embankment 1 Trap Variation

The embankment of this sub-modelling is adding the geometric variation, by adding 1 trap on the embankment that can be seen in Figure 4.4 as follows.

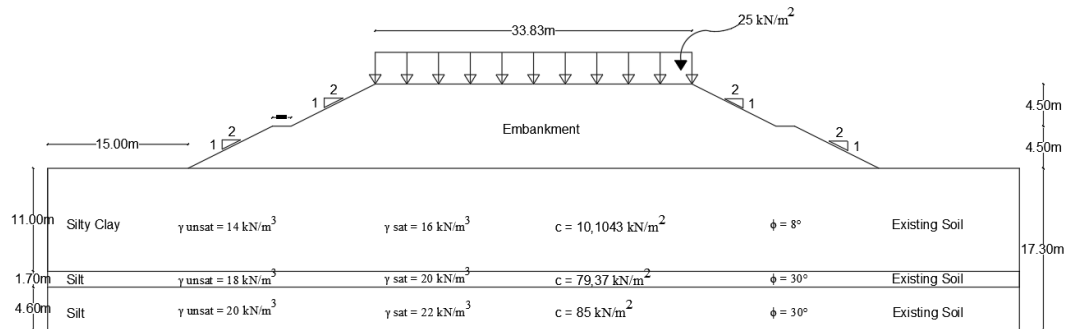


Figure 4.4 Embankment 1 Trap

4.4.3. Embankment 2 Trap Variation

The embankment on this sub-modelling is adding the geometric variation, by adding 2 traps on the embankment that can be seen in Figure 4.5 as follows.

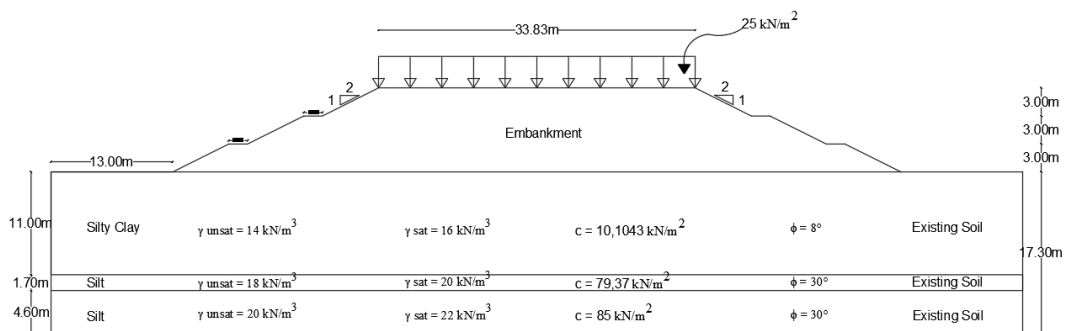


Figure 4.5 Embankment 2 Trap

4.4.4. Embankment 3 Trap Variation

The embankment on this sub-modelling is adding the geometric variation, by adding 3 traps on the embankment that can be seen in Figure 4.6 as follows.

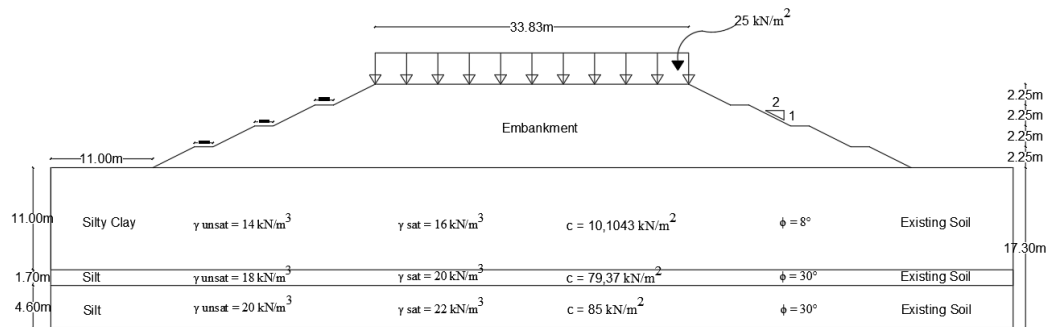


Figure 4.6 Embankment 3 Trap

4.4.5. Existing Embankment with Geotextile Reinforcement

Initial modelling of the existing embankment with the same geometry on the existing embankment. Horizontal installation of geotextiles with an SV of 0,5 m and overlapping length of 1 m. For the total length of the geotextile used along the embankment at the bottom, assuming that the length reached the minimum total length of the geotextile requirement calculation. The Figure of existing embankment with geotextile reinforcement can be seen in Figure 4.7 as follows.

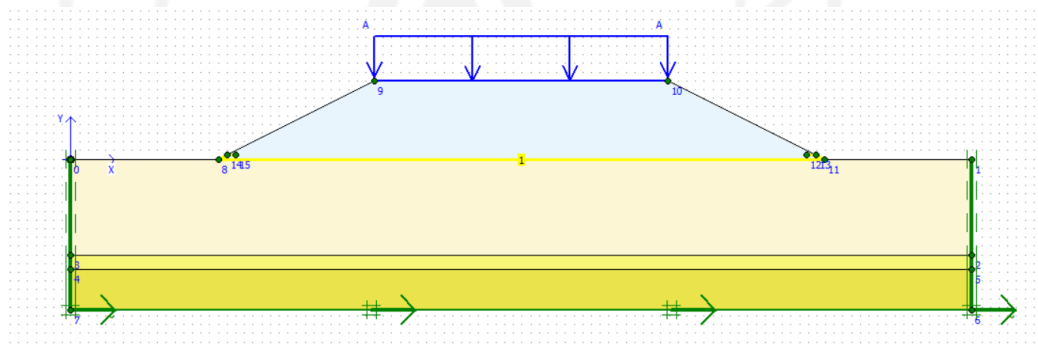


Figure 4.7 Existing Embankment with Geotextile Reinforcement

4.4.6. Embankment 1 Trap with Geotextile Reinforcement

Initial modelling of the embankment 1 trap with geotextile reinforcement are equal with geometry on embankment 1 trap variation, that can be seen in Figure 4.8 as follows.

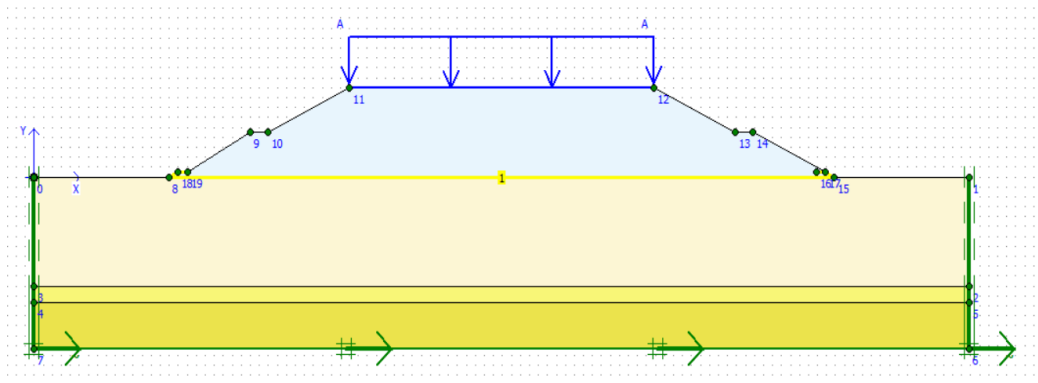


Figure 4.8 Embankment 1 Trap with Geotextile Reinforcement

4.4.7. Embankment 2 Trap with Geotextile Reinforcement

Initial modelling of the embankment 2 trap with geotextile reinforcement are equal with geometry on embankment 2 trap variations, that can be seen in Figure 4.9 as follows.

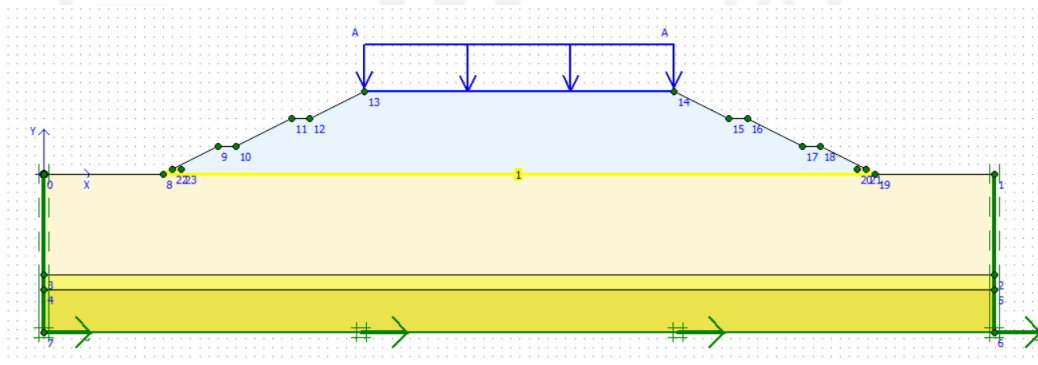


Figure 4.9 Embankment 2 Trap with Geotextile Reinforcement

4.4.8. Embankment 3 Trap with Geotextile Reinforcement

Initial modelling of the embankment 3 trap with geotextile reinforcement are equal to geometry on embankment 3 trap variations, that can be seen in Figure 4.10 as follows.

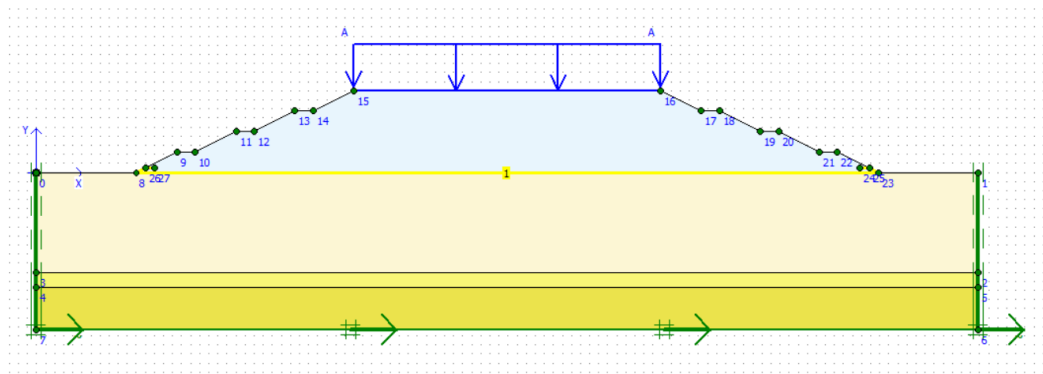


Figure 4.10 Embankment 3 Trap with Geotextile Reinforcement

4.5 Plaxis Program Analysis

The analysis in this research using the Plaxis program was carried out in stages, namely Plaxis input, Plaxis calculation and Plaxis Output.

4.5.1. Plaxis Input

1. Open Plaxis Program

Operate the Plaxis program by double-clicking on the Plaxis input icon. Then a box will appear with the option create/open project, then select new project and click OK to create a new job as shown in Figure 4.11 below.



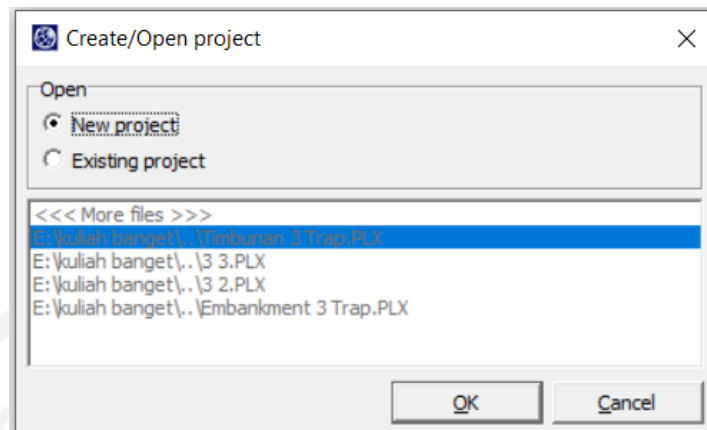


Figure 4.11 Create/Open Project Command Box

2. General Setting

In the general setting there are two command tabs, namely the project and dimensions tab. Select the project tab command, enter the name of the project to be modelled in the command box. Then select the plane strain model analysis in the general box and select the 15-Node basic element type for analysis by generating accurate stress and failure loads, that can be seen in Figure 4.12 as follows.

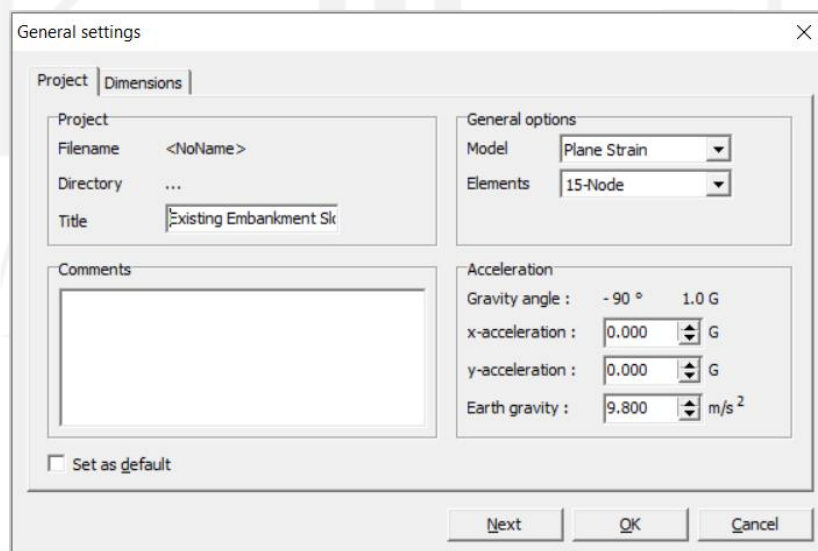


Figure 4.12 Project and Dimension Command

In the geometry dimension tab options, use the pre-selected units in the unit box (Length = m, Force = kN, Time = day). In the geometry dimension box, the size of the drawing fields must be inputted, when inputting the top and bottom coordinates of the geometry to be created. Plaxis will add a small margin so the geometry will be on the drawing plane. Then enter 0,0; 50,0; 0,0; 25,0 each in the left, right, bottom and top fields in the commands box. The grid box contains values for setting the grid spacing.

This grid will form a dotted that is used to enter the exact description of the existing grid during modelling. The distance between the points is determined by the space value. Then for spacing enter value of 0,1 and 1,0 for the number intervals. The Figure 4.13 Dimension tab can be seen as follows.

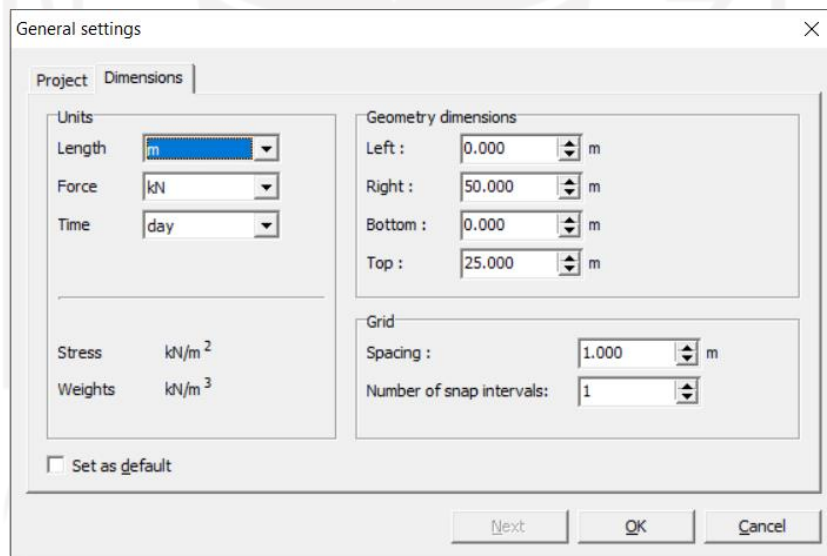



Figure 4.13 Dimension Tab

3. Geometry Modelling

The depiction of the geometric model is carried out with the following stages.

- a.  Select the geometry line option

Position the cursor at the centre of the coordinates. Place the cursor at coordinates 0,0; 0,0; is the starting point in the depiction of geometry, after the geometry is drawn according to the specified coordinates.



- b. Click the standard fixities on the toolbar.



- c. Click the distributed load - load system A button on the toolbar. Then click on the start point and end point on the geometry that received the load, then right click to end the evenly distributed load input. Enter the distributed load (10 kN/m²)

4. Material Parameter

To input material data in this program can be done by using the material sets button on the toolbar or through the options available in the materials menu.



Select the material sets button on the toolbar.

- Click the option (new) at the bottom of the materials sets window. A command box will appear with three-tab sheets namely, general, parameters, interface (See Figure 4.6 and Figure 4.7)
- In the material sets command box type “Embankment” in the identification box.
- Then select Mohr-Coloumb in the material model on command box material type.
- Enter the value to be input in general properties and permeability according to the material parameter that used.
- Click on the parameters tab of the four tab-sheet menu and enter values according to the properties of the materials used. Since the geometry model does not use an interface, the third tab sheet can be passed and then click OK to save the material.
- Click and drag the data set from the material sets window into the soil cluster in the drawing plane and enter above the material.

- g. Then click the OK button on the material sets window to close the database. The Figure 4.14 general tab command and Figure 4.15 parameters tab command can be seen as follows.

Mohr-Coulomb - Sandy Silt II

General | Parameters | Interfaces

Material set

Identification: Sandy Silt II

Material model: Mohr-Coulomb

Material type: Drained

General properties

γ_{unsat} : 17.000 kN/m³

γ_{sat} : 20.000 kN/m³

Comments

Permeability

k_x : 4.300E-05 m/day

k_y : 4.300E-05 m/day

Advanced...

SoilTest Next OK Cancel

Figure 4.14 General Tab Command

Mohr-Coulomb - Sandy Silt II

General | Parameters | Interfaces

Stiffness

E_{ref} : 2.000E+04 kN/m²

ν (nu): 0.300

Strength

c_{ref} : 79.370 kN/m²

ϕ (phi): 30.000°

ψ (psi): 0.000°

Alternatives

G_{ref} : 7692.308 kN/m²

E_{oed} : 2.692E+04 kN/m²

Velocities

V_s : 66.590 m/s


V_p : 124.600 m/s

Advanced...

SoilTest Next OK Cancel

Figure 4.15 Parameters Tab Command

5. Mesh Generation Setup

 Click the generate mesh option on the toolbar or select a menu from the mesh. After the arrangement of the element network, then a new window

will open where the finite element network is shown in Figure 4.16 as follows. Then click the “update” button to enter geometry mode.

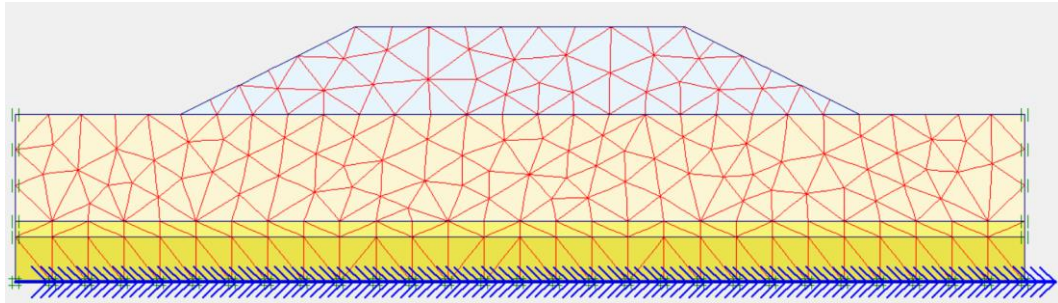





Figure 4.16 Element from Generate Meshing

6. Initial Condition
 - a. Click  Initial conditions button on the toolbar.
 - b.  Since this project neglect the water pressure, then proceed to the initial geometry configuration mode by clicking the button to the right of the switch. The phreatic line will automatically be located on the basis of geometry.
 - c.  Click the general initial stresses option on the toolbar. Command procedure box will appear, then select OK as shown in Figure 4.17 below.

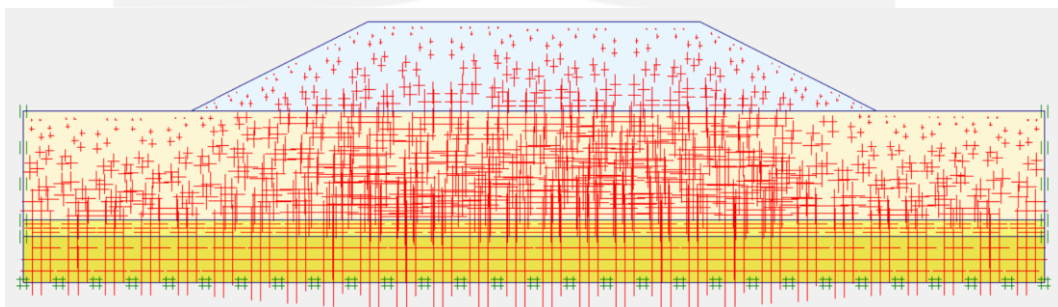


Figure 4.17 Initial Soil Stresses

- d. Click calculate button

4.5.2. Plaxis Calculation

In the calculation section (Figure 4.10) there are four-tab sheets, namely generate, parameters, multipliers and preview. In the general tab sheet, the calculation type, plastic analysis is selected which is used to determine the magnitude of the displacement from the condition under review, phi/c reduction is selected to determine the effect of the earthquake, while on the parameters tab sheet, staged construction is selected for loading input as shown in Figure 4.18 as follows.

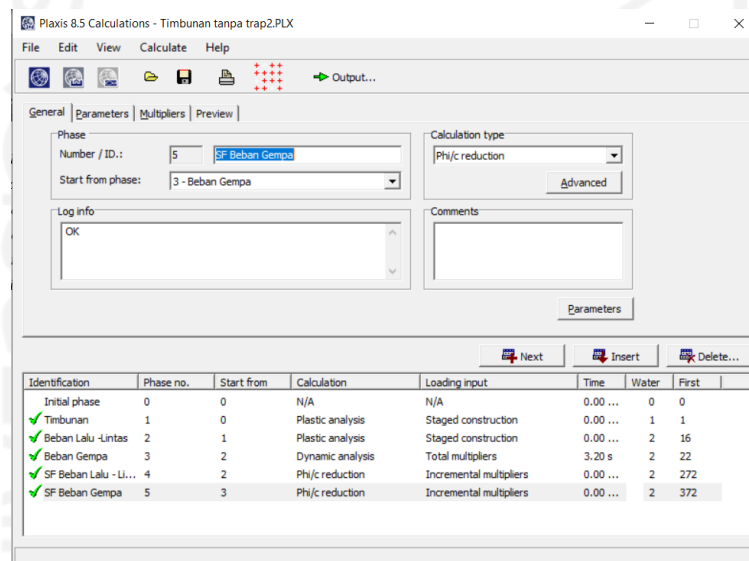



Figure 4.18 Calculation Command

 The next step is to determine the point that will be reviewed to describe the curve display by clicking the select point for curve button as shown in Figure 4.19 as follows.

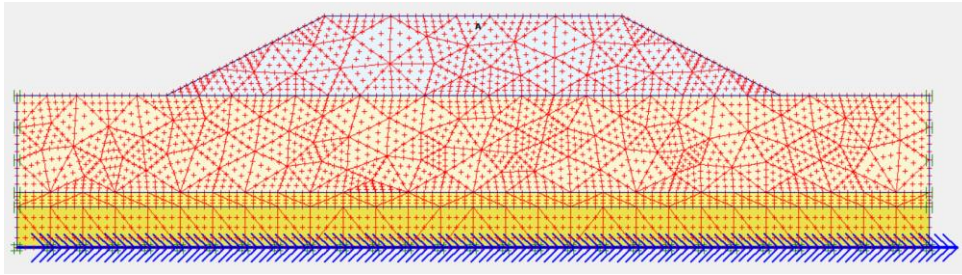
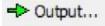


Figure 4.19 Determined the Point Curve

Then the next step is to click the calculation button to run the calculation analysis.

4.5.3. Plaxis Output

After the calculation analysis phases is complete, then click the  Output... button to display the results of the calculation phase that has been carried out.

4.5.4. Research Flowchart

The research flowchart and slope modelling flowchart can be seen in Figure 4.12 and Figure 4.13 as follows.

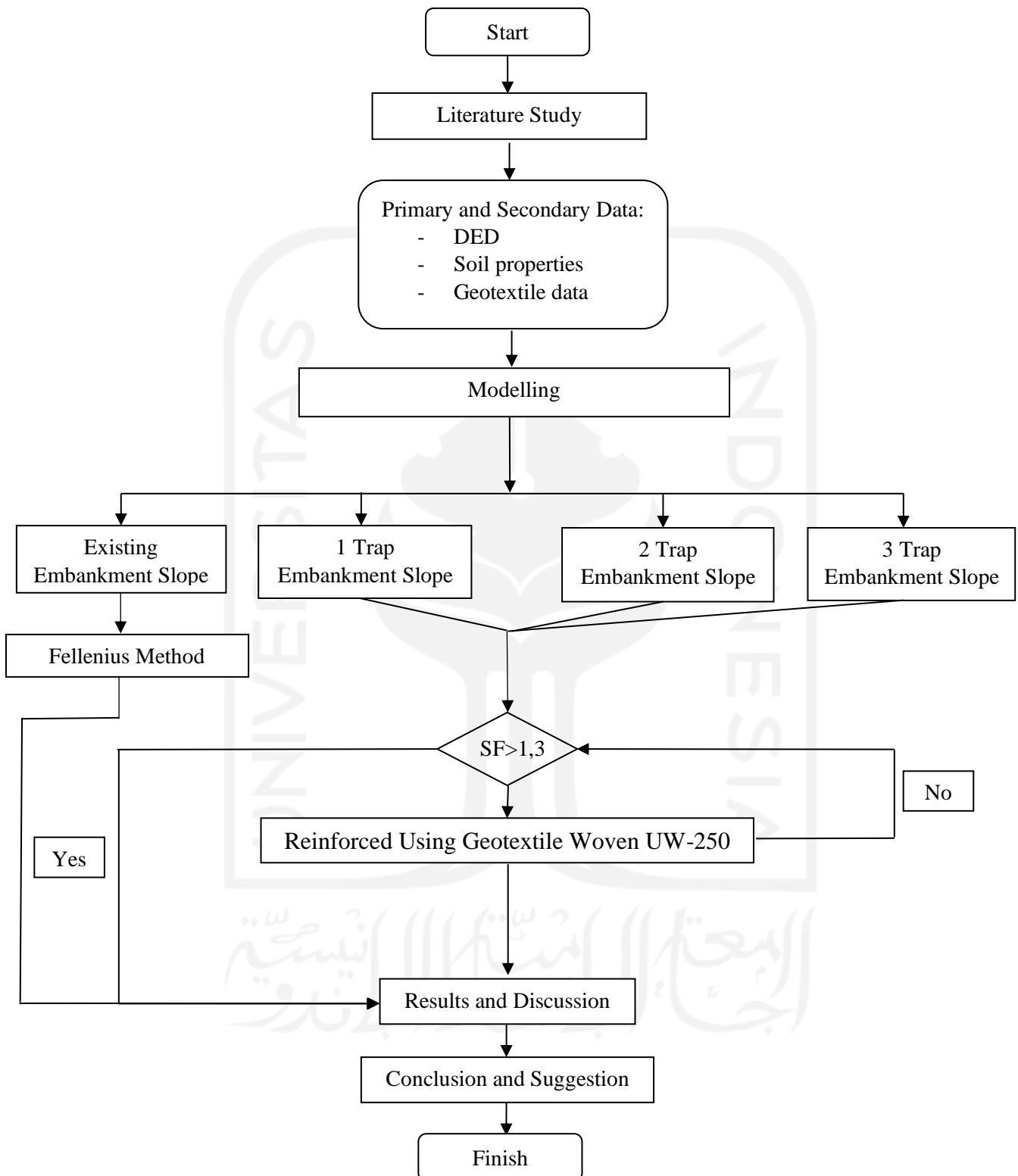


Figure 4.20 Research Steps

CHAPTER V

ANALYSIS AND DISCUSSION

5.1 General Review

Case study that carried out in this research is the condition of the embankments on the Cibitung – Cilincing Toll Road project at STA 7+500. The soil layer at the location is dominated by clay and silt, and the soil layer used is up to third layer with a depth 17.30 meters. While the soil used for embankment is compacted sandy clay. This analysis was carried out to determine the safety factor on the embankment before and after using a trap and reinforced with geotextile that had been determined, whether it experienced a landslide on the slope. The collapse that occurs can be caused because the embankment is no longer able to withstand the forces that occur due to the load when the embankment is about to be used or when the embankment is made.

The analysis was carried out using a variety of traps ranging from 2, 3, and 4 traps. The various embankment of traps is used to determine the safest number of the loads that will occur. The embankment condition will be analysed in two conditions when only using trap variations and after being given geotextile reinforcement.

The load parameters used are the structural load of the road pavement and the traffic load on the road. On embankments with safe numbers that do not meet the safety requirements, reinforcement will be carried out using additional geotextiles. Therefore, it is necessary to do an analysis using reinforcement on unsafe embankments, so that it can be seen whether additional geotextiles are able to withstand landslides that occur and increase the safety factor of road slope embankments.

5.1.1. Analysis Data of Finite element method

The condition of the embankments is in accordance with the Cibitung – Cilincing Toll Road project at Sta 7+500. The soil parameters used were based on the results of the soil data laboratory at the Sta 7+500. The following are the soil parameters, working loads, the slope reinforcement used, and the existing condition of the slope that can be seen in Table 5.1 as follows.

1. Soil Parameter Data

Table 5.1 Soil Parameter Data

Name		Silty Clay	Silt	Silt	Clay Sand (Embankment)
Model	-	MC	MC	MC	MC
Type	-	UNDRAINED	UNDRAINED	UNDRAINED	UNDRAINED
γ unsat	kN/m ³	14	18	20	16
γ sat	kN/m ³	16	20	22	19
Kx	m/day	4,500E-03	4,300E-05	4,300E-05	0,1
Ky	m/day	4,500E-03	4,300E-05	4,300E-05	0,1
E	kN/m ³	4000	20000	24000	11000
ν	-	0,30	0,30	0,334	0,30
Cohesion (C)	kN/m ³	10,1043	79,37	85	10
Friction angle (ϕ)	°	8	30	30	25

(Source: PT. Carina Griya Mandiri, 2017)

2. Rigid pavement and traffic loads data

The structural load used is the load from the rigid pavement. Based on the data used as analytical calculation on the Cibitung – Cilincing Toll

Road project, the load of the pavement structure is 10 kN/m^2 . Based on Traffic load guide for stability analysis (Pt T-10-2002-B) in SE PUPR 42/SE/M/201. The road class on this Toll Road is arterial primary roads, so the traffic load is 15 kN/m^2 . The following is traffic load parameter data can be seen in Table 5.2 as follows.

Table 5.2 Traffic Load Parameter Data

Function	System	LHR	Traffic Load (kN/m^2)
Primary	Artery	All	15
	Collector	>10000	15
		<10000	12
Secondary	Artery	>20000	15
		<20000	12
	Collector	>6000	12
		<6000	10
	Local	>500	10
		<500	10

Source: Ministry of Public Works and Public Housing, (2015)

3. Earthquake Load

The earthquake load used in this analysis comes from Ministry Public Works and Public Housing. The earthquake acceleration used in Plaxis program is selected based on the earthquake zoning in the area of Bekasi which has an earthquake peak acceleration (PGA) of $0,3 - 0,4g$. Earthquake data that matches this value is earthquake data in the American Canyon area of California late 2014 which has an earthquake peak acceleration of $0,3938 \text{ g}$. Earthquake interval time used is $3,2$ seconds assuming it has passed the peak.

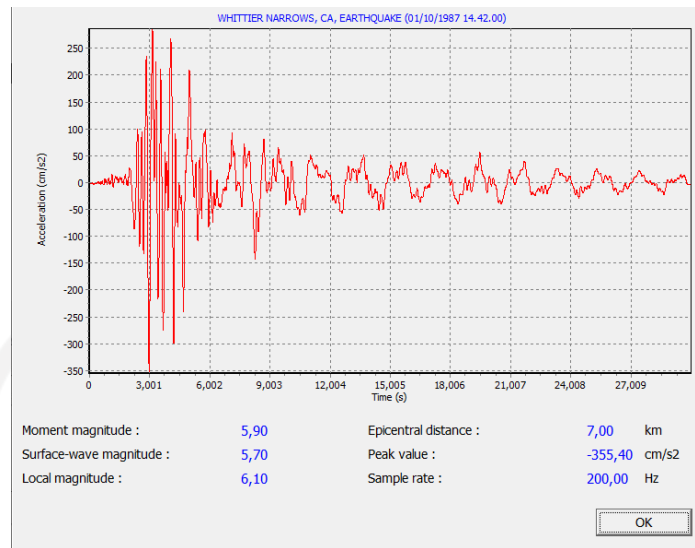


Figure 5.1 Graph of Acceleration and Time of the Whittier Narrows Earth quake

Source: www.usgs.gov, (2018)

4. Geotextile Material Data

The geotextile used is the production of PT. Tekindo Geosistem Unggul with woven type UW 250. The allowable tensile strength and strain values obtained are 52 kN/m². The geotextile values that are used as input into Finite element method can be seen in Table 5.3 below.

Table 5.3 Geotextile Woven UW 250 Parameter

Parameter	Notation	Value	Unit
Tensile Permit	Ta	52	kN/m
Strain	E	20	%
Normal Stiffness	EA	260	kN/m

Source: PT. Tekindo Geosistem Unggul (2020)

5. Existing condition of embankment

Embankment and soil data that has been obtained can be illustrated as follows. The existing condition of the embankment and the existing soil type for each layer can be seen in Figure 5.2 as follows.

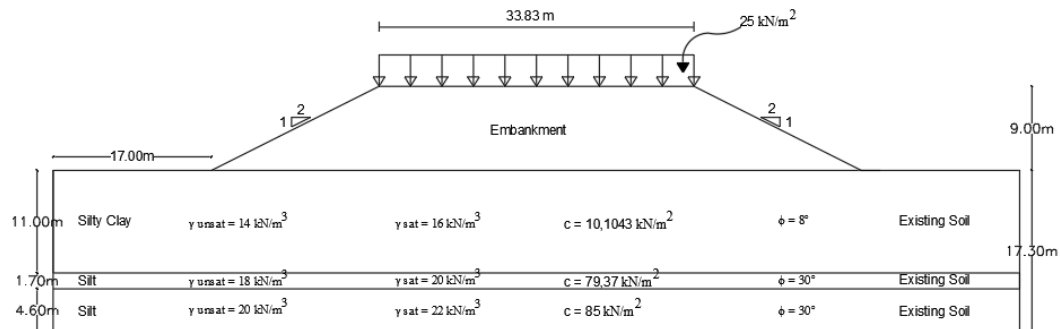


Figure 5.2 Existing Condition of Embankment

5.2 Existing Embankment

5.2.1. Analysis Using Plaxis Program

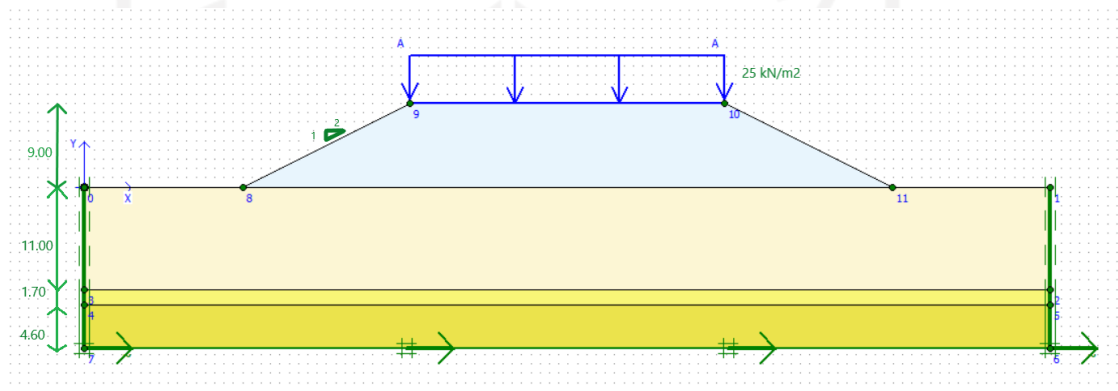
The results of the analysis from the Finite element method that will be displayed in this analysis is the embankments with a height 9 m. The embankment is above the existing soil which consists of 3 layers of soil with a depth of 17,3 m.

1. Initial slope modelling

Slope modelling uses the existing soil at the project site, as well as modelling dynamic earthquake loads and uniform loads. The width of the existing embankment is 69,83 meters. The coordinates that will be input into Plaxis 8.6 can be seen in Table 5.4 and slope modelling can be seen in Figure 5.3 as follows.

Table 5.4 Existing Embankment Coordinates

No.	X (m)	Y (m)
1	86,830	0,00
2	68,830	9,00
3	35,000	9,00
4	17,000	0,00

**Figure 5.3 Modelling of Existing Embankment on Plaxis 8.6**

2. Calculation Analysis of Existing Embankment

The uniform load that used is 25 kN/m^2 due to load from the pavement structure and the traffic load on the road. Thus, do the arrangement of the element network (meshing), after input the soil and material parameters in the embankment modelling. The results of the finite element network (meshing) on the embankment can be seen in Figure 5.4 as follows.

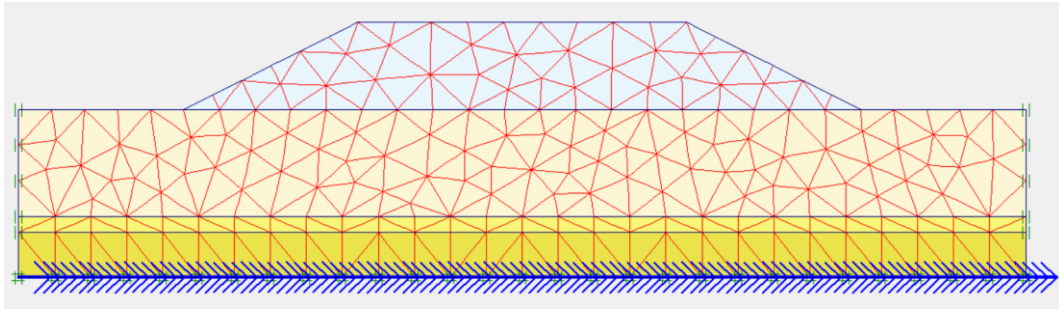


Figure 5.4 Meshing on Existing Embankment

After meshing is complete, it will continue with the initial condition. Then proceed with the initial geometric configuration directly with the calculation of general initial stresses. The results of generating initial stresses as follows.

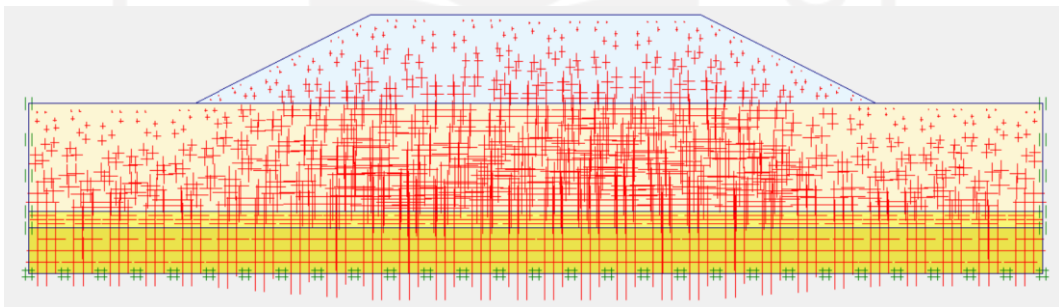


Figure 5.5 Initial Soil Stresses on Existing Embankments

In the next stage, the calculation analysis for the existing embankment 9 m. Firstly, analysed the calculation of the existing embankment. Secondly, analysed the calculation due to load of the road pavement structure, traffic load, and earthquake load on the embankment. The next stage is the calculation of the safety factor based on the due to the load given before. The results of the deformed mesh on the embankment can be seen in Figure 5.6 and Figure 5.7 as follows.

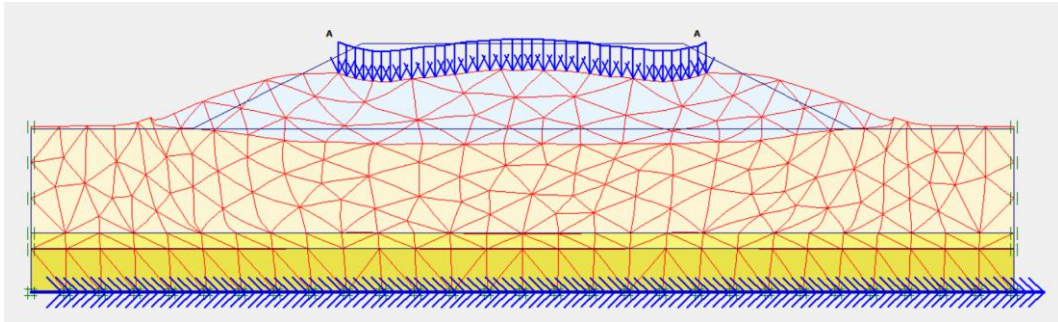


Figure 5.6 Deformed Mesh of Existing Embankment Due to Traffic Load

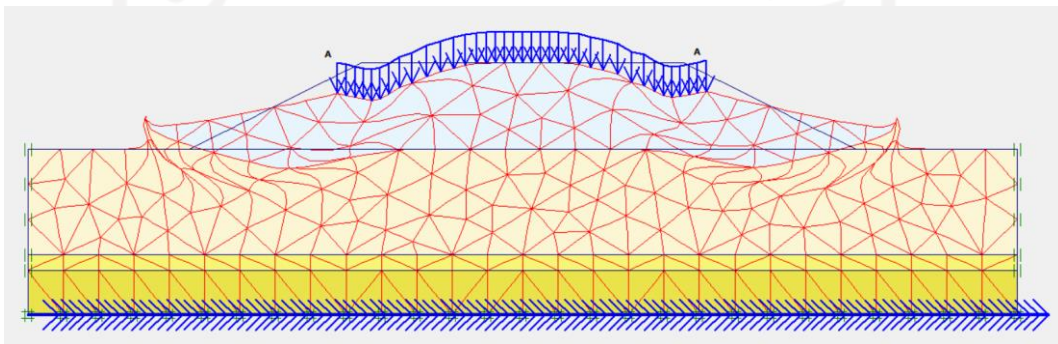


Figure 5.7 Deformed Mesh of Existing Embankment Due to Traffic and Earthquake Load

In embankments that are loaded with pavement structures, traffic load and earthquake load, displacement occurs in the right and left side of the slope embankment. The total displacement value that occurs in the embankment due to traffic load is $258,84 \times 10^{-3}$ m, while the total displacement value due to traffic and earthquake load is $357,52 \times 10^{-3}$ m. The total displacement that occurs can be seen in Figure 5.8 as follows.

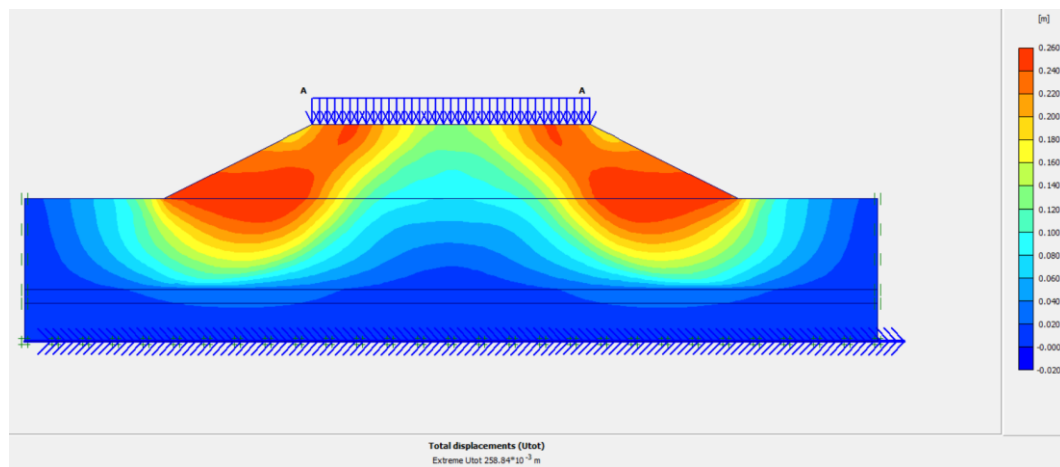


Figure 5.8 Total Displacement of Existing Embankment Due to Traffic Load

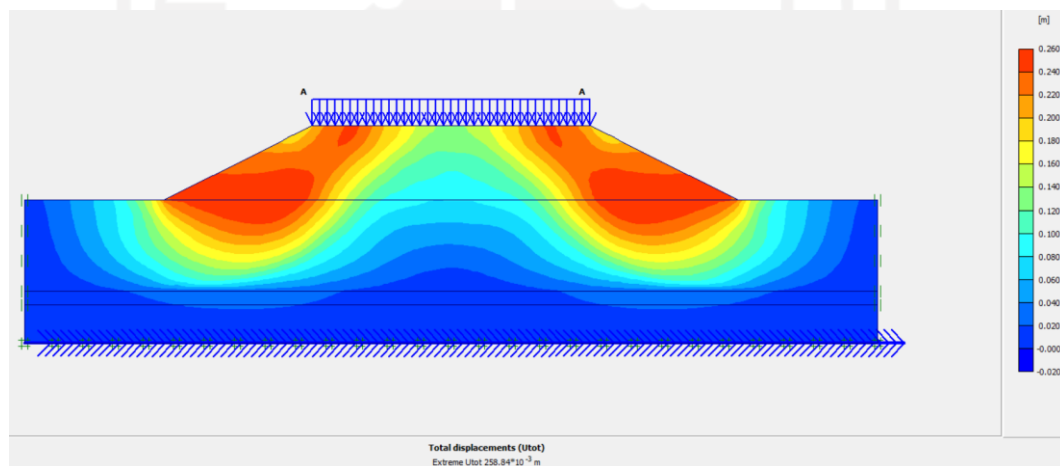


Figure 5.9 Total Displacement of Existing Embankment Due to Traffic and Earthquake Load

المعهد الوطني للبحوث والدراسات
البيئية والهندسية

The results of the direction movement of the existing embankment due to the traffic load can be seen in Figure 5.10 and direction movement of existing embankment due to the traffic load and earthquake load can be seen in Figure 5.11 as follows.

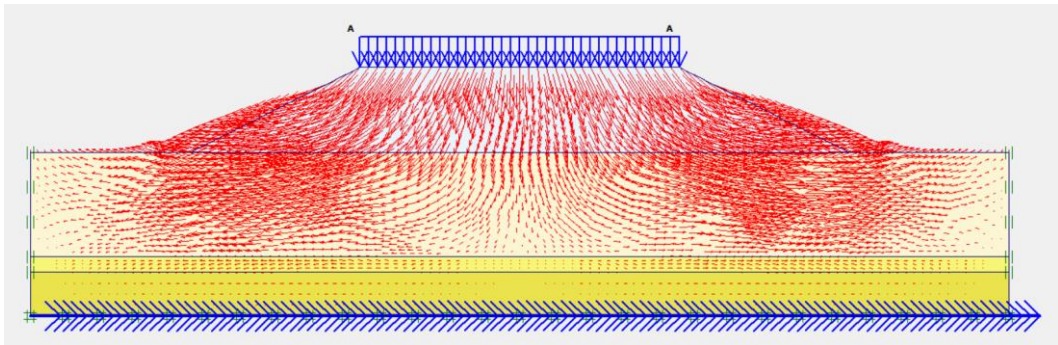


Figure 5.10 Direction Movement of Embankment Due to Traffic Load

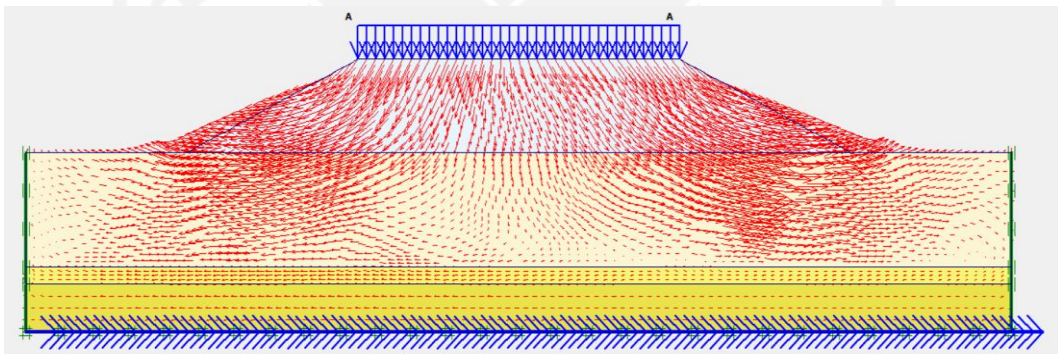


Figure 5.11 Direction Movement of Embankment Due to Traffic and Earthquake Load

The results of the analysis Plaxis program calculations show that, the more lines gradient that show the direction and magnitude of the effective stress, the lower the line the more visible the lines. The value of the effective stresses on the embankments due to traffic loads is $-419,02 \text{ kN/m}^2$, while due to traffic and earthquake load is $-428,24 \text{ kN/m}^2$. These results can be seen in Figure 5.12 and 5.13 as follows.

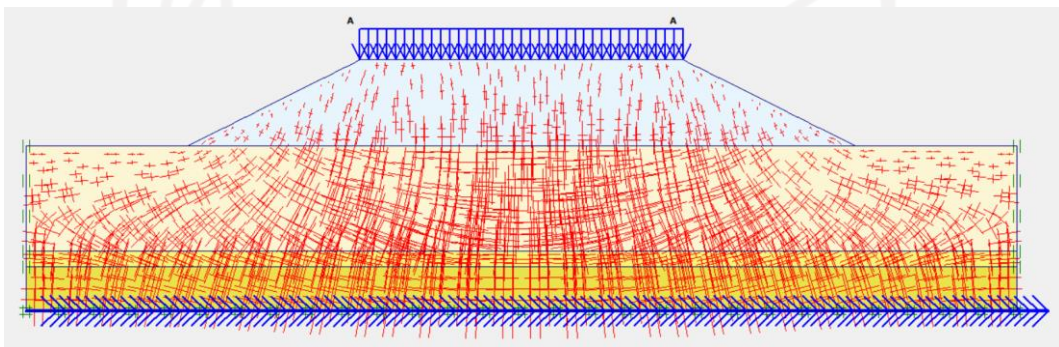


Figure 5.12 Effective Stresses of Existing Slope Embankment Due to Traffic Load

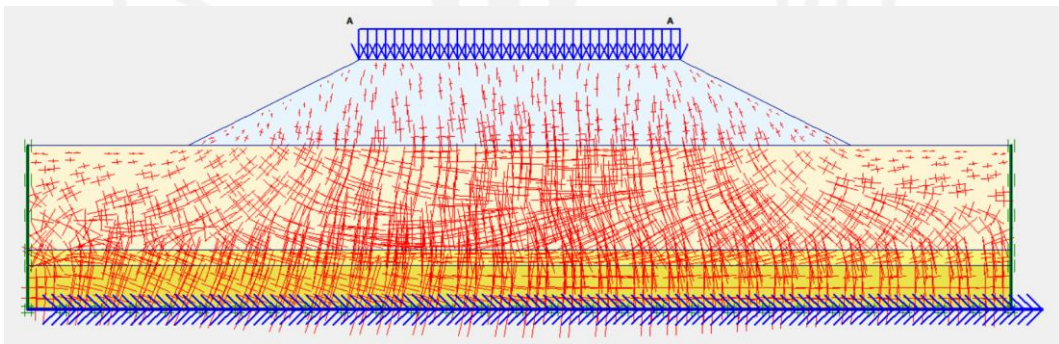


Figure 5.13 Effective Stresses of Existing Embankment Due to Traffic and Earthquake Load

Therefore, the potential for landslide on the existing embankment can be seen in Figure 5.14 and Figure 5.15 as follows.

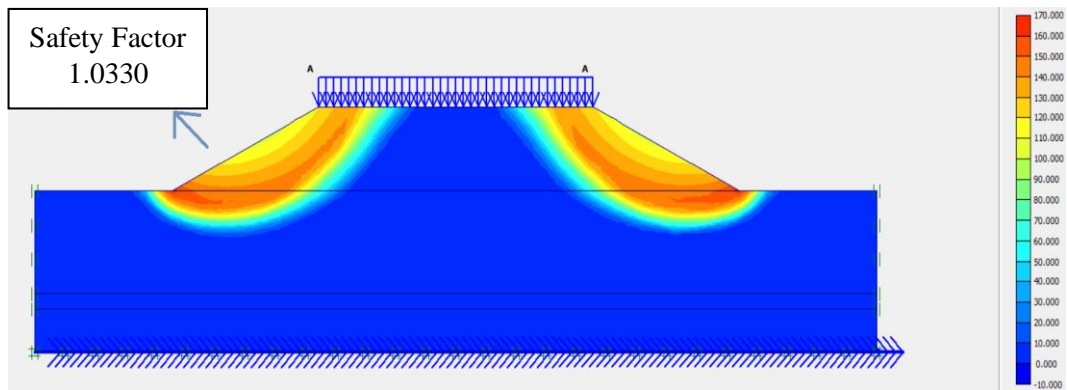


Figure 5.14 Potential Landslides of Embankment Due to Traffic Load

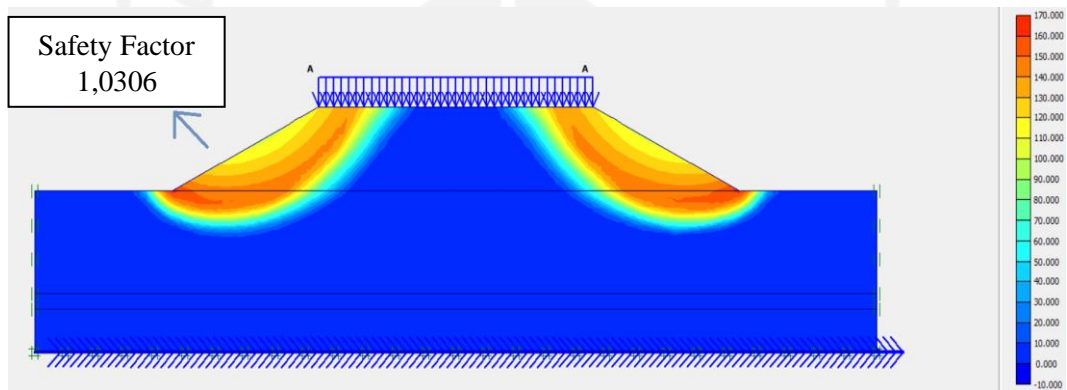


Figure 5.15 Potential Landslides of Embankment Due to Traffic Load and Earthquake Load

The safety factor (SF) of the existing embankment that obtained from the analysis results due to traffic load is 1,0330 while the safety factor due to traffic and earthquake load is 1,0306. The results of the safety factor value can be seen in Figure 5.16 as follows.

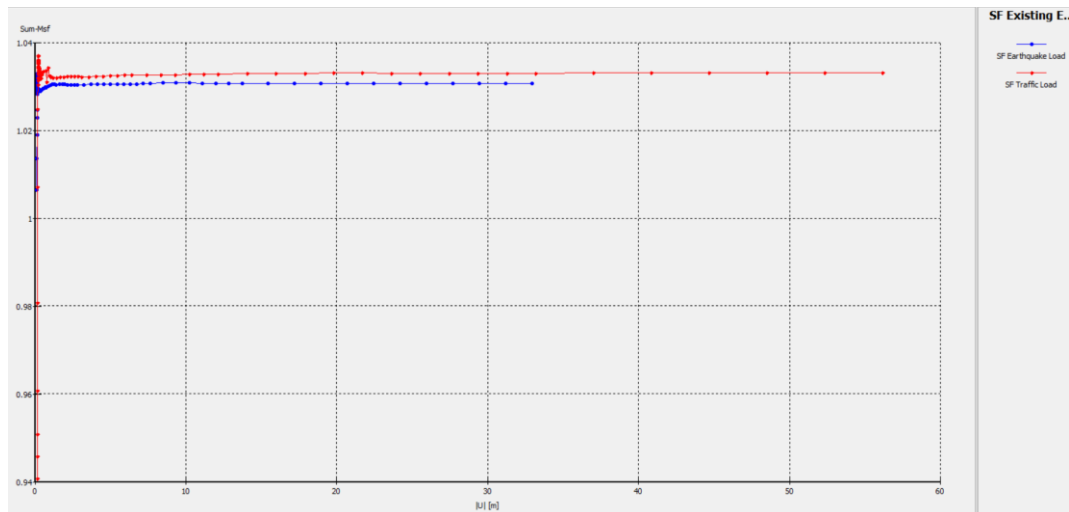


Figure 5.16 SF Curve of Existing Embankment

5.3 Fellenius Calculation Method

Since the analysis using Finite element method on the embankment did not show a safe value according to the safety requirement for road slope embankments, then manual calculations with the fellenius method were used to compare the slope safety values. From the plaxis program, the landslide potential line is shown Figure 5.15 From the figure, it can be seen that the landslide potential line is formed up to the bottom of the slope with a Radius of 24,03 m and in this calculation, it will be divided into 11 slices. The figure of each slice on the embankment can be seen in Figure 5.17 as follows.

$$W_{11} = (\gamma \times A_{11}) + (q \times L) = (16 \times 8,602) + (25 \times 3,22) = 218,132 \text{ kN}$$

3. Measure the size of the angle (α) and radians of each slice on the landslide plane. The recapitulation of the angle in the landslide plane for each slice can be seen in Table 5.6 as follows.

$$\begin{aligned} \text{Rad}_1 &= \alpha \times \frac{\pi}{180} \\ &= -31 \times \frac{\pi}{180} \\ &= -0,54105 \end{aligned}$$

$$\begin{aligned} \text{Rad}_{11} &= \alpha \times \frac{\pi}{180} \\ &= 56 \times \frac{\pi}{180} \\ &= 0,977384 \end{aligned}$$

4. Calculating $W \sin \alpha$ value each slice

$$\begin{aligned} \text{Slice 1} &= W \times \sin \alpha \\ &= 57,294 \times \sin -0,54105 \\ &= -29,508 \text{ kN/m} \end{aligned}$$

$$\begin{aligned} \text{Slice 11} &= W \times \sin \alpha \\ &= 218,132 \times \sin 0,977384 \\ &= 180,839 \text{ kN/m} \end{aligned}$$

Recapitulation from the calculation results $W \sin \alpha$ for every slice can be seen on the Table 5.6 as follows.

5. Calculating $W \cos \alpha$ value each slice

$$\begin{aligned} \text{Slice 1} &= W \times \cos \alpha \\ &= 57,294 \times \cos -0,54105 \\ &= 49,110 \text{ kN/m} \end{aligned}$$

$$\begin{aligned} \text{Slice 11} &= W \times \cos \alpha \\ &= 218,132 \times \cos 0,977384 \\ &= 121,977 \text{ kN/m} \end{aligned}$$

Recapitulation from the calculation results $W \cos \alpha$ for every slice can be seen on the Table 5.6 as follows.

Based on the measurement results of the existing embankment geometry, the length of the curved line on layer 1 (A-B) is 29,46 m, and the length of the curved line on layer 2 (B-C) is 11,97 m. After the length of the curved line is known, it is continued by calculating the value of the sliding resistance deployed by the cohesion component as follows.

$$\begin{aligned}\Sigma c_i a_i &= (10 \times 29,46) + (10,1043 \times 11,97) \\ &= 415,5484 \text{ kN}\end{aligned}$$

The value of the landslide resistance by the friction component in the two layers is as follows.

$$\begin{aligned}W_i \cos \theta - U_i \times \tan \varphi &= (1879,011 \times \tan 25) + (2056,860 \times \tan 8) \\ &= 1165,270 \text{ kN}\end{aligned}$$

On the embankment there is a distributed load resulting from traffic loads of 25 kN/m².

$$\begin{aligned}M_q &= (q \times A) \\ &= (25 \times 17,595) \\ &= 439,875 \text{ kN}\end{aligned}$$

The recapitulation of results of manual calculation using Fellenius method can be seen in Table 5.5 as follows.

Table 5.5 Calculation Recapitulation Using Fellenius Method

Slice No	Soil Layer	Area (m²)	Weight Wi (kN)	θ (°)	Radian	Wi.cos θ (kN)	Wi.sin θ (kN)	Wi.cos θ_i - Ui (kN)
1	2	3,183	57,294	-31	-0,54105	49,110	-29,508	49,110
2	2	8,537	153,666	-22	-0,38397	142,476	-57,564	142,4766
3	1	2,421	38,736	-14	-0,24435	191,656	-47,785	191,6566
	2	11,342	158,788					
4	1	7,612	121,792	-6	-0,10472	310,105	-32,593	310,1058
	2	13,573	190,022					
5	1	12,806	204,896	1	0,017453	401,100	7,001	401,1009
	2	14,019	196,266					
6	1	18	288	9	0,15708	465,043	73,655	465,0431
	2	13,06	182,84					
7	1	23,194	371,104	17	0,296706	497,366	152,060	497,3664
	2	10,642	148,988					
8	1	28,058	533,178	25	0,436332	567,296	264,534	567,2961
	2	6,626	92,764					
9	1	28,368	453,888	34	0,593412	390,693	263,526	390,6939
	2	1,241	17,374					
10	1	21,18	419,38	44	0,767945	301,676	291,325	301,6767
11	1	8,602	218,132	56	0,977384	121,977	180,839	121,9778
TOTAL						3538,5048	1065,4916	

6. Calculating Safety Factor (SF) value

The value of the safety factor on the existing embankment with manual calculations using Fellenius method are as follows.

$$\begin{aligned} SF &= \frac{(\sum c_i \alpha_i) + ((W_i \cos \theta - U_i) \times \tan \varphi)}{(W_i \sin \alpha) + (\text{Load} \times \text{Area})} \\ &= \frac{(415,548) + (1165,270)}{(1065,491) + (422,875)} \\ &= 1,0621 \end{aligned}$$

The value of the safety factor conducted by the existing embankment by the Fellenius method is 1,0621. These results are not much different from the results of the analysis of existing embankment without geometry variation using Plaxis 8.6 which is 1,0306.

5.4 Calculation Analysis Embankment with Topography Variation

Stability of embankment in this sub-part is adding the geometric variation, by adding traps to the embankment up to 3 traps as follows.

5.4.1. Embankment With 1 Trap Variation

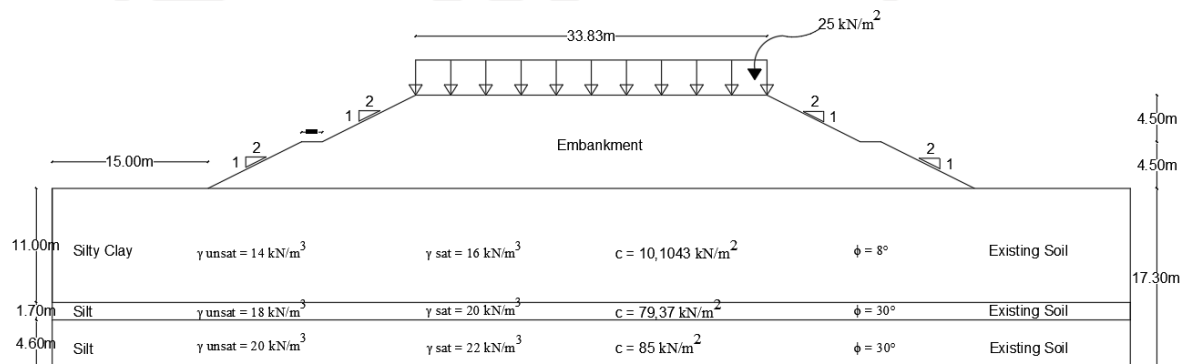


Figure 5.18 Embankment 1 Trap

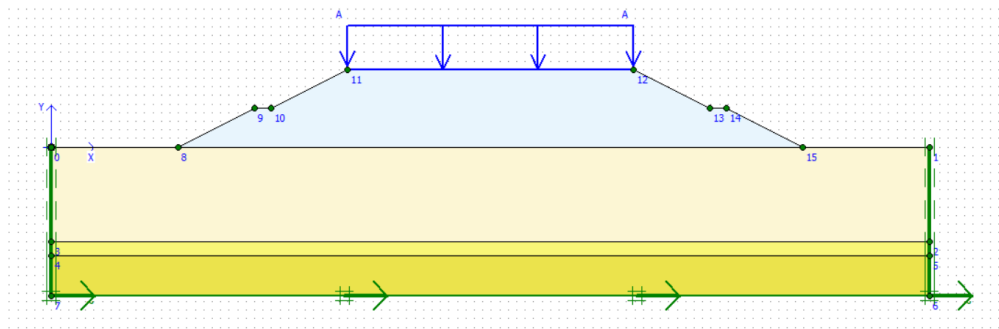


Figure 5.19 Modelling 1 Trap Embankment

In this next following stage is same as the previous part, thus it enters the calculation analysis stage for the embankment with 1 trap variations. The first stage is an analysis of the calculation due to structural load, traffic load and earthquake load on the embankment. The second stage is the calculation of the safety factor due to the load given before. Then the next stage is the calculation of the consolidation of the soil. The results of the embankment can be seen in Figure 5.20 and Figure 5.21 as follows.

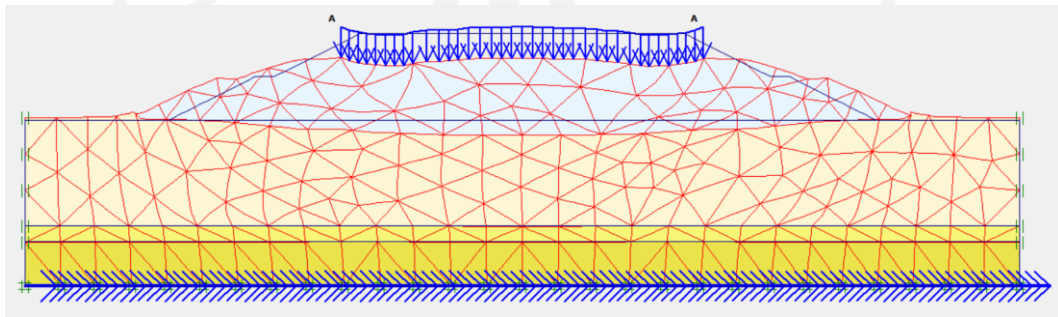


Figure 5.20 Deformed Mesh of Embankment Due to Traffic Load 1 Trap

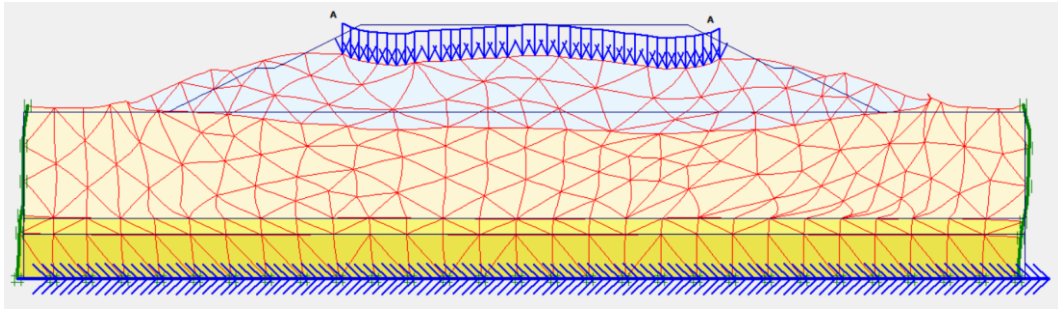


Figure 5.21 Deformed Mesh of Embankment Due Traffic and Earthquake Load 1 Trap

In embankment with variation of 1 trap that are loaded with pavement structures, traffic load and earthquake load. In embankment the total displacement due to the traffic load is $214,34 \times 10^{-3}$ m, while the total displacement due to traffic load and earthquake load is $301,60 \times 10^{-3}$ m. The total displacement that occurs on the embankment with 1 trap variations can be seen in Figure 5.22 and Figure 5.23 as follows.

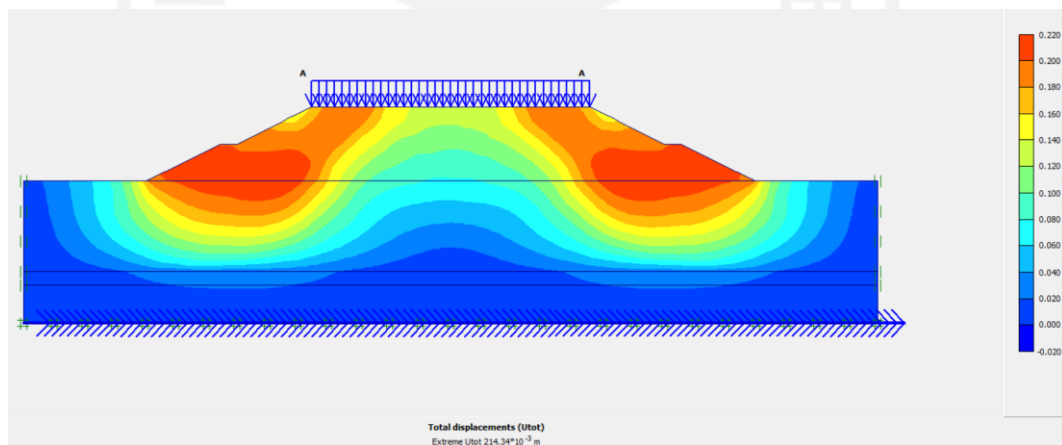


Figure 5.22 Total Displacement of Embankment 1 Trap Due to Traffic Load

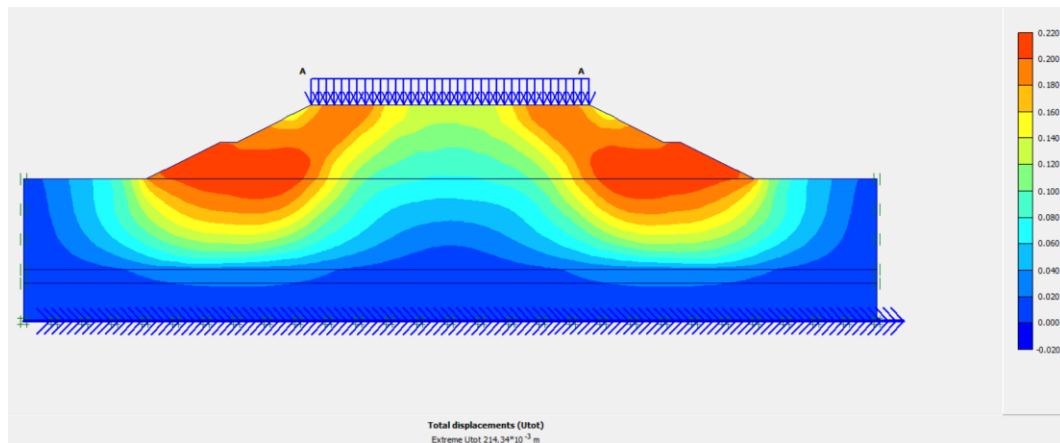


Figure 5.23 Total Displacement of Embankment 1 Trap Due to Traffic Load and Earthquake Load

The results of the soil movement of the Embankment with 1 trap variations due to the structure road pavement load, traffic load and earthquake load can be seen in Figure 5.24 and Figure 5.25 as follows.

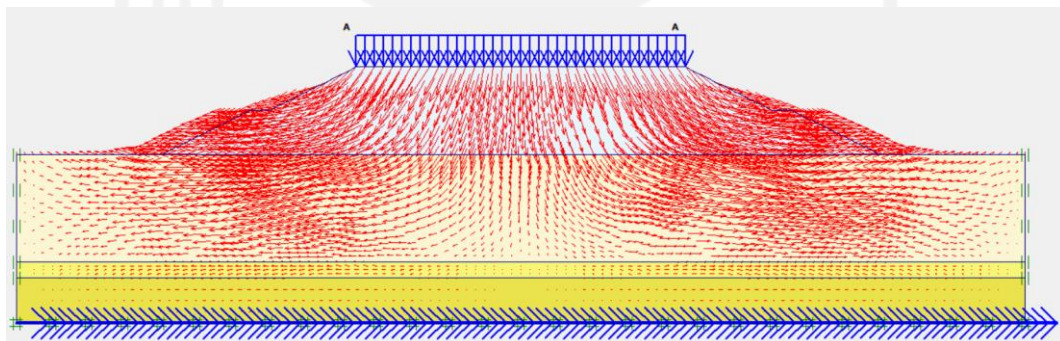


Figure 5.24 Soil Movement of Embankment 1 Trap Due to Traffic Load

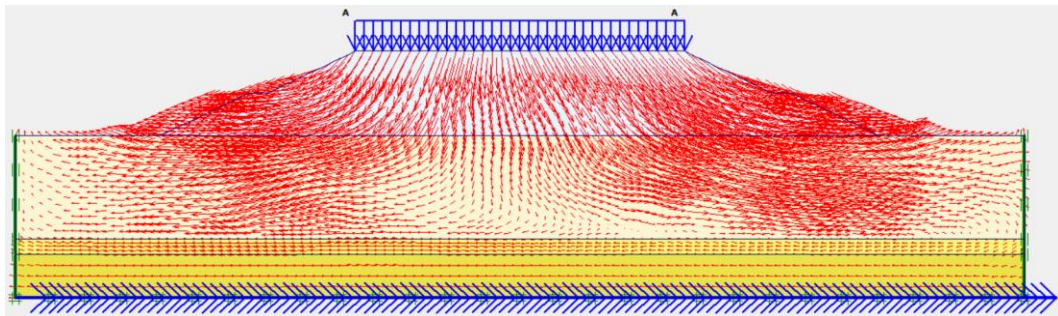


Figure 5.25 Soil Movement of Embankment 1 Trap Due to Traffic Load and Earthquake Load

The results for the effective stresses on the embankment with 1 trap variations due to traffic load is $-419,01 \text{ kN/m}^2$ while the value for the effective stresses due to traffic load and earthquake load is $-426,96 \text{ kN/m}^2$. The results can be seen in Figure 5.26 and Figure 5.27 as follows.

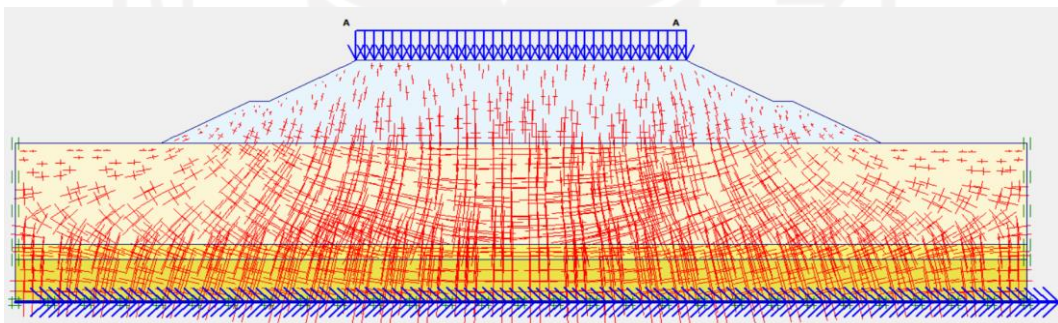


Figure 5.26 Effective Stresses of Embankment 1 Trap Due to Traffic Load

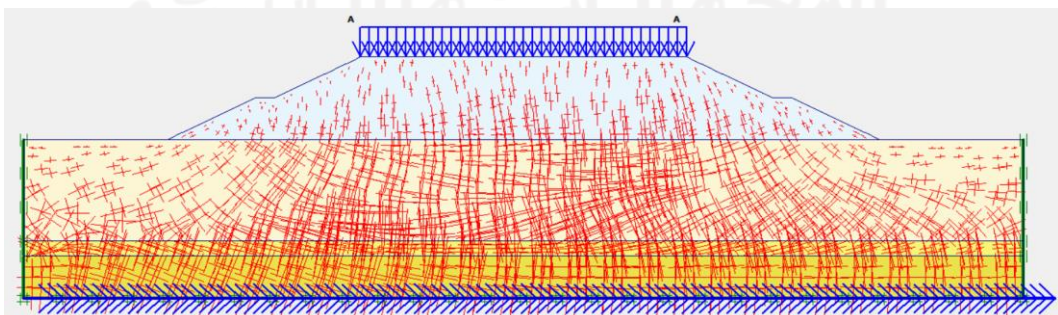


Figure 5.27 Effective Stresses of Embankment 1 Trap Due to Traffic and Earthquake Load

Therefore, the potential for landslide on the embankment with 1 trap variations can be seen in Figure 5.28 and Figure 5.29 as follows.

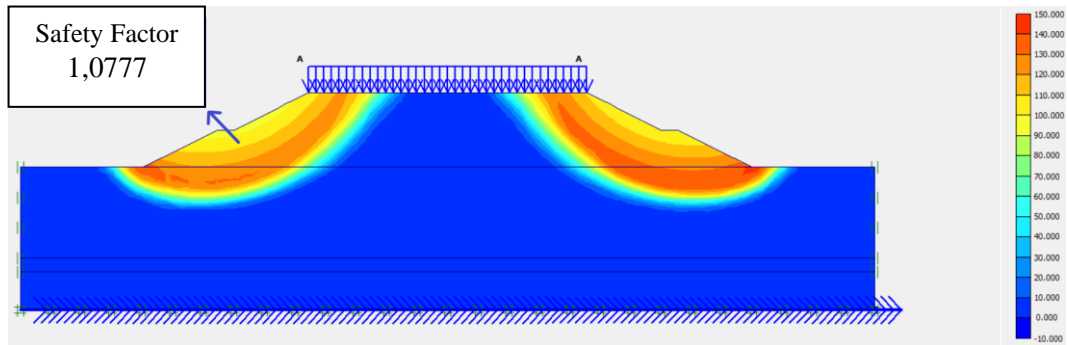


Figure 5.28 Potential Landslides of Embankment 1 Trap Due to Traffic Load

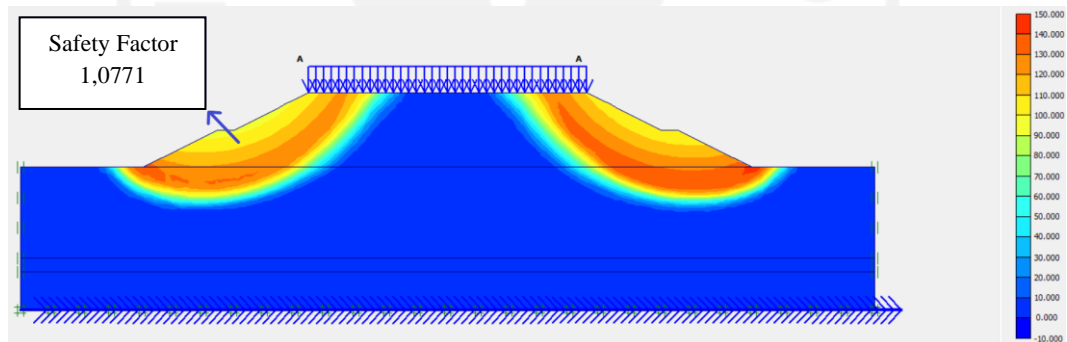


Figure 5.29 Potential Landslides of Embankment 1 Trap Due to Traffic Load and Earthquake Load

The safety factor (SF) of the embankment with 1 trap variation that obtained from the analysis results due to traffic load is 1,07777 while the safety factor due to traffic load and earthquake load is 1,0771. The results of the safety factor value can be seen in Figure 5.30 as follows.

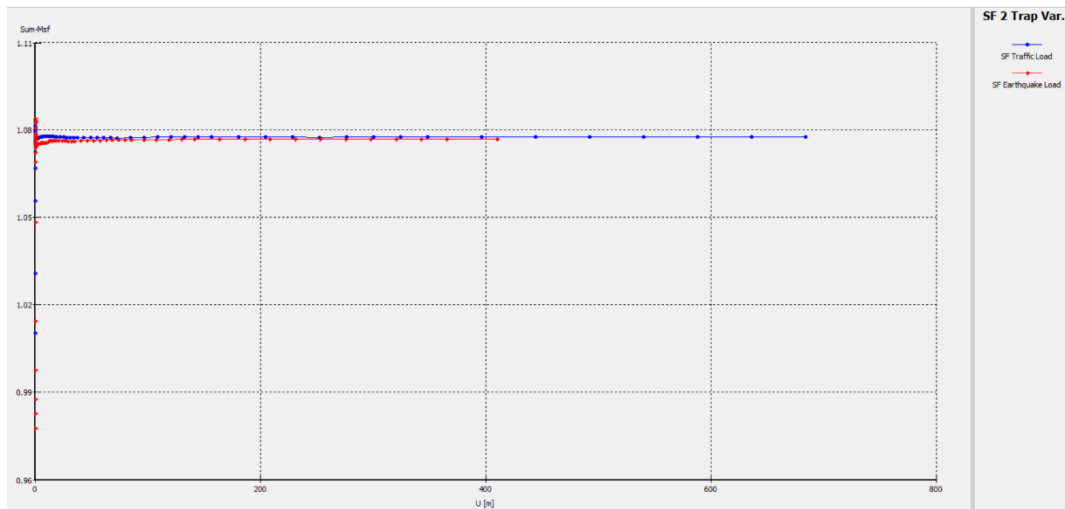


Figure 5.30 SF Curve of Embankment 1 Trap

5.4.2. Embankment with 2 Trap Variation

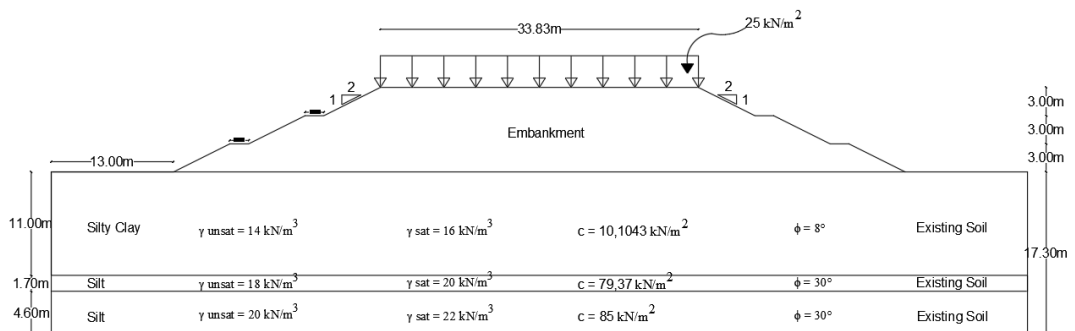


Figure 5.31 Embankment 2 Trap

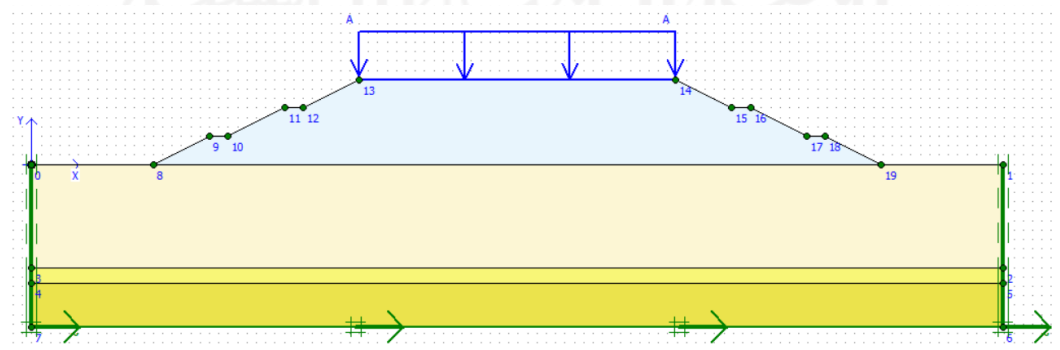


Figure 5.32 Modelling of Embankment 2 Trap

The next stage is adding the variation of trap with embankment with 2 trap variations. The following stage is same as the stage before. The first stage is an analysis of the calculation due to structural load, traffic load and earthquake load on the embankment. The second stage is the calculation of the safety factor due to load given before. Then the next is the calculation of the consolidation of the soil. The results of the embankment with 2 trap variations can be seen in Figure 5.33 and Figure 5.34 as follows.

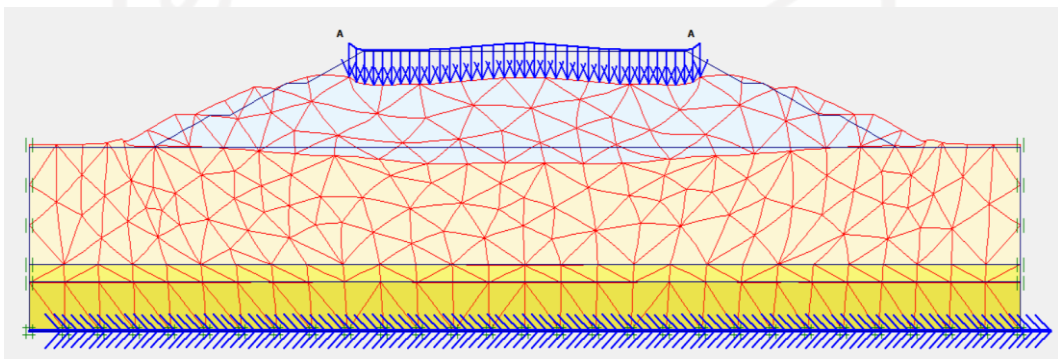


Figure 5.33 Deformed Mesh of Embankment 2 Trap Due to Traffic Load

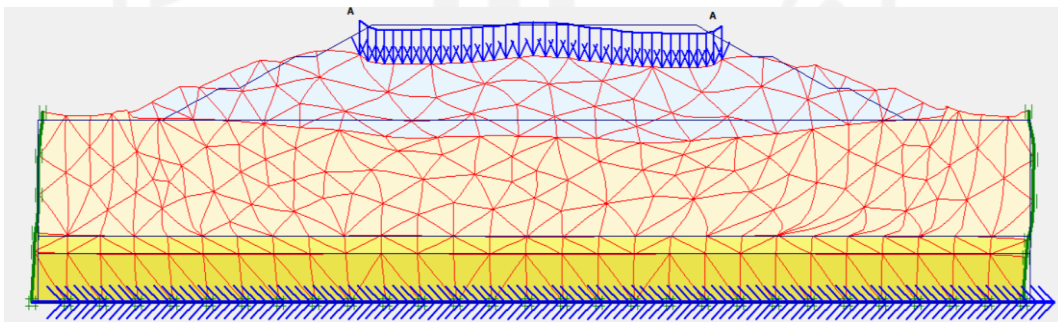


Figure 5.34 Deformed Mesh of Embankment 2 Trap Due to Traffic Load and Earthquake Load

In embankment with 2 trap variation that are loaded with traffic load the total displacement is $190,40 \times 10^{-3}$ m, while the total displacement due to traffic load and earthquake load is $260,40 \times 10^{-3}$ m.

The total displacement that occurs on the embankment with 2 trap variations can be seen in Figure 5.35 and Figure 5.36 as follows.

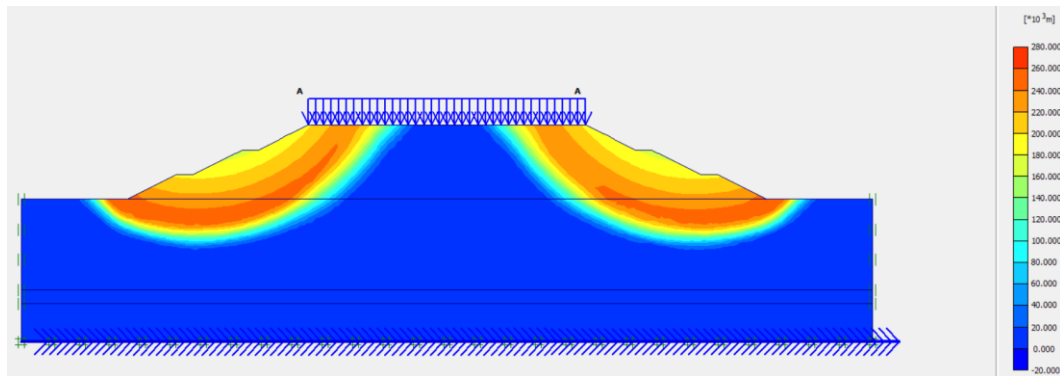


Figure 5.35 Total Displacement of Embankment 2 Trap Due to Traffic Load

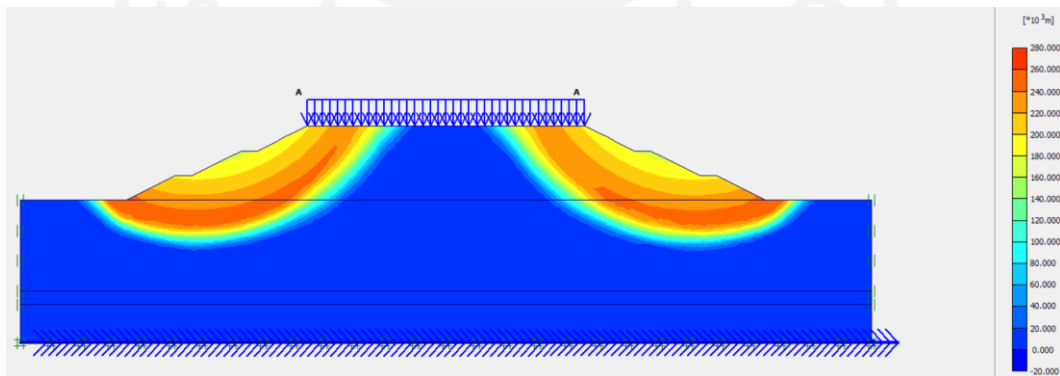


Figure 5.36 Total Displacement of Embankment 2 Trap Due to Traffic Load and Earthquake Load

The results of the soil movement of the embankment with 2 trap variations due to traffic load and earthquake load can be seen in Figure 5.37 and Figure 5.38 as follows.

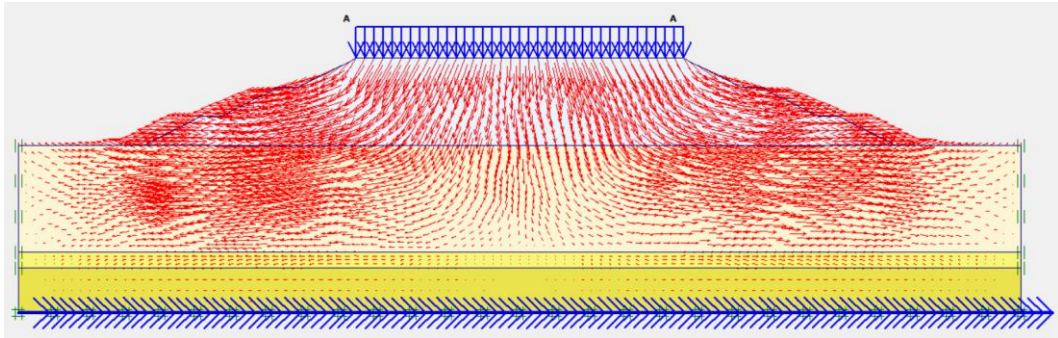


Figure 5.37 Soil Movement Embankment 2 Trap Due to Traffic Load

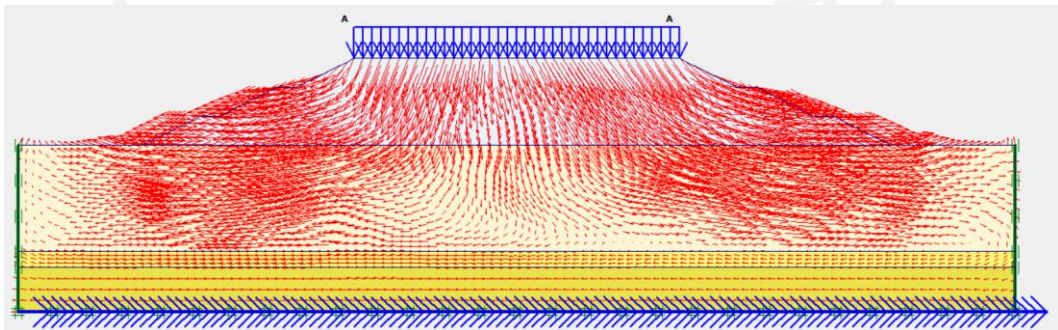


Figure 5.38 Soil Movement Embankment 2 Trap Due to Traffic Load and Earthquake Load

The results for the effective stresses on the embankment with 2 trap variations due to traffic load is $-420,218 \text{ kN/m}^2$ while the value for the effective stresses due to traffic load and earthquake load is $-425,74 \text{ kN/m}^2$. The results can be seen in Figure 5.39 and Figure 5.40 as follows.

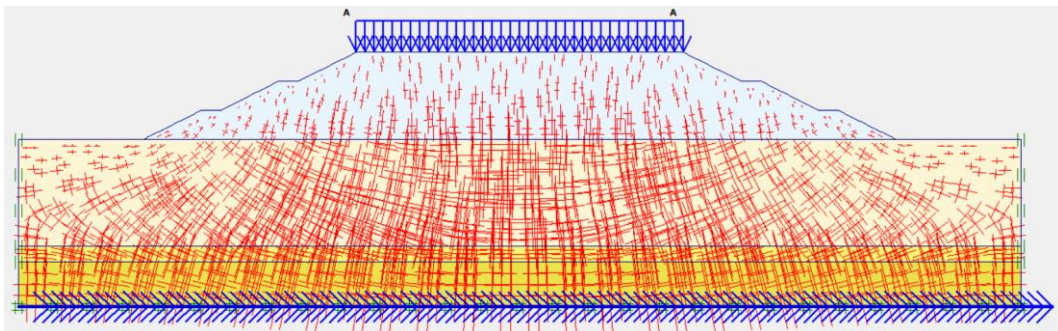


Figure 5.39 Effective Stresses of Embankment 2 Trap Due to Traffic Load

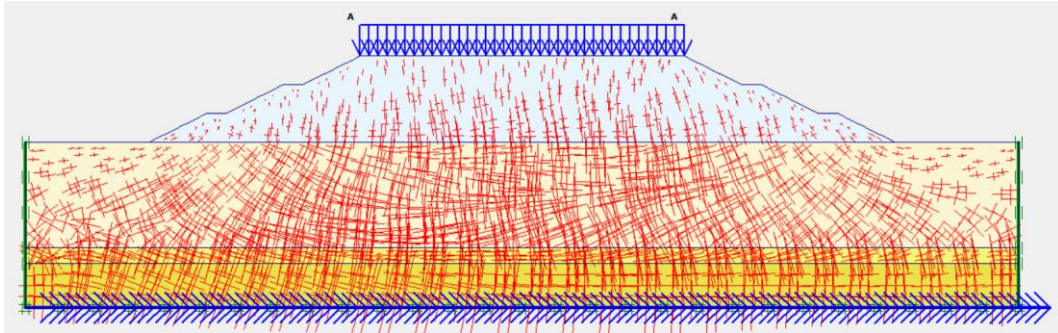


Figure 5.40 Effective Stresses of Embankment 2 Trap Due to Traffic Load and Earthquake Load

The results of the soil movement of the embankment with 2 trap variations due to the traffic load and earthquake load can be seen in Figure 5.41 and Figure 5.42 as follows.

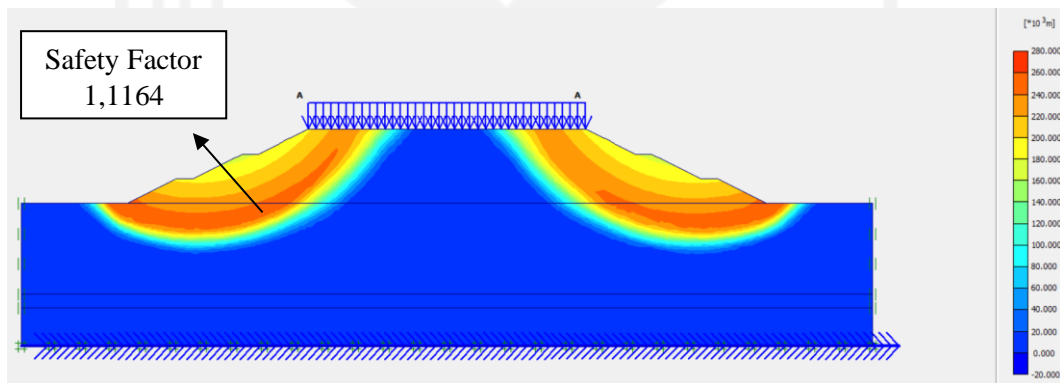


Figure 5.41 Potential Landslides of Embankment 2 Trap Due to Traffic load

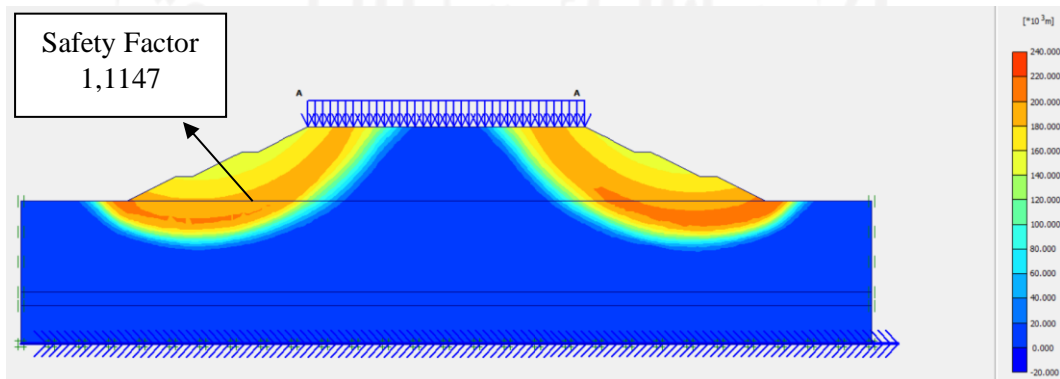


Figure 5.42 Potential Landslides of Embankment 2 Trap Due to Traffic Load and Earthquake Load

The safety factor (SF) of the embankment with 2 trap variation that obtained from the analysis results due to traffic load is 1,1164 while the safety factor (SF) due to traffic load and earthquake load is 1,1147.

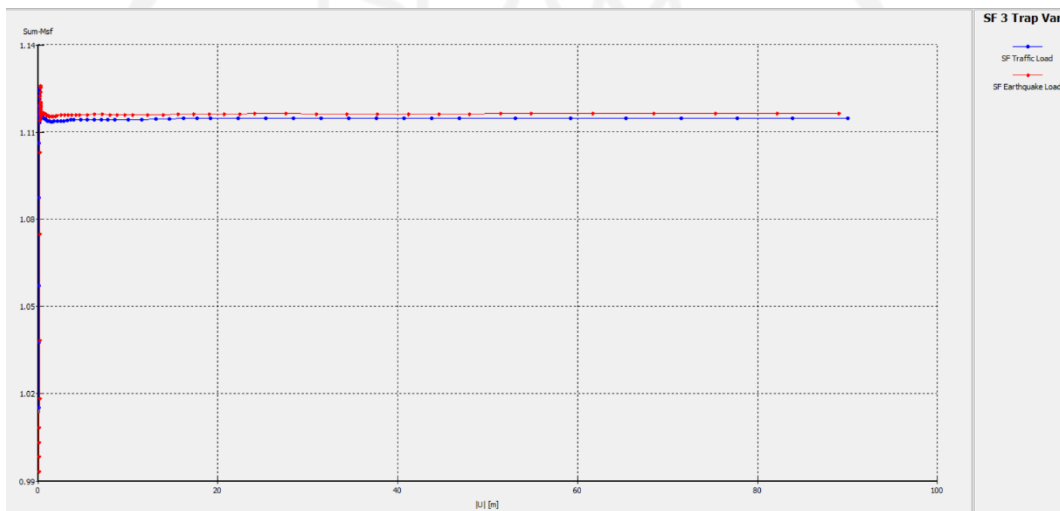


Figure 5.43 SF Curve of Embankment 2 Trap

5.4.3. Embankment with 3 Trap Variation

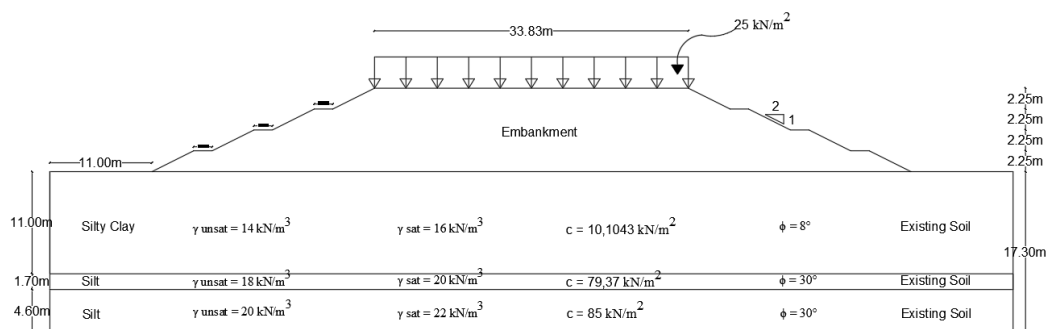


Figure 5.44 Embankment 3 Trap

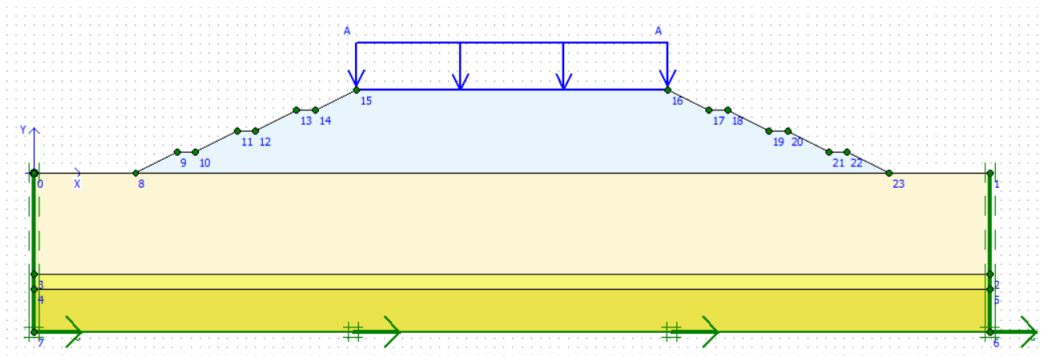


Figure 5.45 Modelling of Embankment 3 Trap

This embankment with 3 trap variations is the addition of geometry variation from the embankment with 2 traps before. The following stage is same as the stage before. The first stage is an analysis of the calculation due to traffic load and earthquake load on the embankment.

The second stage is the calculation of the safety factor due to load given before. Then the next is the calculation of the consolidation of the soil. The results of the embankment with 3 trap variations can be seen in Figure 5.46 and Figure 5.47 as follows.

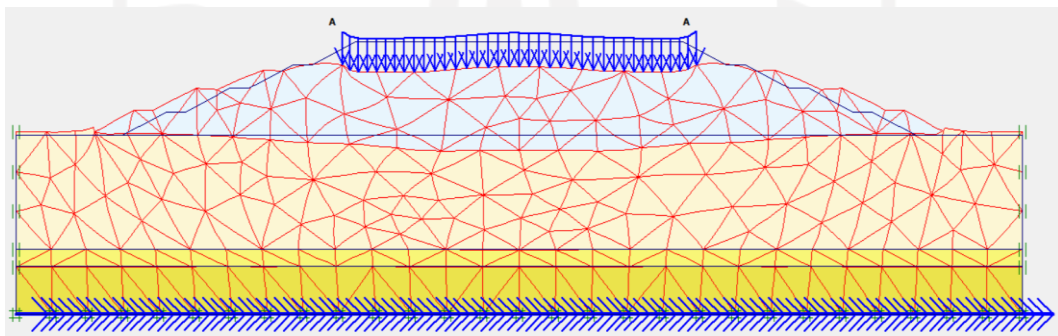


Figure 5.46 Deformed Mesh of Embankment 3 Trap Due to Traffic Load

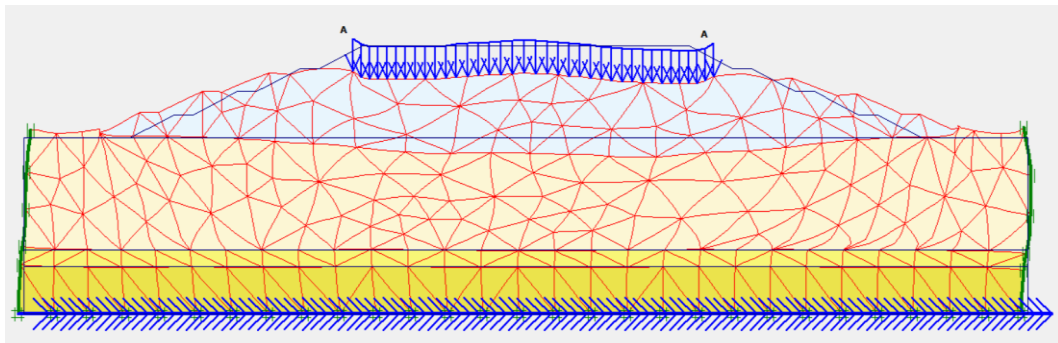


Figure 5.47 Deformed Mesh of Embankment with 3 Trap Due to Traffic and Earthquake Load

In embankment with 3 trap variation that are loaded with traffic load the total displacement is $175,96 \times 10^{-3}$ m, while the total displacement due to traffic load and earthquake load is $234,03 \times 10^{-3}$ m. The total displacement that occurs on the embankment with 3 trap variations can be seen in Figure 5.48 and Figure 5.49 as follows.

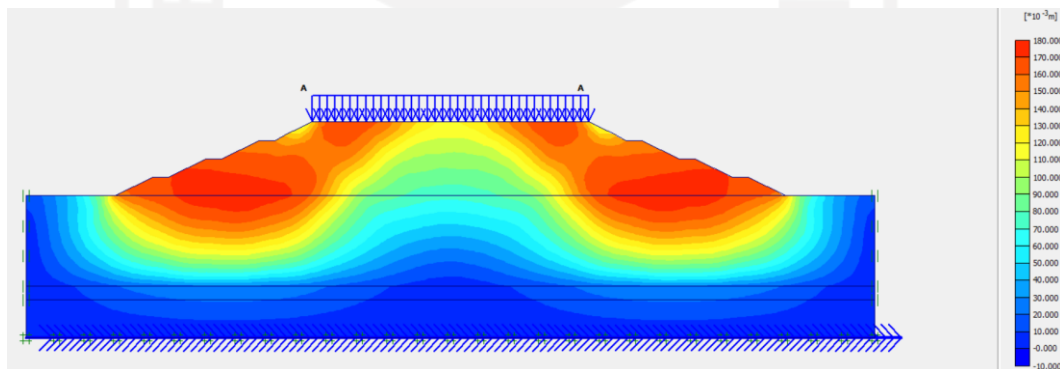


Figure 5.48 Total Displacement of Embankment 3 Trap Due to Traffic Load

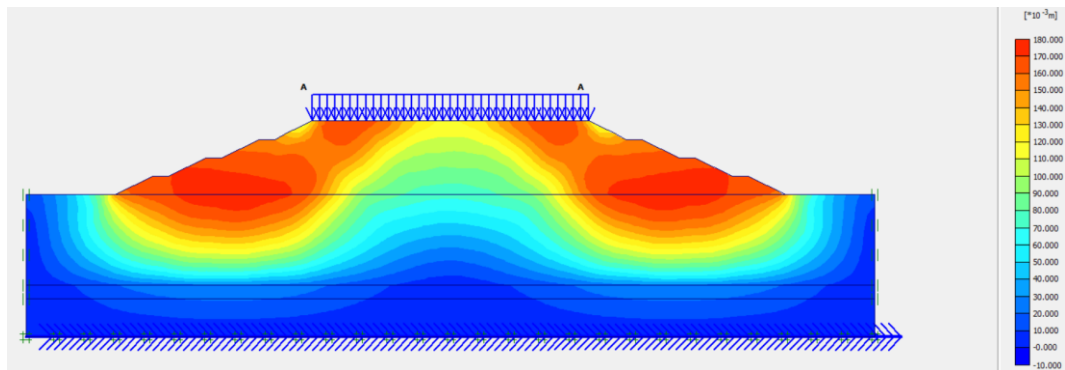


Figure 5.49 Total Displacement of Embankment 3 Trap Due to Traffic and Earthquake Load

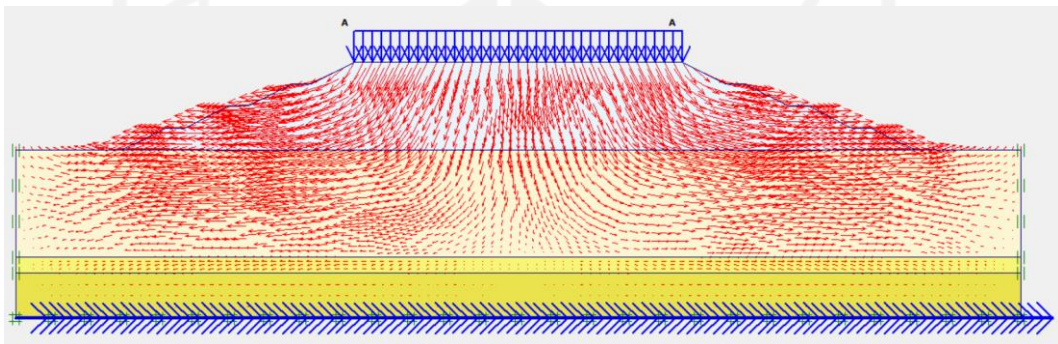


Figure 5.50 Soil Movement of Embankment 3 Trap Due to Traffic Load

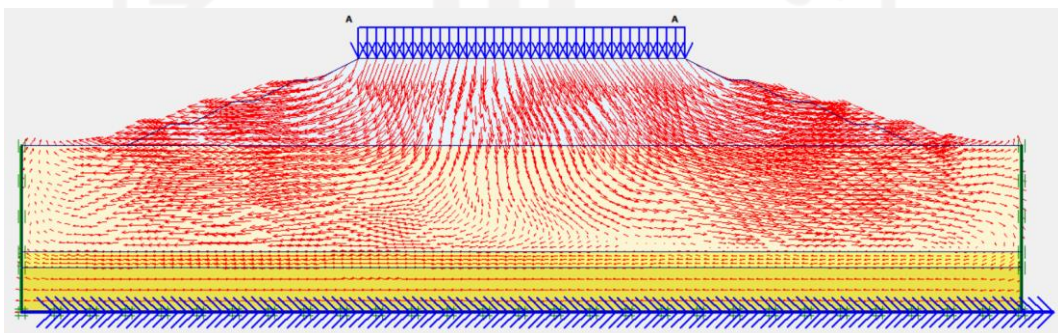


Figure 5.51 Soil Movement of Embankment 3 Trap Due Traffic and Earthquake Load

The results for the effective stresses on the embankment with 3 trap variations due to traffic load is $-420,62 \text{ kN/m}^2$ while the value for the effective stresses due to traffic load and earthquake load is $-426,18 \text{ kN/m}^2$. The results can be seen in Figure 5.52 and Figure 5.53 as follows.

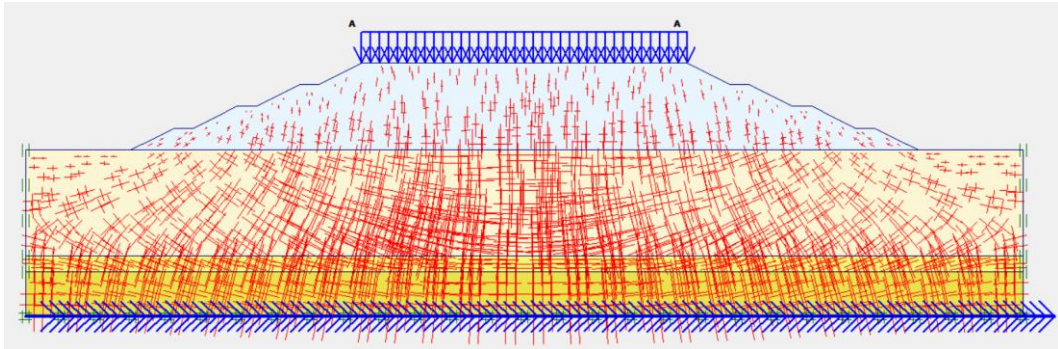


Figure 5.52 Effective Stresses of Embankment 3 Trap Due to Traffic Load

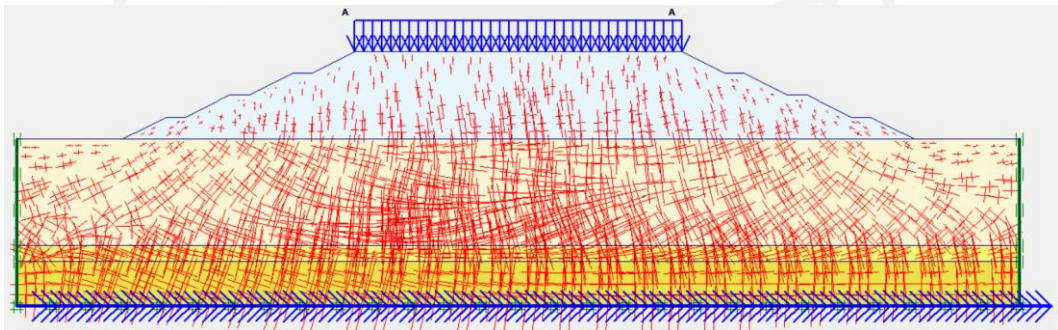


Figure 5.53 Effective Stresses of Embankment 3 Trap Due to Traffic and Earthquake Load

The results of the soil movement of the embankment with 3 trap variations due to traffic load and earthquake load can be seen in Figure 5.54 and Figure 5.55 as follows.

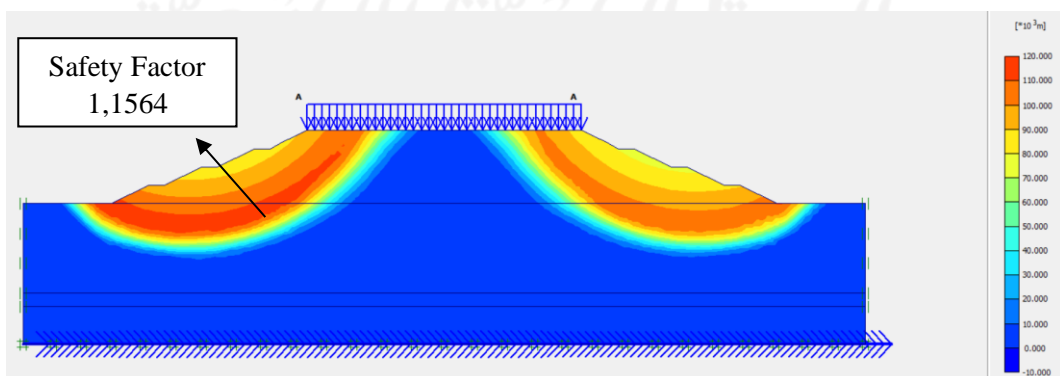


Figure 5.54 Potential Landslides of Embankment 3 Trap Due to Traffic Load

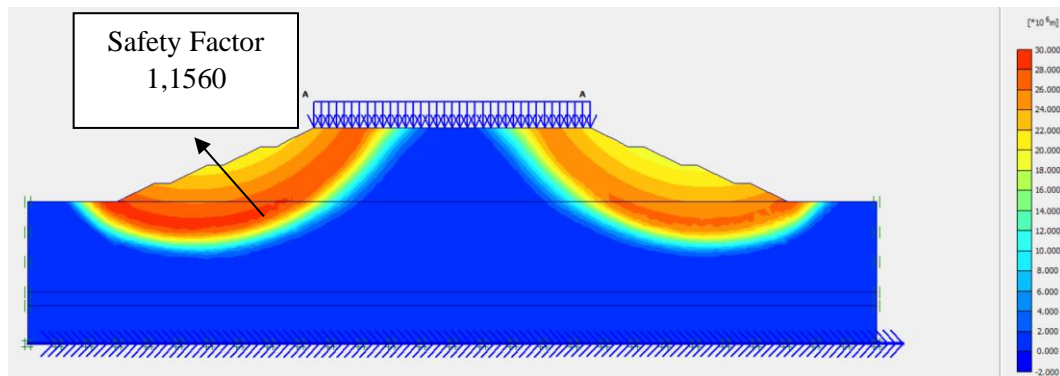


Figure 5.55 Potential Landslides of Embankment 3 Trap Due to Traffic and Earthquake Load

The safety factor (SF) of the embankment with 3 trap geometry variation that obtained from the analysis results due to traffic load is 1,1564 while the safety factor (SF) due to traffic load and earthquake load is 1,1560.

5.4.4. Recapitulation of Safety Factor (SF) Results and Consolidation

The results of the calculation analysis of safety factors on the embankment with geometry variation and consolidation results can be seen in Table 5.6 as follows.

Table 5.6 Recapitulation Results of Safety Factor (SF) and Consolidation on Embankment

Embankment Type	SF Traffic Load		SF Traffic & Earthquake Load		Consolidation (m)
	SF	State	SF	State	
Existing Embankment	1,0330	Unsafe	1,0306	Unsafe	0,27747
1 Trap Embankment	1,0777	Unsafe	1,0771	Unsafe	0,22237
2 Trap Embankment	1,1164	Unsafe	1,1147	Unsafe	0,19339
3 Trap Embankment	1,1564	Unsafe	1,1560	Unsafe	0,17773

It can be seen in Table 5.6 that the safety factor (SF) in the embankments with topography improvement does not have significant effect for the embankment, the safety factor value that is less than the specified safe limit as much as 1,3 so the value of the safety factor (SF) on the embankment still does not meet the SF

requirements. Furthermore, on the embankment that does not meet the requirement, then the analysis is carried out again by adding reinforcement with geotextiles.

5.5 Calculation of Geotextile Needs

5.5.1. Geotextile Calculation Data

1. Embankment Soil Parameter

The soil parameter used and will be strengthened by geotextiles is in the embankment soil section because the largest landslide area is in the soil embankment section. The type of embankment soil used as soil parameter in the calculation of geotextile reinforcement is as follows.

- a. Volume weight of soil (γ_b) = 16 kN/m³
- b. Cohesion (c) = 10 kN/m²
- c. Angle friction (ϕ) = 25°

2. Geotextile Data

In this research, geotextiles with an ultimate tensile strength specification (T_{ult}) of 52 kN/m were used. The type of geotextile that used in this research UW-250 woven geotextile which is the product of PT Teknindo Geosistem Unggul. The geotextile data that will be input into Plaxis program is in the form of the normal stiffness (EA) value which is calculated as follows.

$$\begin{aligned} T_{all} &= \frac{T_{ult}}{SF_{geo}} \\ &= \frac{52}{2} \\ &= 26 \text{ kN/m}^2 \end{aligned}$$

Geotextile parameter data used for calculations and input into the Plaxis program can be seen in Table 5.7 as follows.

Table 5.7 Woven UW-250 Geotextiles Data

Parameter	Notation	Value	Unit
Ultimate Tensile Strength	T_{ult}	52	kN/m
Strain	ϵ	20	%
Normal stiffness	EA	260	kN/m
Allowable Tensile strength	T_{all}	26	kN/m

3. Coefficient of soil bearing capacity

In the analysis of the calculation of geotextile requirements, data on the coefficient of soil bearing capacity is needed. The soil bearing capacity coefficient data in this research used data that obtained from the Ministry of Public Works (2009). The value of the coefficient of soil bearing capacity can be seen in Table 5.8 below.

Table 5.8 Soil Bearing Capacity

ϕ	N_c	N_q	N_γ	ϕ	N_c	N_q	N_γ
10	8,85	2,47	1,22	26	22,25	11,85	12,54
11	8,80	2,71	1,44	27	23,94	13,20	14,47
12	9,28	2,97	1,69	28	25,80	14,72	16,72
13	9,81	3,26	1,97	29	27,86	16,44	19,34
14	10,37	3,59	2,29	30	30,14	18,40	22,40
15	10,98	3,94	2,65	31	32,67	20,63	25,90
16	11,63	4,34	3,06	32	35,49	23,18	30,22
17	12,34	4,77	3,53	33	38,64	26,09	35,19
18	13,10	5,26	4,07	34	42,16	29,44	41,06
19	13,93	5,80	4,68	35	46,12	33,30	48,03
20	14,83	6,40	5,39	36	50,59	37,75	56,31
21	15,82	7,07	6,20	37	55,63	42,92	66,19
22	16,88	7,82	7,13	38	61,35	48,93	78,03
23	18,05	8,66	8,20	39	67,87	55,96	92,25
24	19,32	9,60	9,44	40	75,31	64,20	109,41
25	20,72	10,66	10,8	41	83,86	73,90	130,22

Source: Ministry of Public Works (2009)

5.5.2. External Stability

In planning the embankment with geotextile reinforcement, the slope must be stable against the influence of internal and external forces. The stability that will be reviewed is external stability and internal stability. The external stability calculation will be used to determine the minimum vertical distance of the geotextile layer (SV) and the minimum total length of the geotextile (L).

The uniform load entered is the maximum load in post-construction conditions of 25 kN/m². The value of the safety factor (SF) as a reference in calculating geotextile requirements is 1.5. The forces that will act on the embankment can be seen in Figure 5.56 as follows.

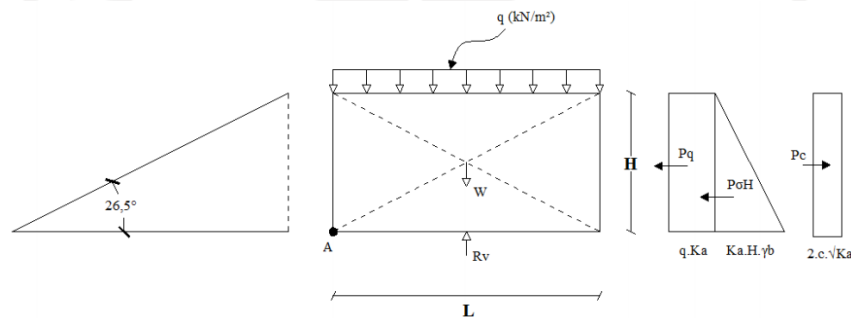


Figure 5.56 Forces Acting on a Slope Embankment

- Determine the minimum vertical distance between geotextile layers (SV) calculation of the active soil coefficient is as follows.

$$K_a = \tan \left(45 - \frac{\phi}{2} \right)$$

$$K_a = \tan \left(45 - \frac{25}{2} \right)$$

$$= 0,40585$$

- Minimum vertical distance of embankment geotextile (SV) layer
2,25 m

$$\text{ohc} = (q \times K_a) + (K_a \times H \times \gamma_b) - (2 \times c \times \sqrt{K_a})$$

$$= (25 \times 0,40586) + (0,40586 \times 2,25 \times 16) - (2 \times 10 \times \sqrt{0,40586})$$

$$= 12,016 \text{ kN/m}^2$$

$$\begin{aligned}
 SV &= \frac{T_{all}}{\sigma_{hc} \times SF} \\
 &= \frac{26}{12,016 \times 1,5} \\
 &= 1,442 \text{ m}
 \end{aligned}$$

Field installed SV = 1m (minimum)

Theoretical number of layers of geotextile = 2m / 1m = 2 layers

In the study for 2,25 m slope embankment, 1 layer of geotextile will be used.

b. Minimum vertical distance of embankment geotextile layer (SV) 4,5m

$$\begin{aligned}
 \sigma_{hc} &= (q \times K_a) + (K_a \times H \times \gamma_b) - (2 \times c \times \sqrt{K_a}) \\
 &= (25 \times 0,40586) + (0,40586 \times 4,5 \times 16) - (2 \times 10 \times \sqrt{0,40586}) \\
 &= 26,626 \text{ kN/m}^2
 \end{aligned}$$

$$\begin{aligned}
 SV &= \frac{T_{all}}{\sigma_{hc} \times SF} \\
 &= \frac{26}{26,626 \times 1,5} \\
 &= 0,650 \text{ m}
 \end{aligned}$$

Field installed SV = 0,5 m (minimum)

Theoretical number of layers of geotextile = 4,5m / 0,5m = 9 layers

In the study for 4,5m slope embankment, 1 layer of geotextile will be used.

c. Minimum vertical distance of embankment geotextile layer (SV) 6,75m

$$\begin{aligned}
 \sigma_{hc} &= (q \times K_a) + (K_a \times H \times \gamma_b) - (2 \times c \times \sqrt{K_a}) \\
 &= (25 \times 0,40586) + (0,40586 \times 6,75 \times 16) - (2 \times 10 \times \sqrt{0,40586}) \\
 &= 41,238 \text{ kN/m}^2
 \end{aligned}$$

$$\begin{aligned}
 SV &= \frac{T_{\text{all}}}{\sigma_{hc} \times SF} \\
 &= \frac{26}{41,237 \times 1,5} \\
 &= 0,420 \text{ m}
 \end{aligned}$$

Field installed SV = 0,5 (minimal)

Theoretical number of layers of geotextile = 6,75 / 0,5m = 13 layers

In the study for 6,75m slope embankment, 1 layer of geotextile will be used.

d. Minimum vertical distance of embankment geotextile layer (SV) 9m

$$\begin{aligned}
 \sigma_{hc} &= (q \times K_a) + (K_a \times H \times \gamma_b) - (2 \times c \times \sqrt{K_a}) \\
 &= (25 \times 0,40586) + (0,40586 \times 9 \times 16) - (2 \times 10 \times \sqrt{0,40586}) \\
 &= 55,848 \text{ kN/m}^2
 \end{aligned}$$

$$\begin{aligned}
 SV &= \frac{T_{\text{all}}}{\sigma_{hc} \times SF} \\
 &= \frac{26}{55,848 \times 1,5} \\
 &= 0,310 \text{ m}
 \end{aligned}$$

Field installed SV = 0,5 (minimal)

Theoretical number of layers of geotextile = 9 / 0,5m = 18 layers

In the study for 9m slope embankment, 1 layer of geotextile will be used.

2. Determine the length of geotextile

a. Stability against rolling

$$SF = \frac{\sum MR}{\sum MD} = \frac{\text{Holding Moment}}{\text{Rolling Moment}} \geq 1,5$$

$$\Sigma MR = \left(\frac{1}{2} \times q \times L^2\right) + \left(\frac{1}{2} \times \gamma b \times H \times L^2\right)$$

$$\Sigma MD = \left(q \times Ka \times \frac{1}{2} H^2\right) + \left(\frac{1}{2} \times Ka \times \gamma b \times H^2 \times \frac{1}{3} \times H\right) - \left(2 \times c \times \sqrt{Ka} \times \frac{1}{2} H^2\right)$$

$$SF = \frac{\left(\frac{1}{2} \times 25 \times L^2\right) + \left(\frac{1}{2} \times 16 \times 9 \times L^2\right)}{(25 \times 0,4058 \times 9^2) + \left(\frac{1}{2} \times 0,4058 \times 16 \times 9^2 \times \frac{1}{3} \times 9\right) - \left(2 \times 10 \times \sqrt{0,4058} \times \frac{1}{2} \times 9^2\right)}$$

$$SF = \frac{84,5 \times L^2}{683,894}$$

$$L^2 = \frac{683,894 \times 1,5}{84,5} = 12,1401 \text{ m}$$

$$L = 3,484 \text{ m}$$

The length of the geotextile to resist overturning on the soil embankment taken is 3,5 m.

b. Stability against shear

$$SF = \frac{(q \times \tan \delta \times L) + (H \times \gamma b \times \tan \delta \times L)}{(q \times Ka \times H) + (0,5 \times Ka \times \gamma b \times H^2) - (2 \times c \times \sqrt{Ka} \times H)}$$

Shear resistance at the base of the reinforcement ($\delta = 2/3 \times 25 = 16,667$)

$$SF = \frac{(25 \times \tan(16,667) \times L) + (12,5 \times 16 \times \tan(16,667) \times L)}{(25 \times 0,4058 \times 12,5) + (0,5 \times 0,4058 \times 16 \times 9^2) - (2 \times 10 \times \sqrt{0,4058} \times 9)}$$

$$SF = \frac{50,5953 \times L}{239,642}$$

$$L = \frac{239,642 \times 1,5}{50,5953} = 7,10467 \text{ m}$$

The length of the geotextile to resist shear in the soil embankment is taken as long as 7 m.

c. Stability against eccentricity

$$\frac{1}{6} \times L \geq e$$

$$e = \frac{\Sigma MD}{Rv}$$

$$= \frac{\left(q \times K_a \times \frac{1}{2} \times H^2 \right) + \left(\frac{1}{2} \times K_a \times \gamma_b \times H^2 \times \frac{1}{3} \times H \right) - \left(2 \times c \times \sqrt{K_a} \times \frac{1}{2} \times H^2 \right)}{(H \times \gamma_b \times L) + (q \times L)}$$

$$\frac{L}{6} \geq \frac{683,894}{169 \times L}$$

$$L^2 = 24,2803 \text{ m}$$

$$L = 4,927 \text{ m}$$

The length of the geotextile to resist eccentricity in the soil embankment is taken as long as 5 m.

d. Stability bearing capacity of soil

$$N_c = 20,72$$

$$N_\gamma = 10,8$$

$$L \leq \frac{\sigma_{ult}}{(H \times \gamma_b) + q}$$

$$\sigma_{ult} = [(c \times N_c) + (0,5 \times L \times \gamma_b \times N_\gamma)] \times SF$$

$$\sigma_{ult} = [(10 \times 20,72) + (0,5 \times L \times 16 \times 10 \times 10,8)] \times 1,5$$

$$\sigma_{ult} = 310,8 + (129,6 \times L)$$

$$L = \frac{310,8}{225,8 - 129,6}$$

$$L = 3,23077 \text{ m}$$

The length of the geotextiles to withstand the bearing capacity of the soil on the embankment is taken as long as 3 m.

From the four parameters above, the maximum length of the geotextile used is 7 m.

Table 5.9 Recapitulation of Geotextile Length Requirement

Embankment Height Zone (H)	Roll Stability	Shear Stability	Eccentricity Stability	Stability of Bearing Capacity	Minimum of Length (L)
2,25	0,532216	0,87054	0,75266	-4.81115	1
4,5	1,495869	2,792977	2,115478	-9.53374	3
6,75	2,484866	4,913139	3,514131	91.4117	5
9	3,484268	7,10467	4,9275	3,230769	7

5.5.3. Internal Stability

1. Overlapping of geotextile length

a. Embankment 2,25m

$$L_o = \frac{\sigma_{hc} \times s_v \times s_f}{2 \times \gamma_b \times H \times \tan \varphi}$$

$$L_o = \frac{12,015 \times 1 \times 1,5}{2 \times 16 \times 2,25 \times \tan 25} = 0,536 \text{ m}$$

Because the minimum overlapping length is 1 meter, thus the length taken is 1 m.

b. Embankment 4,5m

$$L_o = \frac{\sigma_{hc} \times s_v \times s_f}{2 \times \gamma_b \times H \times \tan \varphi}$$

$$L_o = \frac{26,626 \times 0,5 \times 1,5}{2 \times 16 \times 4,5 \times \tan 25} = 0,297 \text{ m}$$

Because the minimum overlapping length is 1 meter, thus the length taken is 1 m.

c. Embankment 6,75m

$$L_o = \frac{\sigma_{hc} \times s_v \times s_f}{2 \times \gamma_b \times H \times \tan \varphi}$$

$$L_o = \frac{41,237 \times 0,5 \times 1,5}{2 \times 16 \times 6,75 \times \tan 25} = 0,307 \text{ m}$$

Because the minimum overlapping length is 1 meter, thus the length taken is 1 m.

d. Embankment 9m

$$L_o = \frac{\sigma_{hc} \times s_v \times s_f}{2 \times \gamma b \times H \times \tan \varphi}$$

$$L_o = \frac{55,848 \times 0,5 \times 1,5}{2 \times 16 \times 9 \times \tan 25} = 0,311 \text{ m}$$

Because the minimum overlapping length is 1 meter, thus the length taken is 1 m.

2. Effective of Geotextile length

a. Embankment 2,25m

$$L_e = \frac{SF \times SV \times Ka \times \gamma b \times H}{2 \times \gamma b \times H \times \tan \varphi}$$

$$L_e = \frac{1,5 \times 1 \times 0,45086 \times 16 \times 2,25}{2 \times 16 \times 2,25 \times \tan 25} = 0,7 \text{ m}$$

The effective length used is 0,5 m

b. Embankment 4,5 m

$$L_e = \frac{SF \times SV \times Ka \times \gamma b \times H}{2 \times \gamma b \times H \times \tan \varphi}$$

$$L_e = \frac{1,5 \times 0,5 \times 0,45086 \times 16 \times 4,5}{2 \times 16 \times 4,5 \times \tan 25} = 0,36 \text{ m.}$$

The effective length used is 0,5 m.

c. Embankment 6,75m

$$L_e = \frac{SF \times SV \times Ka \times \gamma b \times H}{2 \times \gamma b \times H \times \tan \varphi}$$

$$L_e = \frac{1,5 \times 0,5 \times 0,45086 \times 16 \times 6,75}{2 \times 16 \times 6,75 \times \tan 25} = 0,36 \text{ m.}$$

The effective length used is 0,5 m.

d. Embankment 9m

$$L_e = \frac{SF \times SV \times Ka \times \gamma b \times H}{2 \times \gamma b \times H \times \tan \varphi}$$

$$L_e = \frac{1,5 \times 0,5 \times 0,45086 \times 16 \times 9}{2 \times 16 \times 9 \times \tan 25} = 0,36 \text{ m.}$$

The effective length used is 0,5 m.

5.5.4. Tensile Strength Check Between Geotextile - Soil

To determine whether the geotextile used is able to withstand the tensile force that occurs with an SV value of 0,5 m, thus the working shear stress is calculated. The image of the geotextile-soil friction can be seen in Figure 5.57 as follows.

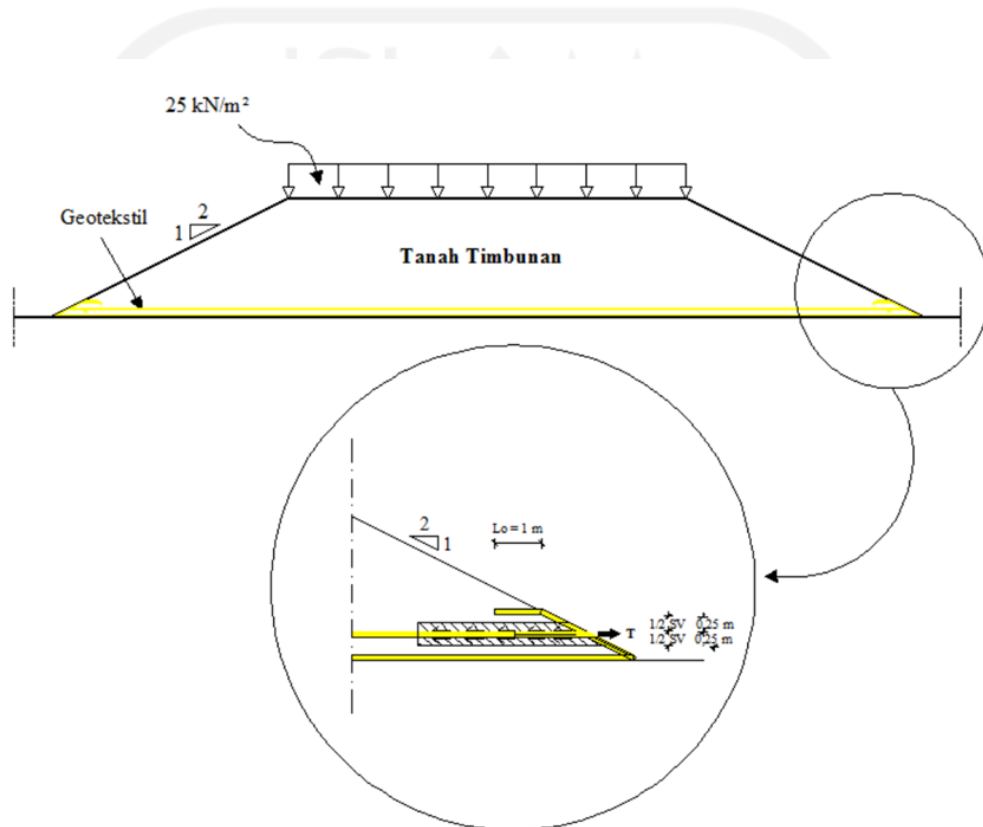


Figure 5.57 Soil – Geotextile Friction Transfer

When the geotextile receives a load from above (soil), the geotextile will stiffen and transfer the stress to the passive area. So, the geotextile must be able to withstand the tensile forces that acting on it. Therefore, it is necessary to design a type of geotextile that is able to withstand the tensile force. The tensile force acting on the geotextile can be found using following equation.

$$\begin{aligned}
 T &= \tan \varphi \times 2 \times \sigma_n \times b \times L \\
 &= \tan(25) \times 2 \times \left(\frac{1}{2} \times 0,5 \times 16 \right) \times 1 \times 7 \\
 &= 26,113 \text{ kN}
 \end{aligned}$$

From the calculation of the tensile force acting above on the geotextile is 26,113 kN, while the type of geotextile used has a tensile strength of 52 kN/m. So, the geotextile strength is strong enough to withstand the tensile force that will work because $52 \text{ kN/m} > 26,113 \text{ kN}$ (safe).

5.6 Calculation of Embankment Reinforced by 1 Layer Geotextile

From the results of the calculation on the analysis that has been carried out with the existing slope embankment without any reinforcement, it is found that the embankments still do not meet the safe number criteria. Therefore, it is necessary to re-do the analysis of the soil embankment with additional geotextile reinforcement with an analysis of the same geometric conditions and in accordance with the calculation of geotextile needs. The results of the calculation analysis using the Finite element method that will be displayed in this analysis are the existing embankment and variations of trap with geotextile reinforcement. For the results on the analysis of the embankment can be seen as follows.

5.6.1. Existing embankment with Geotextile Reinforcement

Initial modelling of the existing embankment with the same geometry on an unreinforced 9m embankment. Horizontal installation of geotextiles with an SV of 0,5 m and overlapping length of 1m. For the total length of the geotextile used along the embankment at the bottom, assuming that the length reached the minimum total length of the geotextile requirement calculation. The input coordinates for Plaxis 8.6 can be seen in Table 5.10 and for slope modelling, it can be seen in Figure 5.58 as follows.

Table 5.10 Input Coordinate of Existing Embankment with Geotextile Reinforcement

No	X (m)	Y (m)	No	X (m)	Y (m)
1	0	0	9	103,830	-17,300
2	103,830	0	10	0	-17,300
3	103,830	-11	11	0	-12,700
4	0	-11	12	86,830	0
5	0	0	13	68,830	9
6	0	-12,700	14	35	9
7	103,830	-12,700	15	17	0
8	103,830	-11			

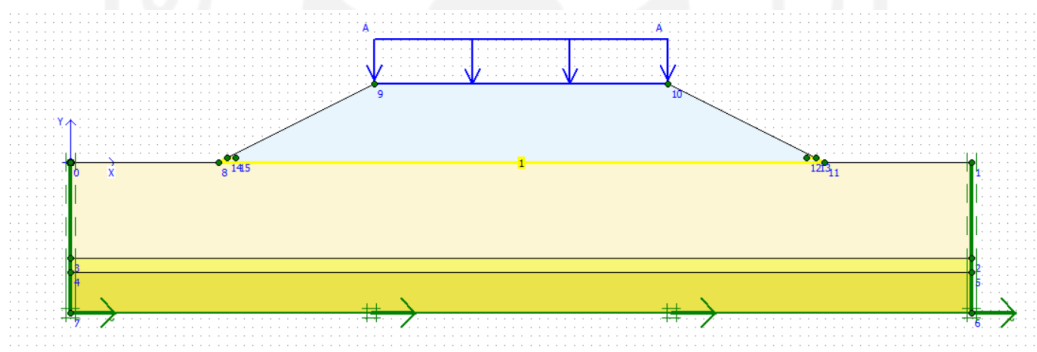


Figure 5.58 Modelling of Embankment Reinforced with Geotextile

The process of the meshing on the existing embankment can be seen in Figure 5.59 as follows.

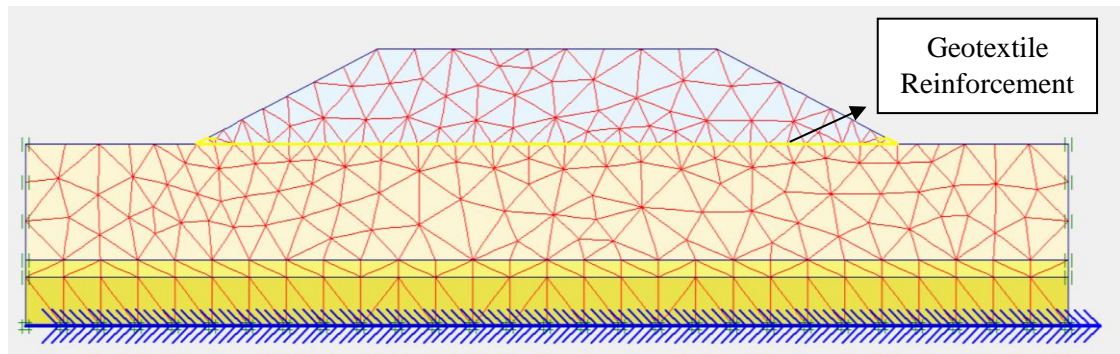


Figure 5.59 Meshing of Existing Embankment with Geotextile Reinforcement

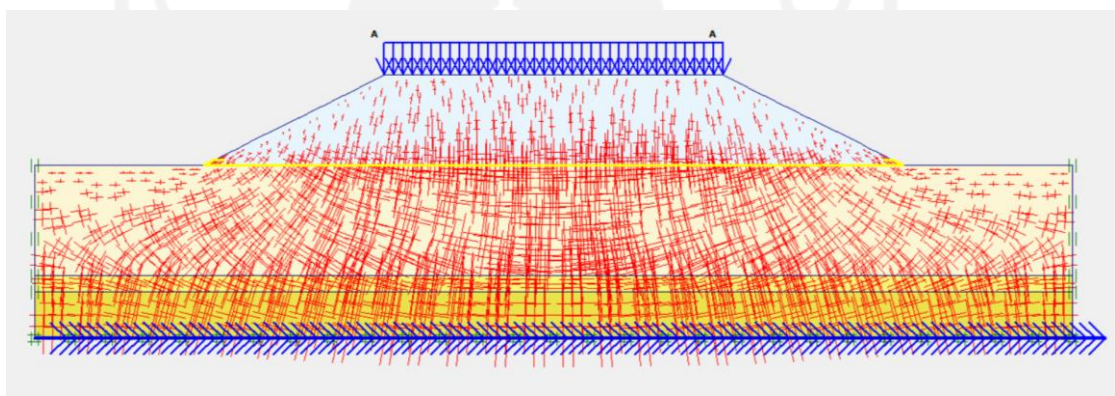


Figure 5.60 Initial Soil Stresses of Existing Embankment with Geotextile Reinforcement

Then after the meshing process is carried out, it is continued with the initial conditions.

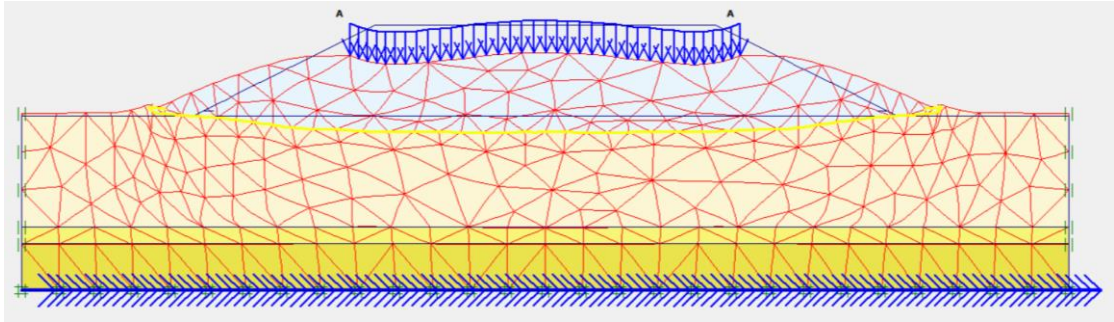


Figure 5.61 Deformed Mesh on Existing Embankment with geotextile Reinforcement Due to Traffic Load

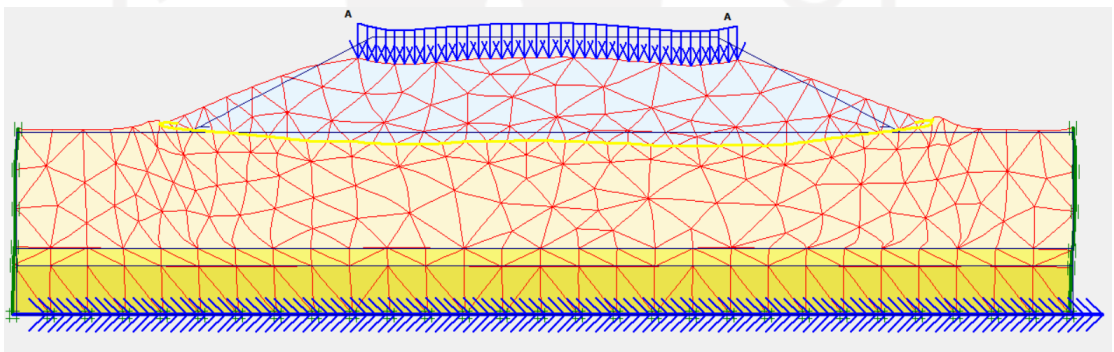


Figure 5.62 Deformed Mesh on Existing Embankment with Geotextile Reinforcement Due to Traffic and Earthquake Load

الجامعة الإسلامية
الاستاذ الدكتور
الشيخ الدكتور

The results of the total displacement that occurs in the existing embankments due to traffic load is $253,12 \times 10^{-3}$ m, while on the existing embankments with the effects of traffic load and earthquake load is $370,49 \times 10^{-3}$ m. The total displacement that occurs on the embankment can be seen in Figure 5.63 and Figure 5.64 as follows.

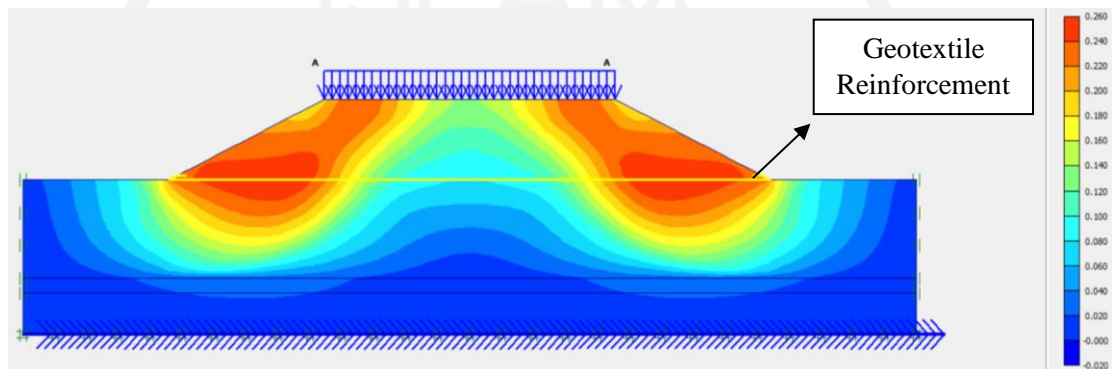


Figure 5.63 Total Displacement of Existing Embankment with Geotextile Reinforcement Due to Traffic Load

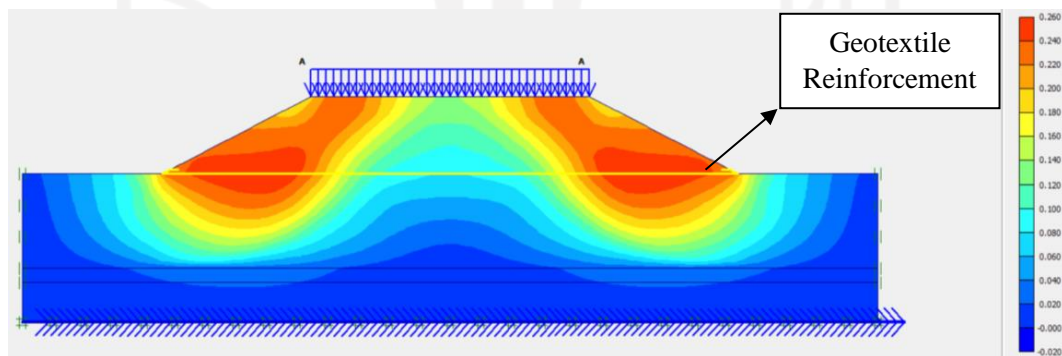


Figure 5.64 Total Displacement of Existing Embankment with Geotextile Reinforcement Due to Traffic and Earthquake Load

Thereafter the direction of movement that occurs in the existing embankment can be seen in Figure 5.65 and Figure 5.66 as follows.

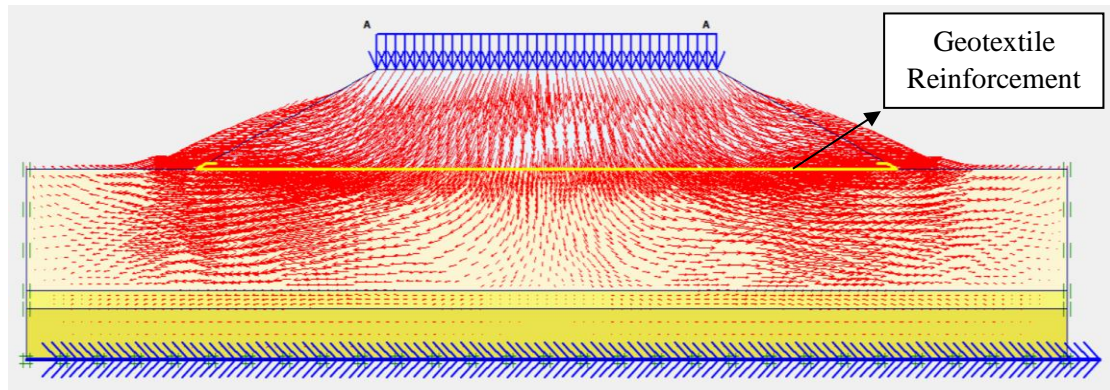


Figure 5.65 Soil Movement of Existing Embankment Due to Traffic Load

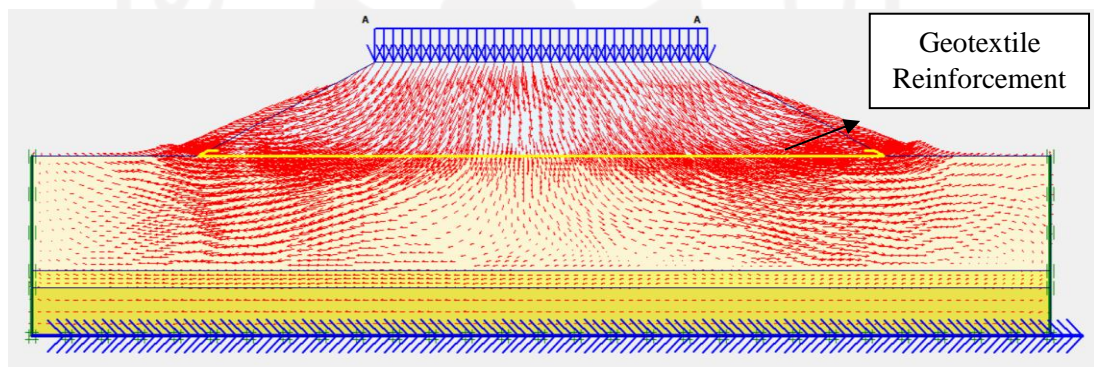


Figure 5.66 Soil Movement of Existing Embankment Due to Traffic and Earthquake Load

The results of the effective stresses on the existing embankments with reinforced geotextile due to traffic load is $-418,92 \text{ kN/m}^2$ while the results of effective stresses due to traffic load and earthquake load is $-428,42 \text{ kN/m}^2$. The results of the analysis can be seen in Figure 5.67 and Figure 5.68 as follows.

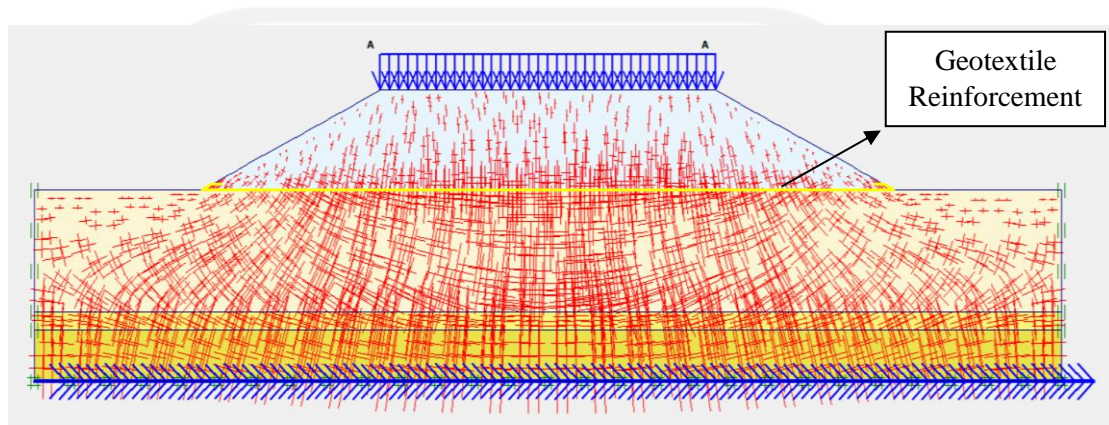


Figure 5.67 Effective Stresses of Existing Embankment with Geotextile Reinforcement Due to Traffic Load

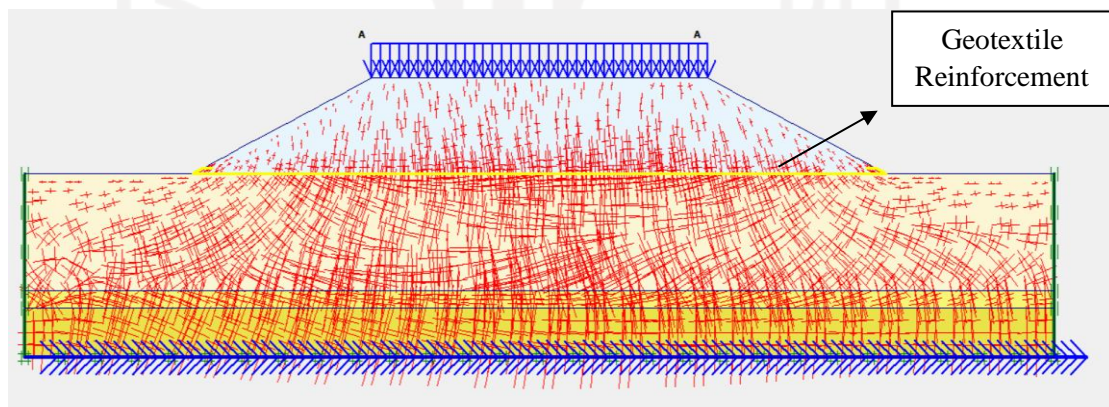


Figure 5.68 Effective Stresses of Existing Embankment with Geotextile Reinforcement Due to Traffic and Earthquake Load

The potential for landslides that occur due to traffic load and earthquake loads can be seen in Figure 5.69 and Figure 5.70 as follows.

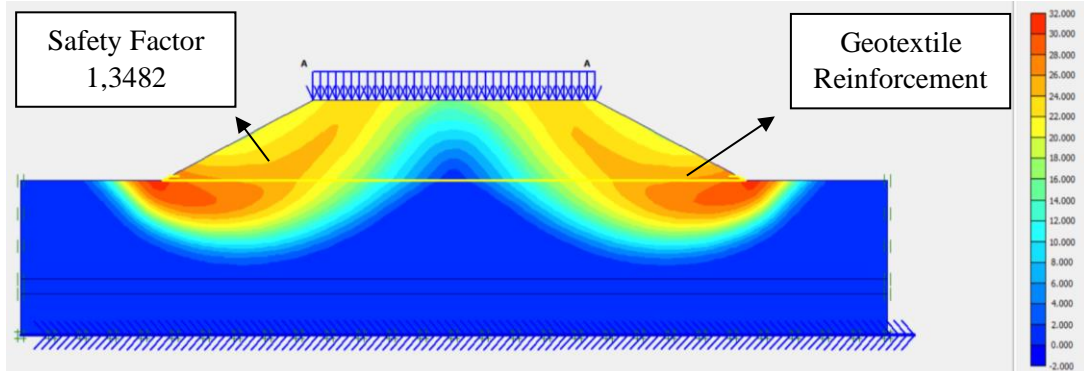


Figure 5.69 Potential Landslides of Existing Embankment Due to Traffic Load

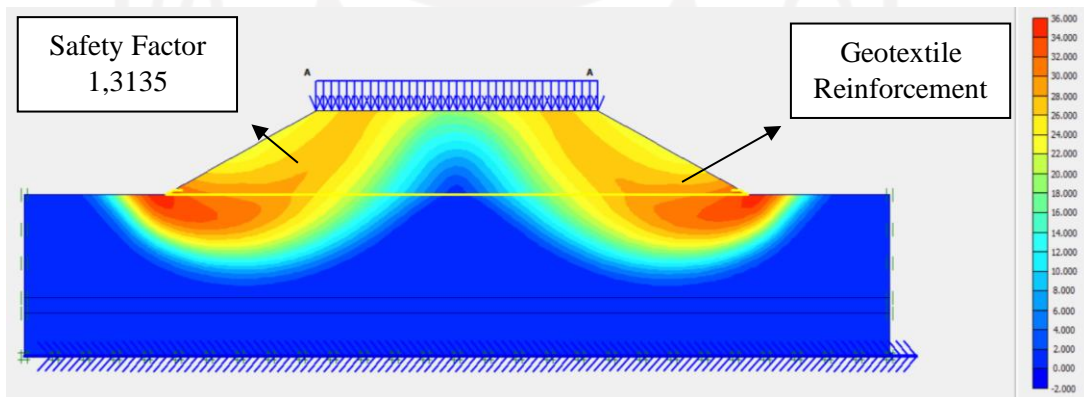


Figure 5.70 Potential Landslides of Existing Embankment Due to Traffic and Earthquake Load

The safety factor of existing embankment with reinforced geotextile due to traffic load is 1,3482 while the safety factor due to traffic load and earthquake load is 1,3135. The results of the safe number values can be seen in the Figure 5.71 as follows.

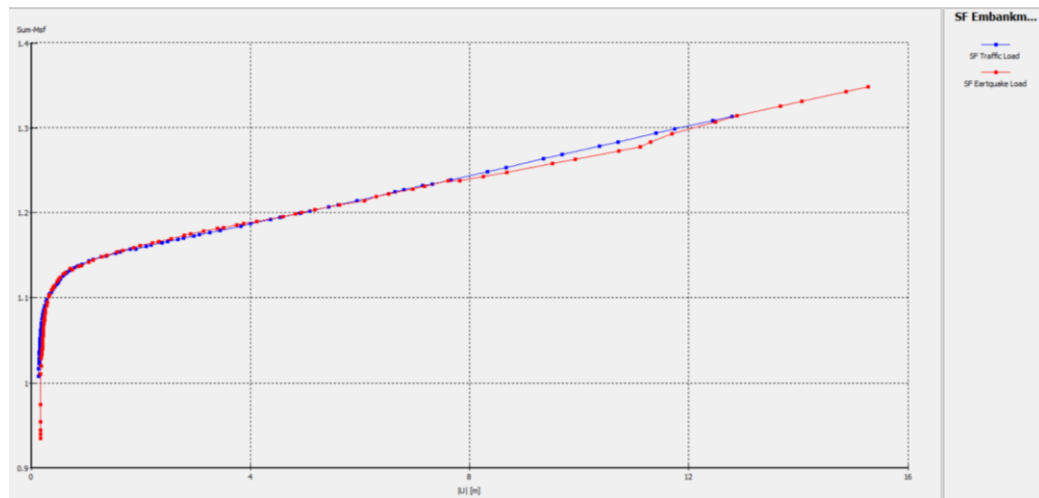


Figure 5.71 SF Curve of Existing Embankment with Reinforced Geotextile

5.6.2. Embankment 1 Trap Variation with Geotextile Reinforcement

Initial modelling of the embankment with the same geometry on an embankment 1 trap variation with geotextile reinforcement. The input coordinates for Plaxis 8.6 can be seen in Table 5.11 and for slope modelling, it can be seen in Figure 5.72 as follows.

Table 5.11 Input Coordinate of Embankment 1 Trap Variation with Geotextile Reinforcement

No	X (m)	Y (m)	No	X (m)	Y (m)
1	0	0	11	0	-12,700
2	103,830	0	12	15	0
3	103,830	-11	13	24	4,5
4	0	-11	14	26	4,5
5	0	0	15	35	9
6	0	-12,700	16	68,830	9
7	103,830	-12,700	17	77,830	4,5
8	103,830	-11	18	79,830	4,5
9	103,830	-17,300	19	88,830	0

Continuity Table 5.11 Input Coordinate of Embankment 1 Trap Variation with Geotextile Reinforcement

10	0	-17,300			
----	---	---------	--	--	--

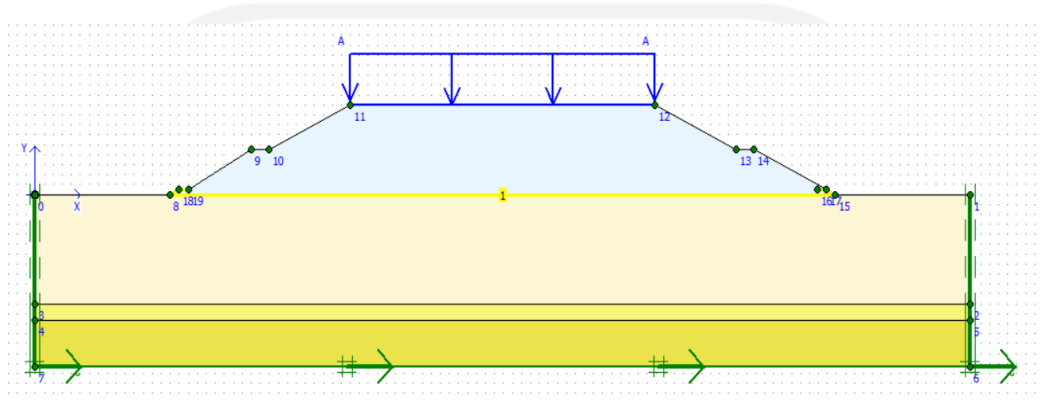


Figure 5.72 Modelling of Embankment 1 Trap with Geotextile Reinforcement

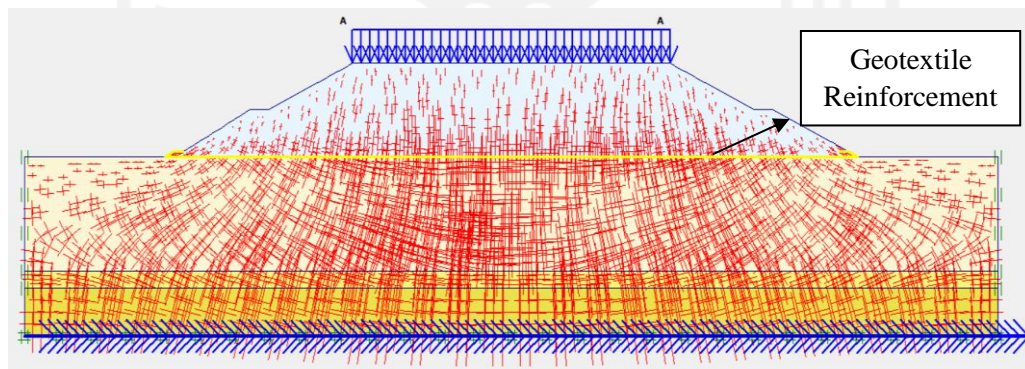


Figure 5.73 Initial Soil Stresses of Embankment 1 Trap with Geotextile Reinforcement

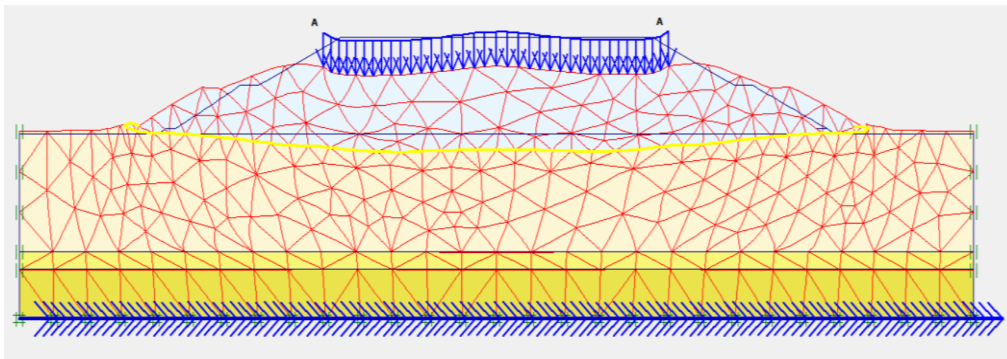


Figure 5.74 Deformed Mesh of Embankment 1 Trap with Geotextile Reinforcement Due to Traffic Load

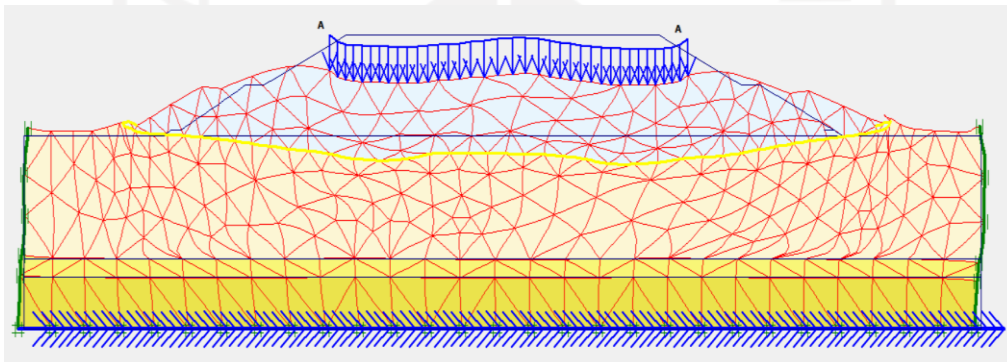


Figure 5.75 Deformed Mesh of Embankment 1 Trap with Geotextile Reinforcement Due to Traffic and Earthquake Load

The result of the total displacement value that occurs on the embankment 1 trap with geotextile reinforcement due to traffic load is $220,57 \times 10^{-3}$ m, while the total displacement due to traffic load and earthquake load is $292,74 \times 10^{-3}$ m. The results of the total displacement that occurs can be seen in Figure 5.76 and Figure 5.77 as follows.

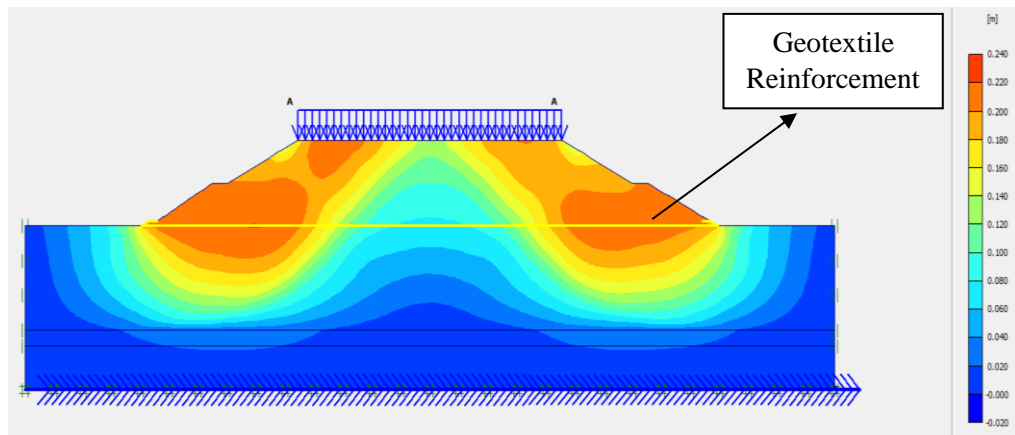


Figure 5.76 Total Displacement of Embankment 1 Trap with Geotextile Reinforcement Due to Traffic Load

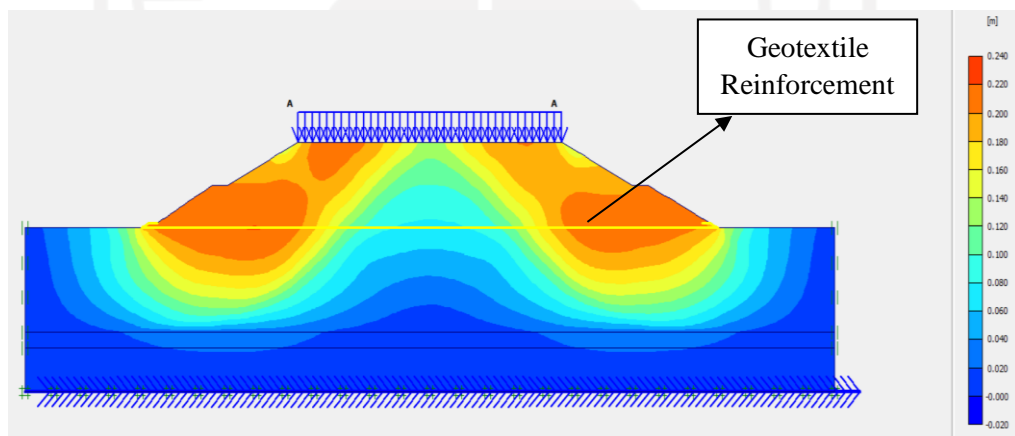


Figure 5.77 Total Displacement of Embankment 1 Trap with Geotextile Reinforcement Due to Traffic and Earthquake Load

المعهد الوطني للبحوث والدراسات
البيئية والهندسة المدنية

Thereafter the direction of movement that occurs in the embankment can be seen in Figure 5.78 and Figure 5.79 as follows.

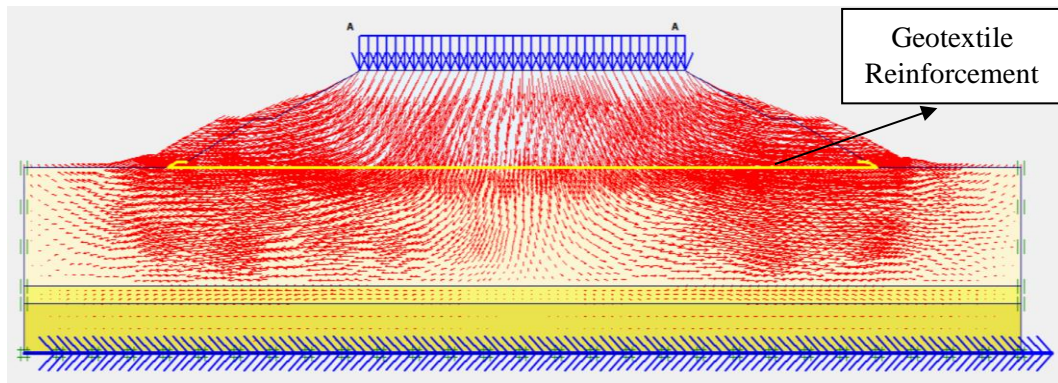


Figure 5.78 Soil Movement of Embankment 1 Trap with Geotextile Reinforcement Due to Traffic Load

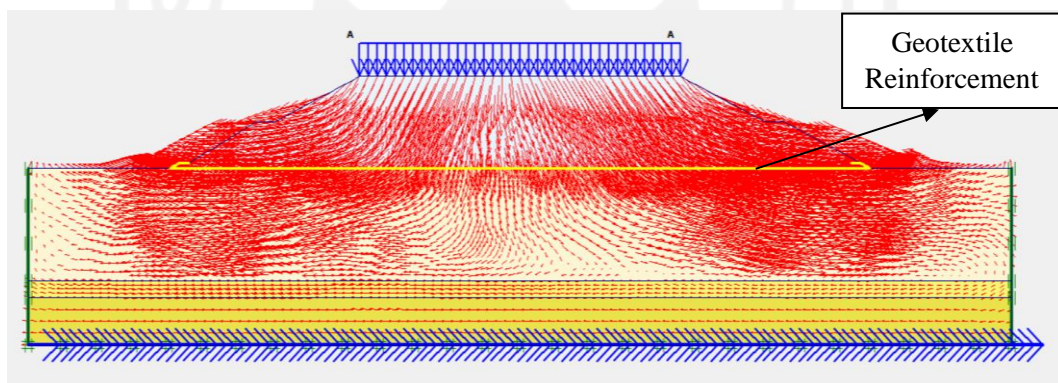


Figure 5.79 Soil Movement of Embankment 1 Trap with Geotextile Reinforcement Due to Traffic and Earthquake Load

Thereafter, the value of effective stresses that occur on the embankments 1 trap with geotextile reinforcement due to traffic load is $-419,53 \text{ kN/m}^2$, while the effective stresses due to traffic load and earthquake load is $-425,72 \text{ kN/m}^2$. The results of these calculations can be seen in Figure 5.80 and Figure 5.81 as follows.

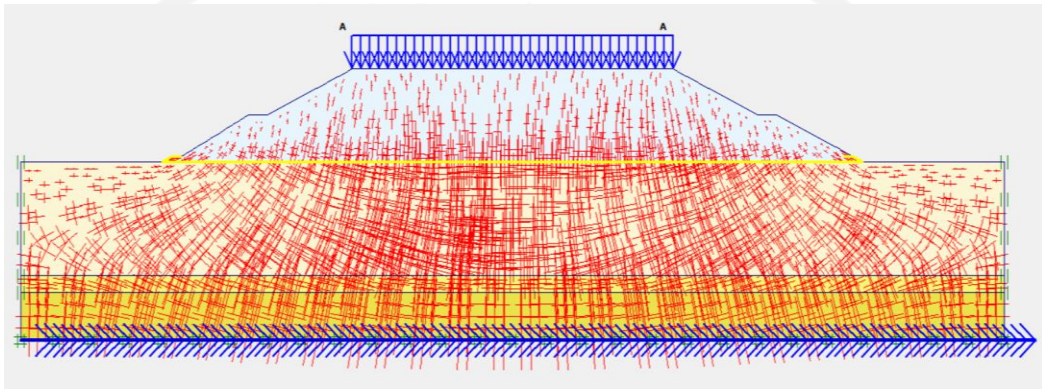


Figure 5.80 Effective Stresses of Embankment 1 Trap with Geotextile Reinforcement Due to Traffic Load

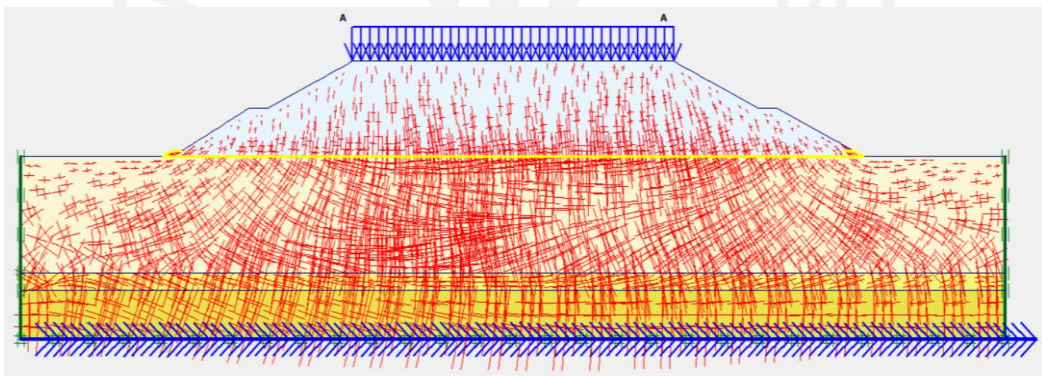


Figure 5.81 Effective Stresses of Embankment 1 Trap with Geotextile Reinforcement Due to Traffic and Earthquake Load

The occurrence of landslide due to traffic loads and earthquake loads can be seen in Figure 5.82 and Figure 5.83 as follows.

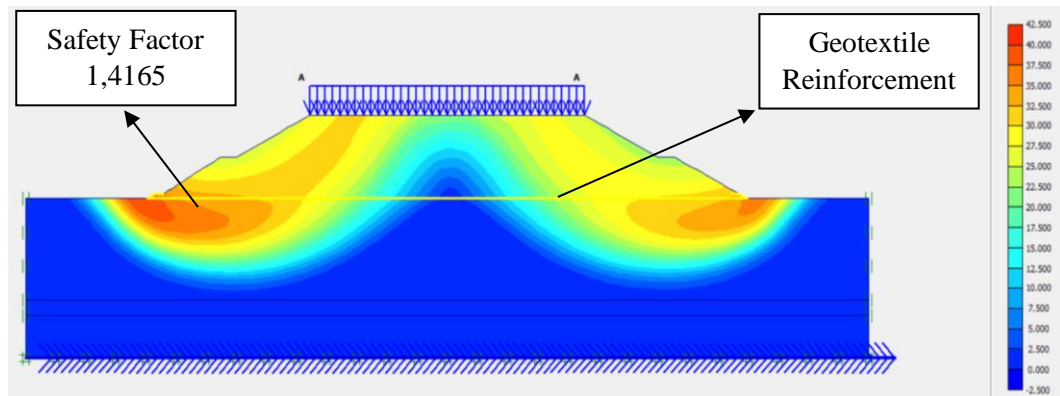


Figure 5.82 Potential Landslides of Embankment 1 Trap with Geotextile Reinforcement Due to Traffic Load

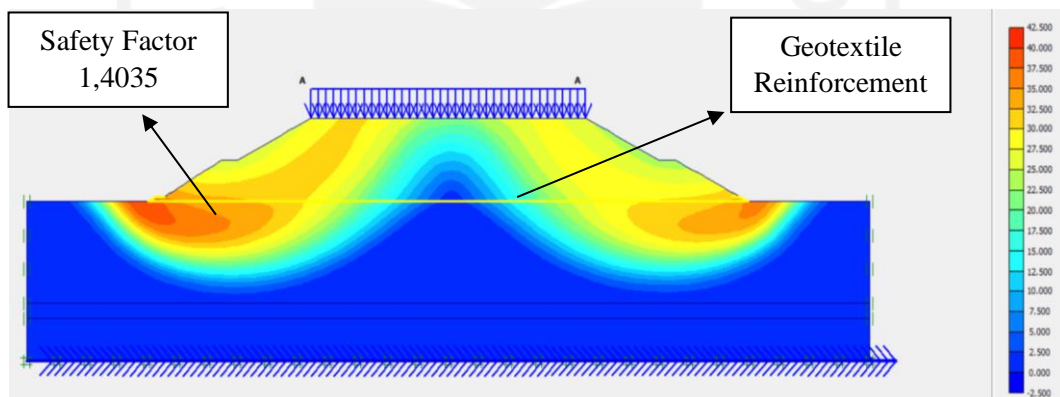


Figure 5.83 Potential Landslide of Embankment 1 Trap with Geotextile Reinforcement Due to Traffic and Earthquake Load

The safety factor of embankment 1 trap with reinforced geotextile due to traffic load is 1,4165 while the safety factor due to traffic load and earthquake load is 1,4035. The results of the safe number values can be seen in the Figure 5.84 as follows.

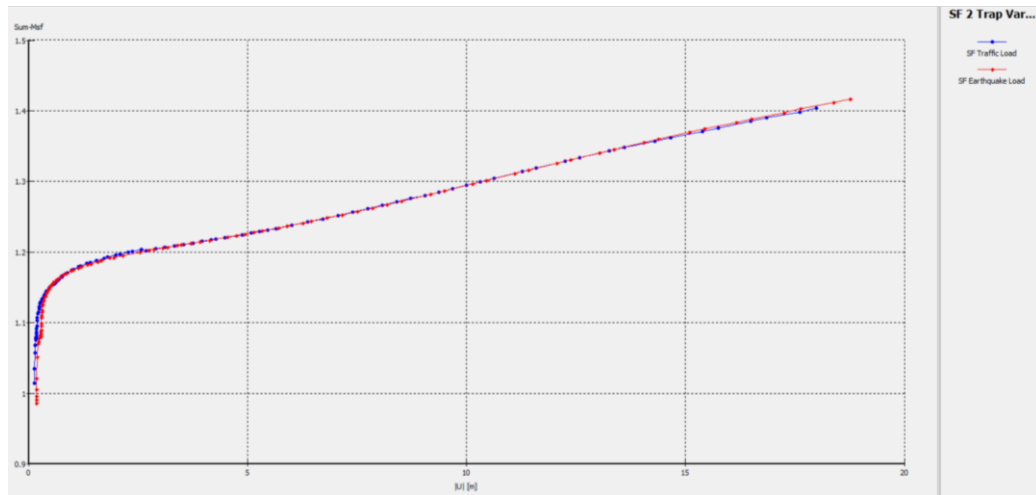


Figure 5.84 SF Curve of Embankment 1 Trap with Reinforced Geotextile

5.6.3. Embankment 2 Trap Variation with Geotextile Reinforcement

Initial modelling of the embankment with the same geometry on an embankment 2 trap variation with geotextile reinforcement. The input coordinates for Plaxis 8.6 can be seen in Table 5.12 and for slope modelling, it can be seen in Figure 5.85 as follows.

Table 5.12 Input Coordinate of Embankment 2 Trap Variation with Geotextile Reinforcement

No	X (m)	Y (m)	No	X (m)	Y (m)
1	0,00	0,00	13	19	3,00
2	103,830	0,00	14	21	3,00
3	103,830	-11	15	27	6,00
4	0,00	-11	16	29	6,00
5	0,00	0,00	17	35	9,00

Continuity of Table 5.12 Input Coordinate of Embankment 2 Trap Variation with Geotextile Reinforcement

6	0,00	-12,700	18	68,830	9,00
7	103,830	-12,700	19	74,830	6,00
8	103,830	-11,00	20	76,830	6,00
9	103,830	-17,300	21	82,830	3,00
10	0,00	-17,300	22	84,830	3,00
11	0,00	-12,700	23	90,830	0,00
12	13	0,00			

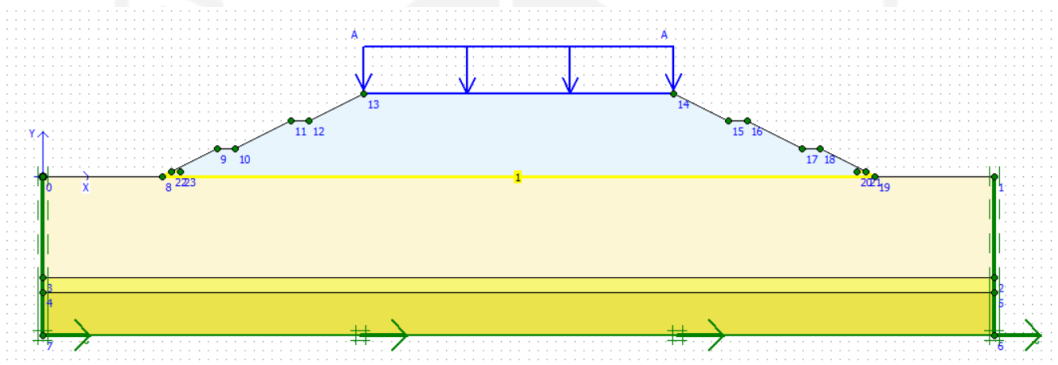


Figure 5.85 Modelling of Embankment 2 Trap with Geotextile Reinforcement

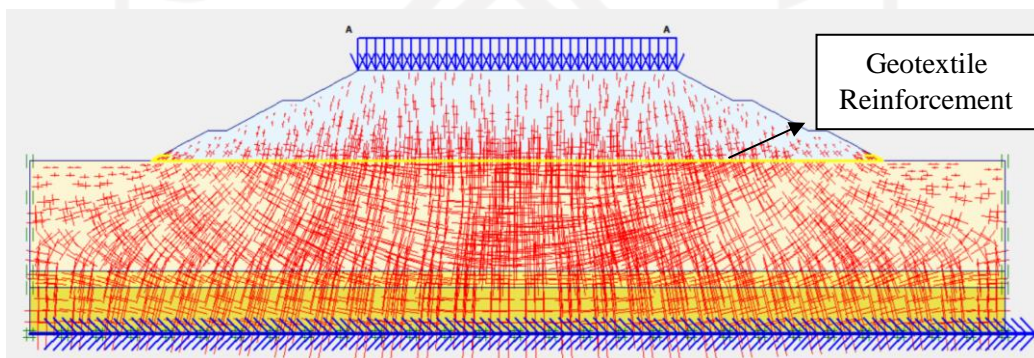


Figure 5.86 Initial Stresses of Embankment 2 Trap with Geotextile Reinforcement

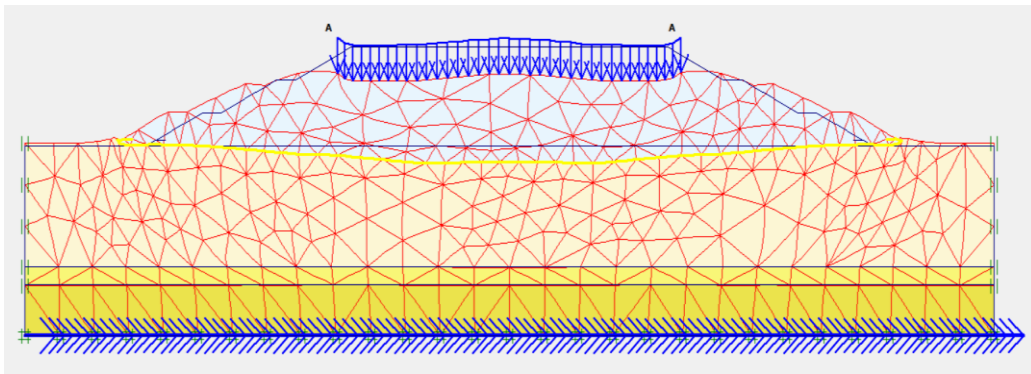


Figure 5.87 Deformed Mesh of Embankment 2 Trap with Geotextile Reinforcement Due to Traffic Load

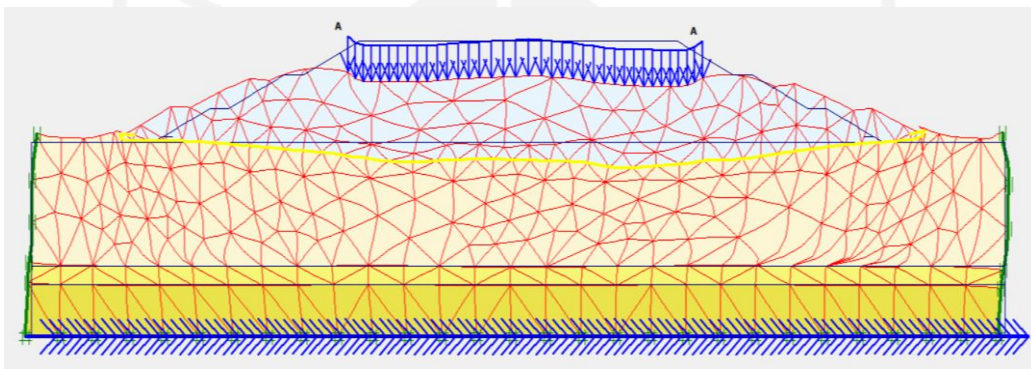


Figure 5.88 Deformed Mesh of Embankment 2 Trap with Geotextile Reinforcement Due to Traffic and Earthquake Load

The result of the total displacement value that occurs on the embankment 2 trap with geotextile reinforcement due to traffic load is $189,11 \times 10^{-3}$ m, while the total displacement due to traffic load and earthquake load is $259,58 \times 10^{-3}$ m. The results of the total displacement that occurs can be seen in Figure 5.89 and Figure 5.90 as follows.

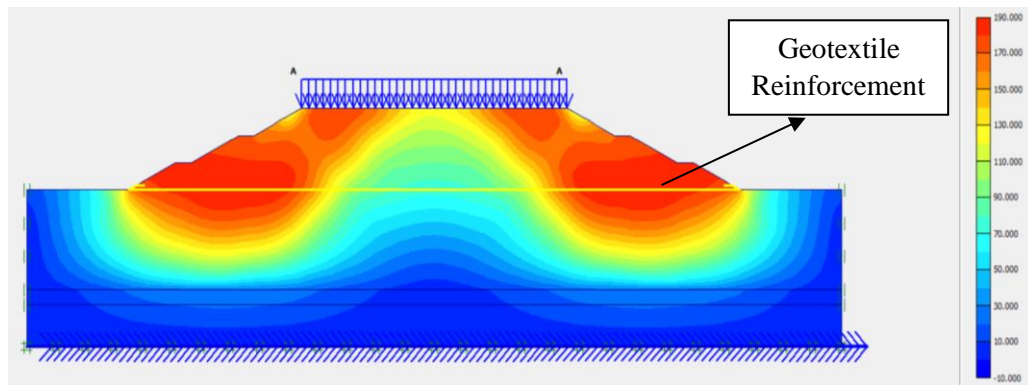


Figure 5.89 Total Displacement of Embankment 2 Trap with Geotextile Reinforcement Due to Traffic Load

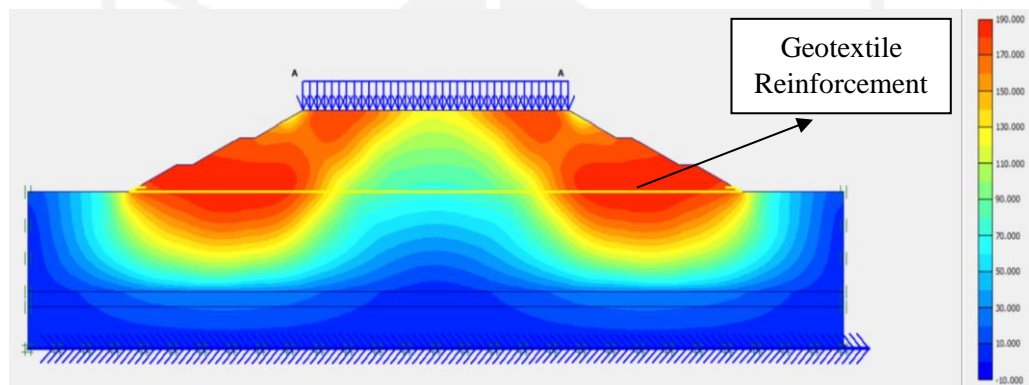


Figure 5.90 Total Displacement of Embankment 2 Trap with Geotextile Reinforcement Due to Traffic and Earthquake Load

Thereafter the direction of movement that occurs in the embankment can be seen in Figure 5.91 and Figure 5.92 as follows.

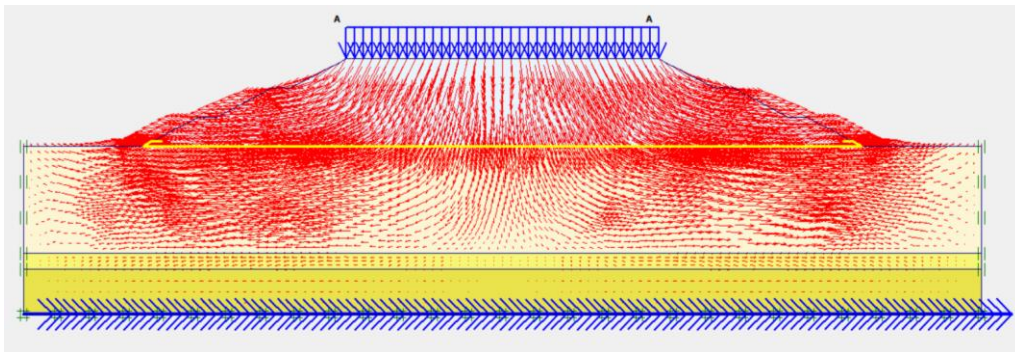


Figure 5.91 Soil Movement of Embankment 2 Trap with Geotextile Reinforcement Due to Traffic Load

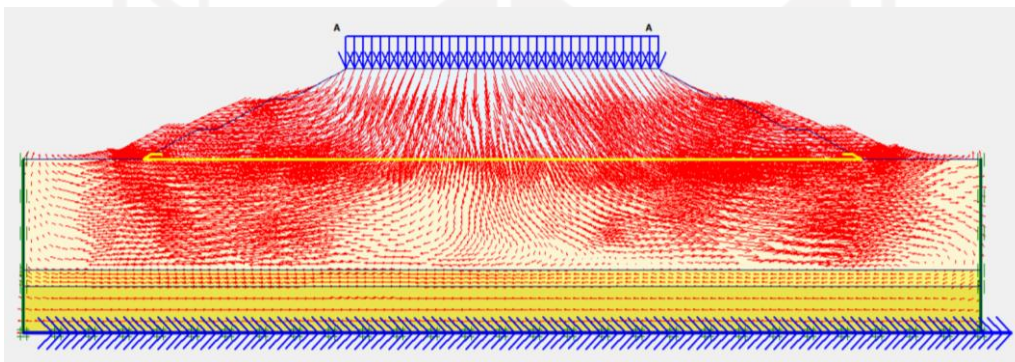


Figure 5.92 Soil Movement of Embankment 2 Trap with Geotextile Reinforcement Due to Traffic Load

Thereafter, the value of effective stresses that occur on the embankments 2 trap with geotextile reinforcement due to traffic load is $-420,03 \text{ kN/m}^2$, while the effective stresses due to traffic load and earthquake load is $-426,84 \text{ kN/m}^2$. The results of these calculations can be seen in Figure 5.93 and Figure 5.94 as follows.

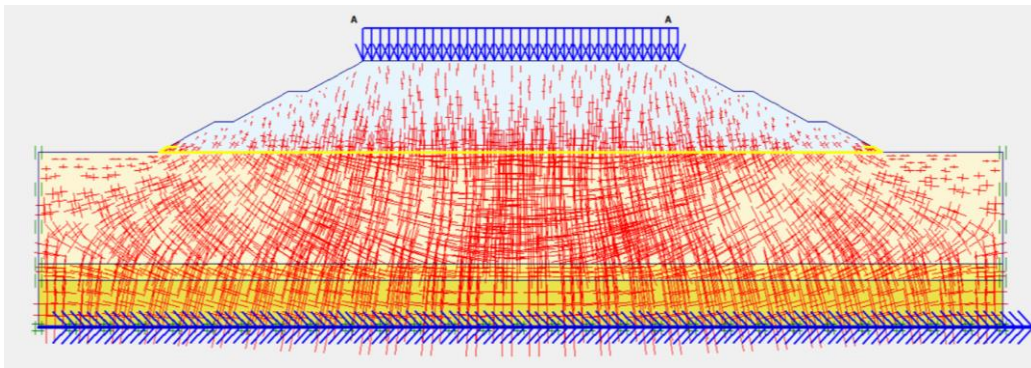


Figure 5.93 Effective Stresses of Embankment 2 Trap with Geotextile Reinforcement Due to Traffic Load

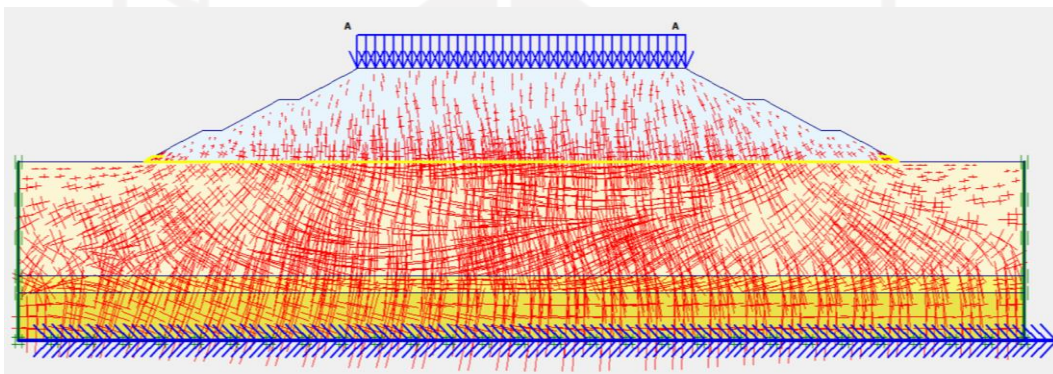


Figure 5.94 Effective Stresses of Embankment 2 Trap with Geotextile Reinforcement Due to Traffic Load

The occurrence of landslide due to traffic loads and earthquake loads can be seen in Figure 5.95 and Figure 5.96 as follows.

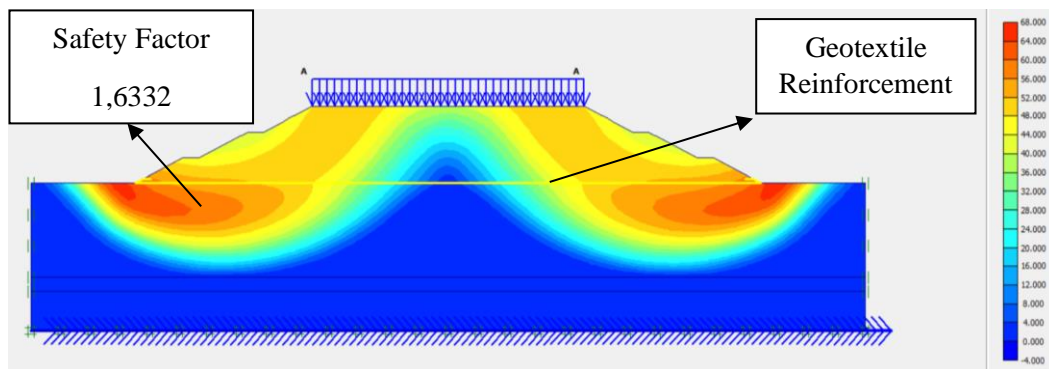


Figure 5.95 Potential Landslide of Embankment 2 Trap with Geotextile Reinforcement Due to Traffic Load

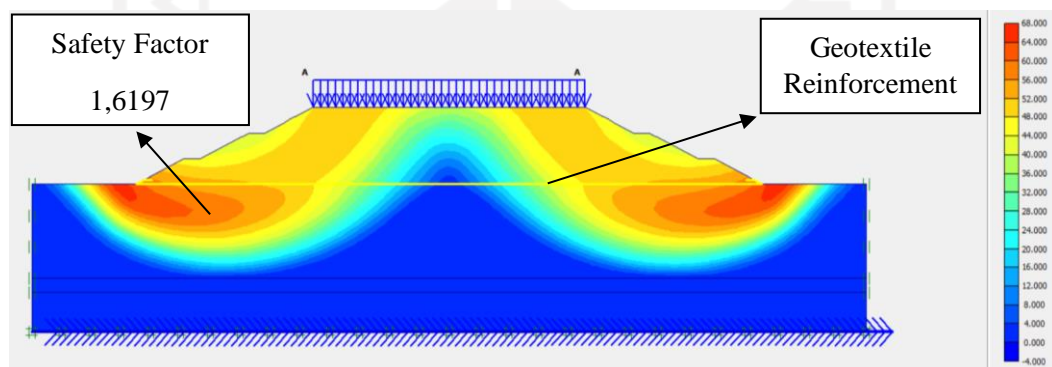


Figure 5.96 Potential Landslide of Embankment 2 Trap with Geotextile Reinforcement Due to Traffic Load

The safety factor of embankment 2 trap with reinforced geotextile due to traffic load is 1,6332 while the safety factor due to traffic load and earthquake load is 1,6197. The results of the safe number values can be seen in the Figure 5.97 as follows.

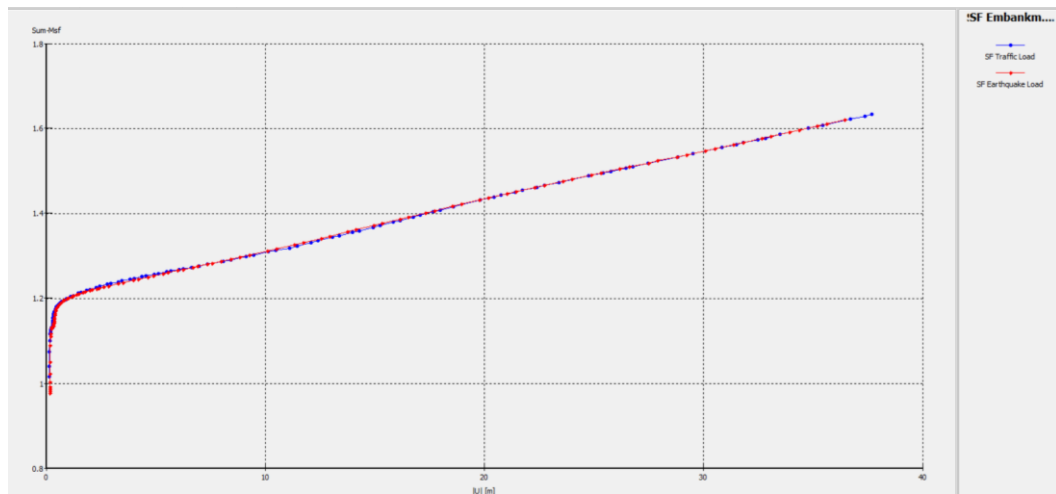


Figure 5.97 SF Curve of Embankment 2 Trap with Reinforced Geotextile

5.6.4. Embankment 3 Trap Variation with Geotextile Reinforcement

Initial modelling of the embankment with the same geometry on an embankment 3 trap variation with geotextile reinforcement. The input coordinates for Plaxis 8.6 can be seen in Table 5.13 and for slope modelling, it can be seen in Figure 5.98 as follows.

Table 5.13 Input Coordinate of Embankment 3 Trap Variations with Geotextile Reinforcement

No	X (m)	Y (m)	No	X (m)	Y (m)
1	0,00	0,00	13	15,500	2,250
2	103,830	0,00	14	17,500	2,250
3	103,830	-11	15	22,00	4,500
4	0,00	-11	16	24,00	4,500
5	0,00	0,00	17	28,500	6,750
6	0,00	-12,700	18	30,500	6,750
7	103,830	-12,700	19	35,000	9,00
8	103,830	-11,00	20	68,830	9,00
9	103,830	-17,300	21	73,330	6,750

**Continuity of Table 5.13 Input Coordinate of Embankment 3 Trap
Variations with Geotextile Reinforcement**

10	0,00	-17,300	22	75,330	6,750
11	0,00	-12,700	23	79,830	4,500
12	11	0,00	24	81,830	4,500

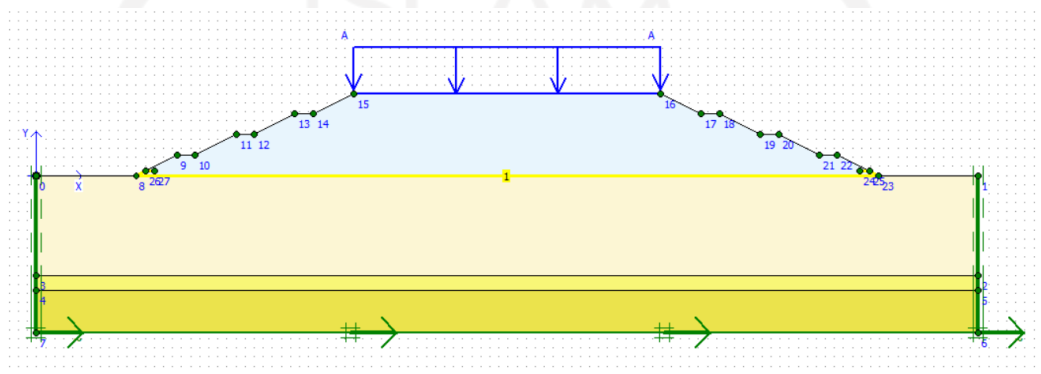


Figure 5.98 Modelling of Embankment 3 Trap with Geotextile Reinforcement

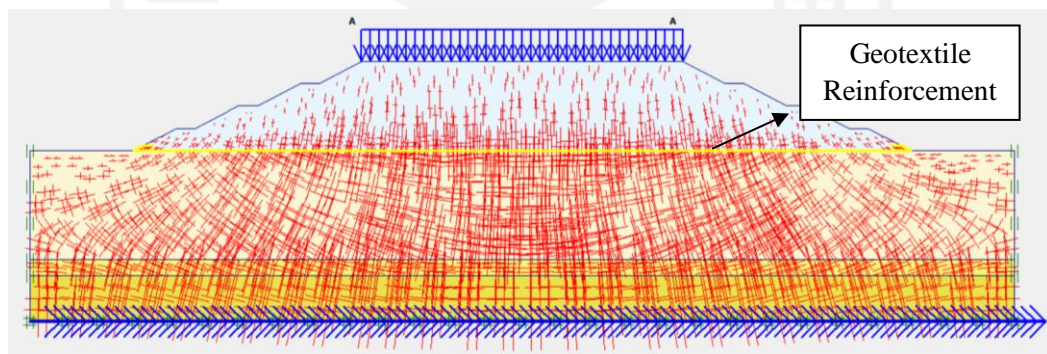


Figure 5.99 Initial Stresses of Embankment 3 Trap with Geotextile Reinforcement

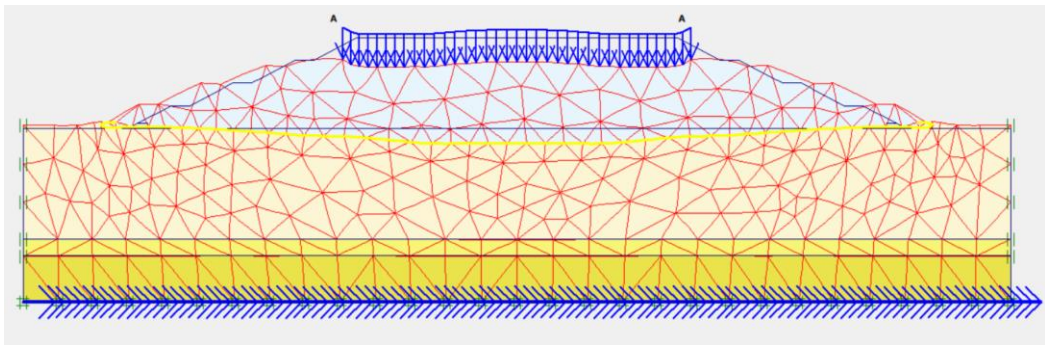


Figure 5.100 Deformed Mesh of Embankment 3 Trap with Geotextile Reinforcement Due to Traffic Load

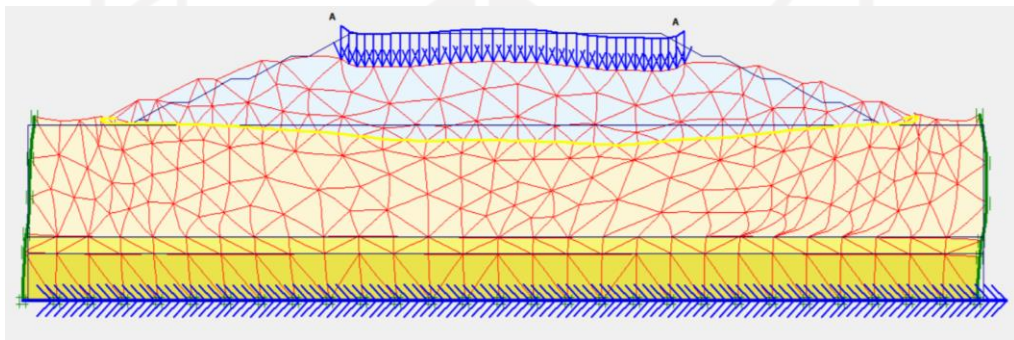


Figure 5.101 Deformed Mesh of Embankment 3 Trap with Geotextile Reinforcement Due to Traffic and Earthquake Load

The result of the total displacement value that occurs on the embankment 3 trap with geotextile reinforcement due to traffic load is $175,01 \times 10^{-3}$ m, while the total displacement due to traffic load and earthquake load is $233,77 \times 10^{-3}$ m. The results of the total displacement that occurs can be seen in Figure 5.102 and Figure 5.103 as follows.

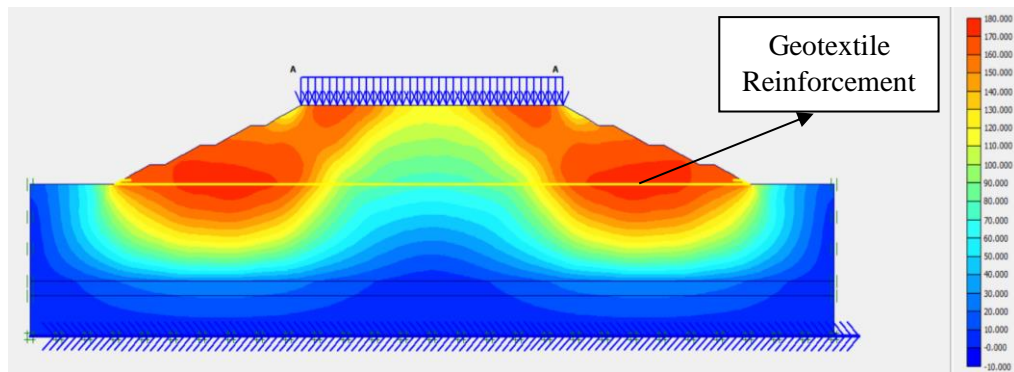


Figure 5.102 Total Displacement of Embankment 3 Trap with Geotextile Reinforcement Due to Traffic Load

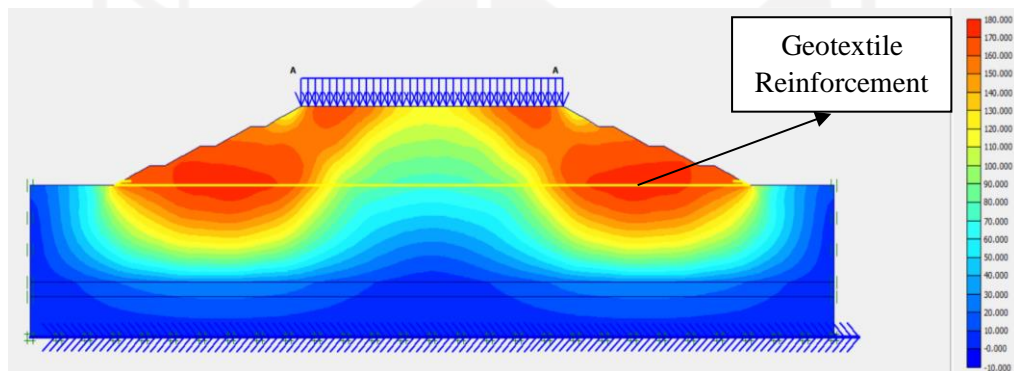


Figure 5.103 Total Displacement of Embankment 3 Trap with Geotextile Reinforcement Due to Traffic and Earthquake Load

Thereafter the direction of movement that occurs in the embankment can be seen in Figure 5.104 and Figure 5.105 as follows.

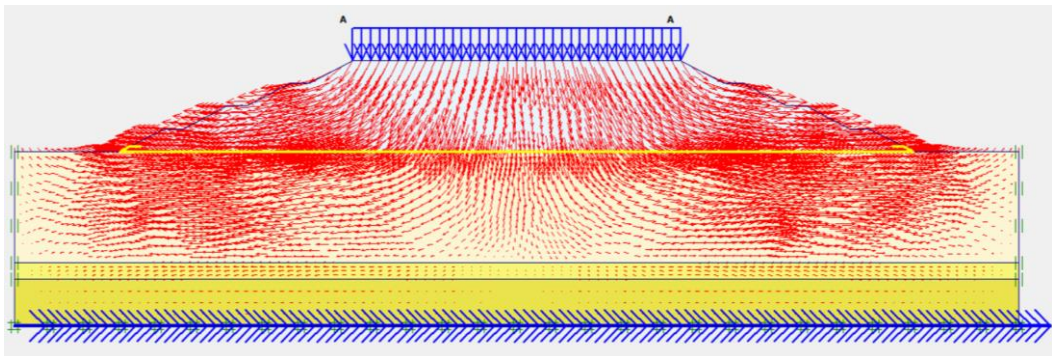


Figure 5.104 Soil Movement of Embankment 3 Trap with Geotextile Reinforcement Due to Traffic Load

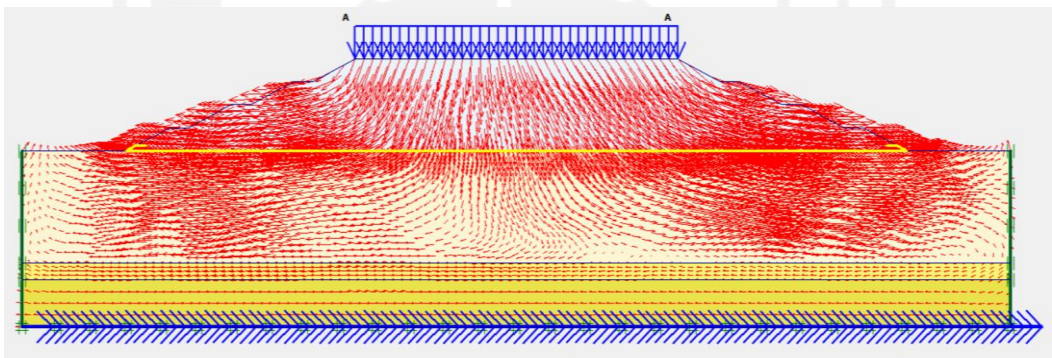


Figure 5.105 Soil Movement of Embankment 3 Trap with Geotextile Reinforcement Due to Traffic and Earthquake Load

Thereafter, the value of effective stresses that occur on the embankments 3 trap with geotextile reinforcement due to traffic load is $-420,52 \text{ kN/m}^2$, while the effective stresses due to traffic load and earthquake load is $-426,99 \text{ kN/m}^2$. The results of these calculations can be seen in Figure 5.106 and Figure 5.107 as follows.

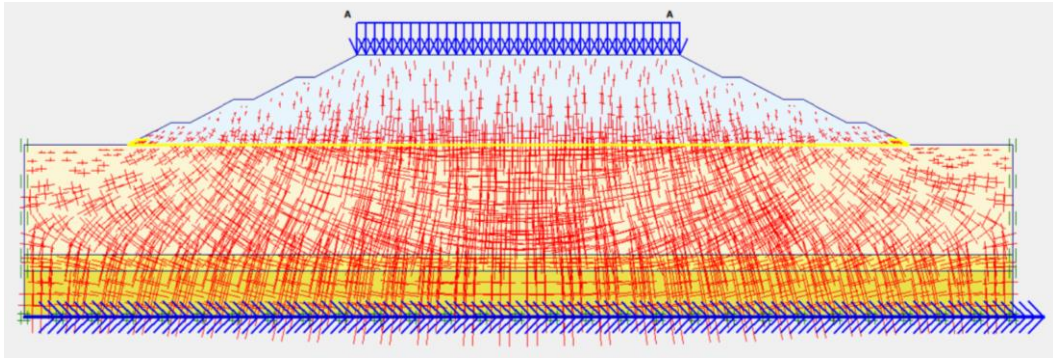


Figure 5.106 Effective Stresses of Embankment 3 Trap with Geotextile Reinforcement Due to Traffic Load

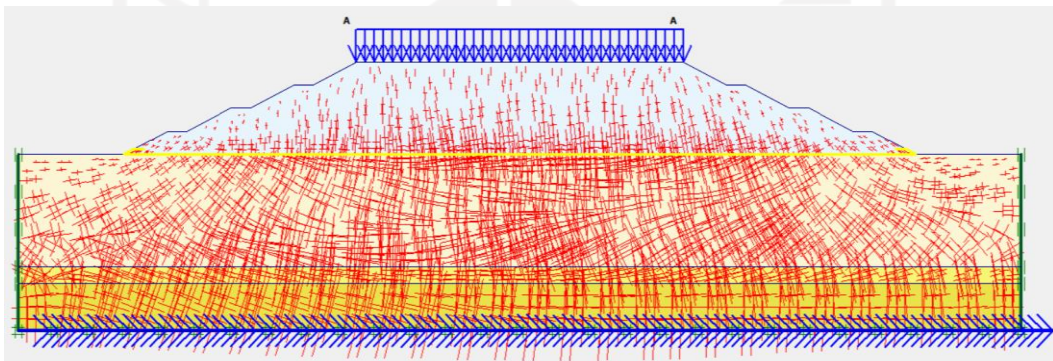


Figure 5.107 Effective Stresses of Embankment 3 Trap with Geotextile Reinforcement Due to Traffic and Earthquake Load

The occurrence of landslide due to traffic loads and earthquake loads can be seen in Figure 5.108 and Figure 5.109 as follows.

المعهد الإسلامي
الاستدائات الأندلسية

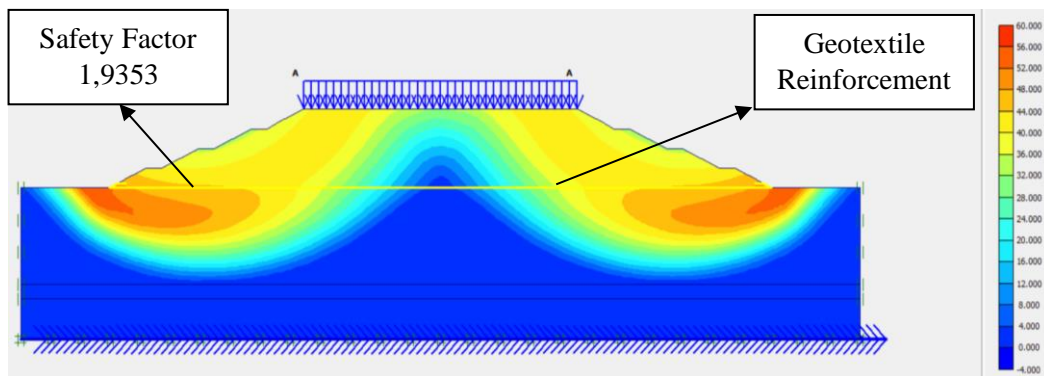


Figure 5.108 Potential Landslide of Embankment 3 Trap with Geotextile Reinforcement Due to Traffic Load

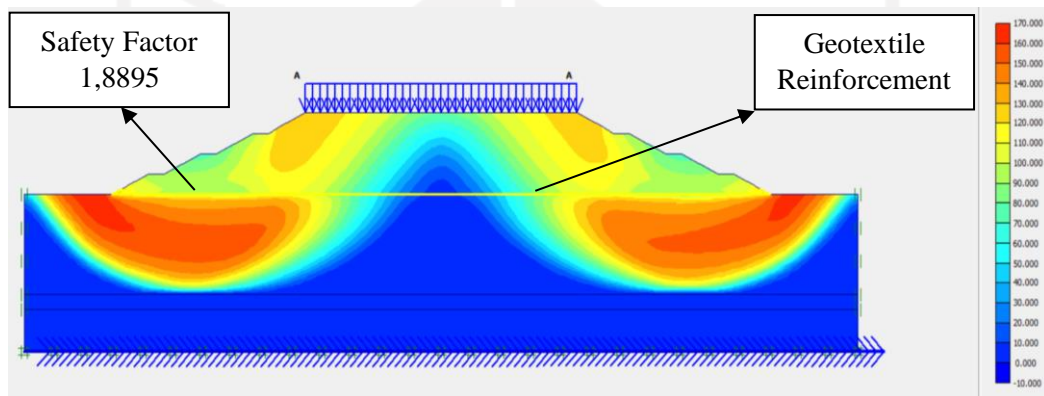


Figure 5.109 Potential Landslide of Embankment 3 Trap with Geotextile Reinforcement Due to Traffic and Earthquake Load

The safety factor of embankment 3 trap with reinforced geotextile due to traffic load is 1,9353 while the safety factor due to traffic load and earthquake load is 1,8895. The results of the safe number values can be seen in the Figure 5.110 as follows.

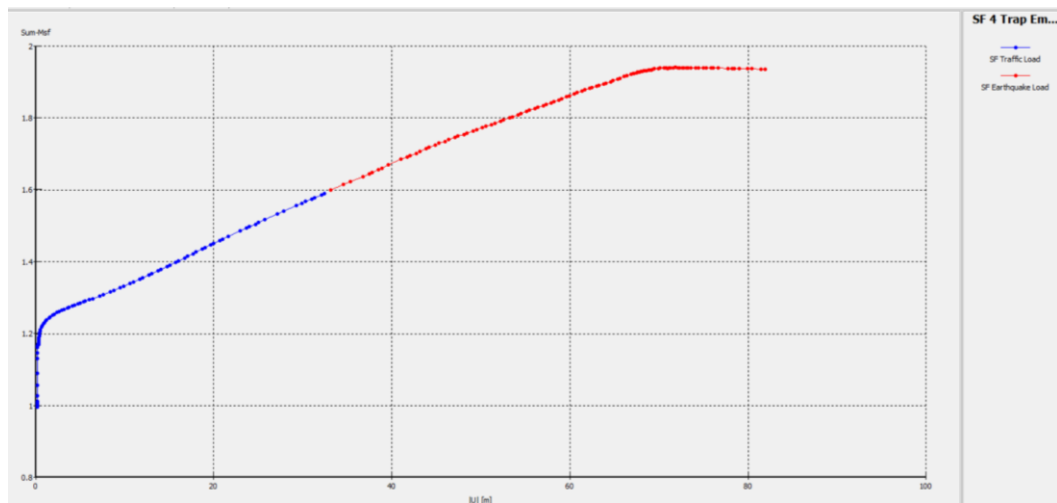


Figure 5.110 Curve of Embankment 3 Trap with Reinforced Geotextile

5.7 Recapitulation of Safety Factor (SF) and Consolidation

The results of the recapitulation on embankments 1, 2 and 3 traps with geotextile reinforcement can be seen in Table 5.14 as follows.

Table 5.14 Recapitulation of Safety Factor for Embankment with 1 Layer Geotextile Reinforcement

Embankment Type	SF Traffic Load		SF Traffic & Earthquake Load		Consolidation (m)
	Value	Status	Value	Status	
Existing Embankment	1,3482	Safe	1,3135	Safe	0,13874
1 Trap Embankment	1,4165	Safe	1,4035	Safe	0,11119
2 Trap Embankment	1,6332	Safe	1,6197	Safe	0,09670
3 Trap Embankment	1,9353	Safe	1,8895	Safe	0,08887

From the results of the calculation analysis, it can be concluded that the embankment with geotextile reinforcement has a significant effect, the reinforced embankment has become safe and exceed the safety factor because it is greater than the required safety number of 1,3.

5.8 Discussion

In Cibitung -Cilincing construction project, there are several types of soil conditions, especially in the Cibitung, Bekasi area at Sta. 7+500. The project being carried out is located on soft soil condition and the height of the embankment is 9m with 1V: 2V slope tilt. So, there are possibilities of the embankment to landslide.

For this reason, the soil needs to be repaired first by stabilizing or strengthening and carry out the quality control before it is used as a road structure above it so that the soil meets quality requirements, both physically and technically.

The load parameters that inputted in this analysis are uniform loads due to the load on the road structure and traffic load, as well as earthquake load in accordance with the earthquake zoning in the Bekasi area.

5.8.1. Results Analysis of Existing Embankment

This research analyses of the stability existing embankments on Cibitung – Cilincing toll road project that was conducted to determine the safety factor on the embankments of the road. The calculation analysis existing embankment carried out by using Finite element method. Based on the results of the calculation analysis, the safety factor for existing embankment is 1,0330 due to traffic load and 1,0306 due to traffic load and earthquake load. While, the results from the Fellenius method of the existing embankment are 1,0621. So, the existing embankment is in an unsafe condition, because the safety factor results is still lower than the safety factor requirement for the toll road specification, which is 1,3.

In addition to analysing the safety factor, this study also compares the value of consolidation that occurs on the slopes for one year (365 days). Consolidation is a settlement that occurs due to the load on the slope and the release of water through the soil pores for a certain period. The consolidation of the embankments that occurred in this study can be seen in Table 5.5 and Table 5.14. On the existing embankment the consolidation that occurred is 0,2774m.

5.8.2. Results of Embankment Analysis with Topography Improvement

Improvement topography with variations of trap, namely variations in 1 trap embankments, 2 traps embankments and 3 traps embankments. The calculation analysis of the embankment with topography improvement carried out by using Finite element method. Based on the results of the calculation analysis, the safety factor on the embankment with variation of 1 trap, 2 traps and 3 traps have a value of 1,0777; 1,1164; 1,1564 due to traffic load and 1,0771; 1,1147; 1,1560 due to traffic load and earthquake load. So, the embankment without geotextile reinforcement is in an unsafe condition, because the safety factor is still lower than the safety factor requirement for the toll road specification, which is 1,3.

The consolidation of the embankments that occurred in embankment with topography improvement with variation of 1 trap, 2 traps and 3 traps have a value with one-year calculation of 0,22237m; 0,19339m; 0,17773m.

5.8.3. Results of Embankment Analysis with Geotextile Reinforcement

In this study, to overcome the problem of embankments which have a safety number lower than the requirement, reinforcement is used geosynthetic materials of the woven geotextile type UW-250 produced by PT. Teknindo Superior Geosystems. The ultimate tensile strength of this type of geotextile is 52 kN/m² with a strain of 20%. Before analysing the embankment with geotextile reinforcement, it is necessary to calculate the amount of geotextile needed. Geotextiles are installed horizontally on the soil and then covered with compacted embankment.

The results of the embankment analysis with geotextile reinforcement conducted a safety number greater than the required safety number for the toll road specification. On the existing embankment the safety factor with reinforcement is 1,3482 due to traffic load and 1,3135 due to traffic and earthquake load, while on the 1 trap embankment the safety factor is 1,4165 due to traffic load and 1,4035 due to traffic and earthquake load, for the 2 traps embankment the safety factor is 1,6332 due traffic load and 1,6197 due to traffic and earthquake load and for 3 traps

embankments slope the safety factor is 1,9353 due to traffic load and 1,8895 due to traffic and earthquake load. So, the embankment with geotextile reinforcement is in safe condition, because the safety factor more than the safety factor requirement for the toll road specification, which is 1,3.

The results analysis of the consolidation with one-year calculation of the embankment with geotextile reinforcement is more safety than the embankments with topography improvement. Consolidation on the existing embankment with geotextile reinforcement is 0,13874m, while the embankment 1 trap with reinforced geotextile is 0,11119m, the consolidation of 2 traps embankment with reinforced geotextile is 0,09670m and 3 traps embankments with reinforced geotextile is 0,08887m.

The following is a recapitulation of the analysis results on the conditions of the embankment before reinforced with geotextile and embankment after reinforced with geotextile and the value of the consolidation, which is presented in Table 5.15

**Table
5.15**

Embankment Type	SF Soil Embankment		Settlement Consolidation (m)
	Traffic Load	Traffic & Earthquake Load	
a. Existing Embankment	1,0330	1,0306	0,27747
b. Topography Improvement			
1. Embankment 1 Trap	1,0777	1,0771	0,22237
2. Embankment 2 Traps	1,1164	1,1147	0,19339
3. Embankment 3 Traps	1,1564	1,1560	0,17773
c. Geotextile Reinforcement			
1. Existing Embankment	1,3482	1,3135	0,13874
2. Embankment 1 Trap	1,4165	1,4035	0,11119
3. Embankment 2 Traps	1,6332	1,6197	0,09670
4. Embankment 3 Traps	1,9353	1,8895	0,08887

Recapitulation of Safety Factor and Consolidation of Embankment



The overall recapitulation graph of the embankment stability analysis using trap variations in condition without geotextile reinforcement and with geotextile reinforcement and consolidation results without being given geotextile reinforcement and being given geotextile reinforcement can be seen in Figure 5.111, Figure 5.112 and Figure 5.113 as follows.

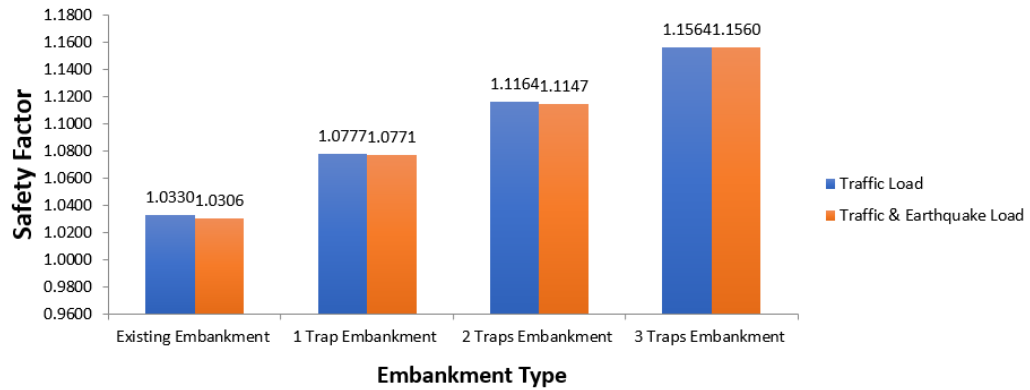


Figure 5.111 Comparison of Safety Factor with Variations of Trap without Geotextile Reinforcement

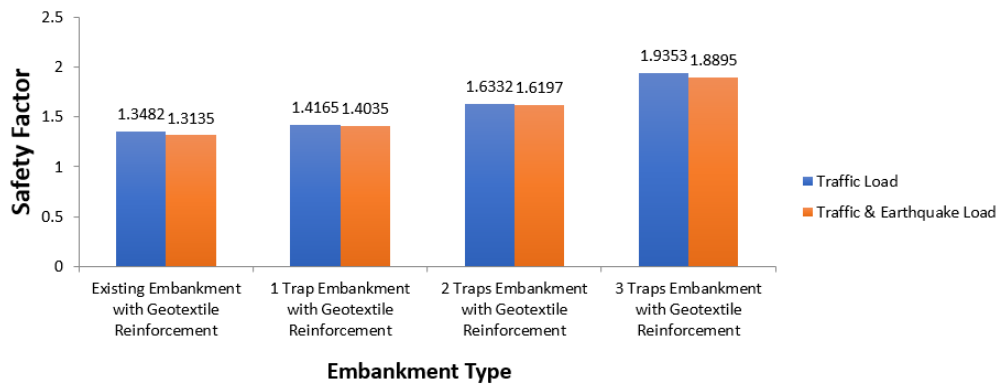


Figure 5.112 Comparison of Safety Factor with Variations of Trap with Geotextile Reinforcement

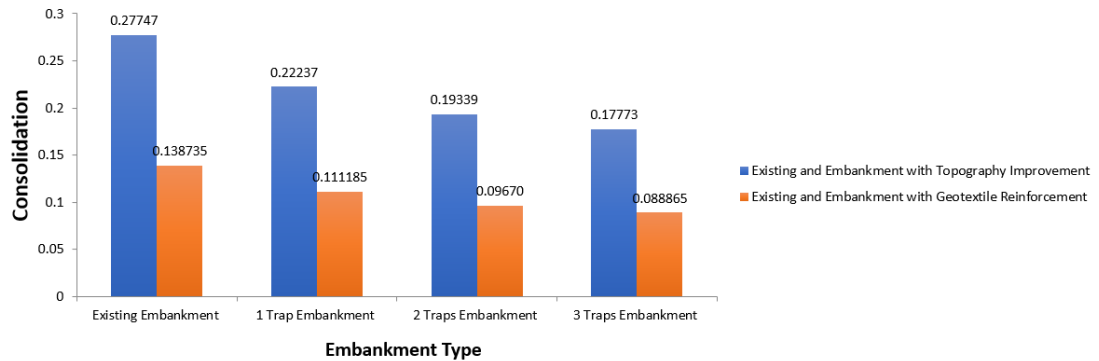


Figure 5.113 Comparison Consolidation of Embankment Improvement

From this analysis, it can be seen that the embankment soil using trap variations and reinforced with geotextiles has an increasing impact on the safety of slope stability. Embankment that given a variety of traps with geotextile reinforcement can be considered in planning as an additional material for strengthening slope stability. Comparison of slope stability with geotextile reinforcement with and without geotextile also affect the results of consolidation that occurred. From the results of the consolidation, the embankment with geotextile reinforcement has a smaller consolidation value than the embankment that are not reinforced with geotextile.

CHAPTER VI

CONCLUSION AND SUGGESTION

6.1 Conclusion

Based on the results of the analysis of calculations and discussions that have been described in the previous chapter, it can be concluded as follows.

1. The results safety factor of embankment stability analysis on the existing embankment due to traffic load is 1,0330 and the results of safety factor due to traffic load and earthquake load is 1,0306. While, the results of safety factor based on the Fellenius method is 1,0621.
2. The results safety factor of embankment stability analysis on the embankment with topography improvement, namely 1 trap, 2 traps and 3 due to traffic load is 1,0777; 1,1164; and 1,1564; while 1,0771; 1,1147; and 1,1560 due to traffic load and earthquake load.
3. The results safety factor of embankment stability analysis on the embankment with geotextile reinforcement are as follows; for the existing embankment with geotextile reinforcement due to traffic load is 1,3482 and 1,3135 due to traffic load and earthquake load, for the embankment with topography improvement with geotextile reinforcement, namely 1 trap, 2 traps and 3 traps is 1,4165; 1,6332; 1,9353 due to traffic load while 1,4035; 1,6197; 1,8895 due to traffic load and earthquake load.
4. The results for consolidation settlement of existing embankment stability analysis conducted is 0,27747 m.
5. The results for consolidation settlement of embankment with topography improvement namely 1 trap, 2 traps and 3 traps respectively are 0,22237 m; 0,19339 m; and 0,17773 m.
6. The results for consolidation settlement of embankment with geotextile reinforcement namely, the existing embankments, 1 trap embankments, 2 traps embankments and 3 traps embankments with geotextile reinforcement respectively are 0,13874 m; 0,11119 m; 0,09670 m; and 0,08887 m.

The results analysis of the stability on the embankment with geotextile reinforcement conducted in greater safety factor than the embankments without geotextile reinforcement also embankment with topography variations. Meanwhile, in the consolidation analysis that has been carried out, the results on the reinforced embankment are smaller than the embankments without geotextile reinforcement.

6.2 Suggestion

Based on the results of case studies from the analysis, the authors provide some suggestion as follows.

1. For further research, it can be using additional another replacement reinforcement parameters such as retaining wall, sheet pile, or bore pile.
2. For researchers who will conduct further research with the use of alternative materials to add soil stability, such as chemical stability with the soil on the existing embankment add with chemicals materials such as lime, cement and others.
3. The soil parameters of embankments can be analysed using variations in soil types with variations in soil density (γ_b), cohesion (c), or soil shear strength (ϕ), to determine the effect of changes in soil parameters on slope stability.

Bibliography

- Abdul, B. H. (2018). *Analisis Stabilitas Lereng dengan Perkuatan Geotekstil*. Yogyakarta, Indonesia: Fakultas Teknik Sipil dan Perencanaan, Universitas Islam Indonesia.
- Abramson L. W., T. S. (2002). *Slope Stability and Stabilization Methods*. New York: John Wiley & Sons, Inc.
- Aisyah, A. A. (2018). *Analisis Stabilitas Timbunan pada Konstruksi Badan Jalan dengan Perkuatan Geotekstil Menggunakan Metode Fellenius*. Yogyakarta, Indonesia: Fakultas Teknik Sipil dan Perencanaan, Universitas Islam Indonesia.
- Arif, K. R. (2005). *Analisis Stabilitas Tanah Timbunan Diatas Tanah Lunak dengan Perkuatan Geomembran*. Yogyakarta, Indonesia: Penelitian. Universitas Islam Indonesia.
- Azizah F. N., S. N. (2014). *Penggunaan Geotekstil pada Lereng Sungai Putih Surakarta*. Surakarta: Universitas Sebelas Maret.
- Bowles, J. E. (1984). *Sifat -Sifat Fisis dan Geoteknis Tanah (Mekanika Tanah) Edisi I*. Jakarta, Indonesia: Erlangga.
- Bowles, Joseph E. (1986). *Physical and Geotechnical Characteristics of the Soil*.
- Cruden, D. M. (1996). *Landslide Types and Processes in Special Report 247: Landslide, Investigation and Mitigation (A.K Turner and R.L. Schuster, eds)*. Washington DC: Transportation Research Board, National Research Council, National Academy Press.
- Das, B. M. (1985). *Mekanika Tanah Jilid I*. Jakarta, Indonesia: Erlangga.
- Das, B. M. (1998). *Mekanika Tanah (Prinsip-Prinsip Rekayasa Geoteknik) Jilid I*. Jakarta, Indonesia: Erlangga.
- Dayanum, S. (2012). *Evaluasi Gerakan Masa Tanah Timbunan dengan Sistem Subdrain dan Perkuatan Berdasarkan Simulasi Murneris pada Jalan Tol Semarang-Solo*. Yogyakarta, Indonesia: Universitas Gajah Mada.
- Hardiyatmo, C. H. (2013). *Geosintetik Untuk Rekayasa Jalan Raya (Perancangan dan Aplikasi)*. Yogyakarta, Indonesia : Gadjah Mada University Press.



- Henry, S. (2006). *Stabilisasi Tanah Lempung Lunak dengan Bahan Aditif Kapur Karbid dan Perkuatan Tanah dengan Geotekstil*. Yogyakarta, Indonesia: Fakultas Teknik Sipil dan Perencanaan, Universitas Islam Indonesia.
- Hoek, J. a. (1981). *Rock Slope Engineering*. London: Institution of Mining and Metallurgy.
- Holtz, R. a. (1996). *Stabilization of Soil Slopes (In: Landslides Investigation and Mitigation)*. Washington DC: National Academy Press.
- Ismanti, S. (2012). *Analisis Perilaku Timbunan dengan Perkuatan Geosintetik Menggunakan Software Plaxis*. Yogyakarta, Indonesia: Universitas Gajah Mada.
- John, N. W. (1987). *Geotextiles*. New York, USA: Blackie.
- Krahn, J. (2003). *The Limits of Limit Equilibrium Analysis*. Canada: Canadian Journal.
- Lazarte, C. A. (2003). *Soil Nail Walls (Geotechnical Engineering Circular)*. Washington DC: Federal Highway Administration.
- Liu, H. a. (2007). Unified Elastoplastic-Viscoplastic Bounding Surface Model of Geosynthetic and Its Applicants to Geosynthetic Reinforced Soil Retaining Wall Analysis. *Journal of Engineering Mechanism*, Vol 133, pp. 801-815.
- Ministry of Public Works and Public Housing (2009). Traffic Load Data.
- Morgenstern, N. R. (1965). The Analysis of The Stability of General Slip Surface. *Geotechnique*, Vol. 15, No. 1, pp 79 - 93.
- PT. Carina Griya Mandiri, (2017). *Soil Data*.
- Simatupang, A. I. (2013). *Perbandingan antara Metode Limit quilibrium dan Metode Finite Element dalam Analisa Stabilitas Lereng* . Medan: Jurnal Teknik Sipil USU .
- SNI-1726. (2019). *Indonesia Earthquake Zoning Map, Tata Cara Perencanaan Tahan Gempa Gedung dan Non Gedung*. Jakarta: Badan Standarisasi Nasional.
- Sowers, G. B. (1975). *Introductory Soil Mechanics and Foundation*. New York: Macmillan.
- Sukartaatmadja. (2004). *Konservasi Tanah dan Air*. Bogor: IPB Press.
- Surjandari, N. S. (2012). *Analisis Stabilitas Lereng dengan Perkuatan Geotekstil*. Universitas Sebelas maret Surakarta.
- Suryolelono K. B. (2000). *Geosintetik Geoteknik*. Yogyakarta, Indonesia.

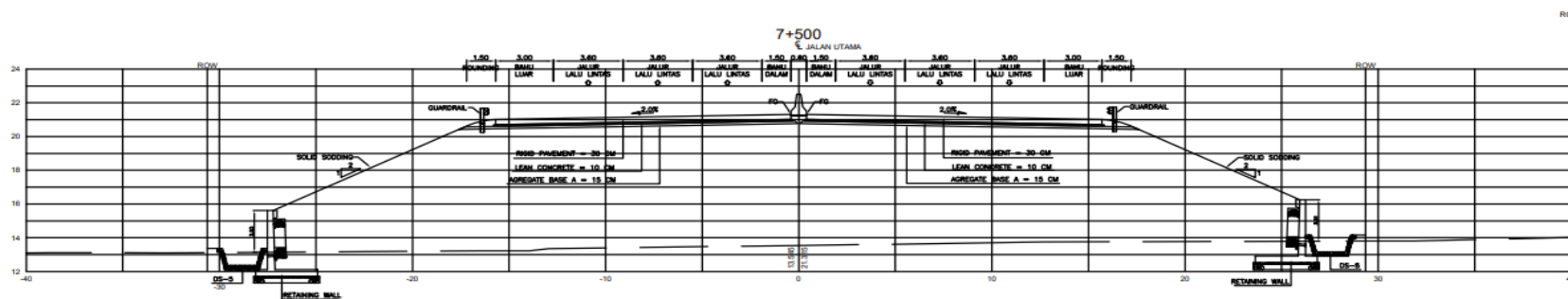
- Suryolelono, B. K. (2001). *Konsep dan Analisa Penanggulangan Bahaya Tanah Longsor*. Yogyakarta, Indonesia: KMTS UGM.
- Suryolelono, K. B. (1993). *Teknik Fondasi Bagian I (Fondasi Telapak dan Dinding Penahan Tanah)*. Yogyakarta, Indonesia: Nafiri.
- Terzaghi K., P. R. (1943). *Theoretical Soil Mechanic*. New York: John Willey & Sons.
- Terzaghi, K. a. (2014). *Theoretical Soil Mechanic*. New York: John Willey & Sons.
- W. Ratih., M. (1998). *Penelitian Laboratorium Stabilitas Tanah Lempung dengan Menggunakan Geotekstil sebagai Alternatif Perkuatan Tanah Dasar Struktur Pondasi Gedung*. Yogyakarta, Indonesia: Penelitian. Universitas Islam Indonesia.
- Zakaria, Z. (2009). *Analisis Kestabilan Lereng Tanah*. Bandung, Indonesia: Universitas Padjajaran.



Appendix

Appendix 1.1 Cross Section

 <p>PT CIBITUNG TANJUNG PRIK PORT TOLLWAYS</p>	<p>DETAIL ENGINEERING DESIGN REVIEW DESAIN INTERCHANGE CIBITUNG - SUMBER SAKA (STA. 0+440 - STA. 8+291) JALAN TOL CIBITUNG - CILINCING</p>	<p>Consultant</p>  <p>PT BINA KARYA Engineering & Development Studio</p>	DIGAMBAR OLEH	DIREKANAKAN OLEH	DIBETUJUI OLEH	DIKETAHUI OLEH	<p>Judul Gambar :</p>	No. Gbr :
			DRAFTSMAN SOETARNO	HIGHWAY ENGINEER I. WAWAN SETAWAN, MT	TEAM LEADER I. PETRUS WISNU WIBOWO	PEMIMPIN PROYEK YAYA RUSPEYA		Skala :



Appendix 1.2 Results Bor Log Test Data



PT. CARINA GRIYA MANDIRI
 ENGINEERING & MANAGEMENT CONSULTANT
 Jl. Pahlawan Revolusi No. 2A Jakarta 13430. Telp.021-8613824. Mail : pt_cg_mandiri@yahoo.com

- ENGINEERING DESIGN
- SOIL INVESTIGATION
- SUPERVISION
- MINING EXPLORATION
- SURVEY / MAPPING

PROJECT : RENCANA PEMBANGUNAN JALAN TOL LINGKAR LUAR JAKARTA II, RUAS CIBITUNG - CILINCING		BORING NO : BH-28															
LOCATION : STA. 7+500, ABT-2 (JU. SUNGAI SADANG 2)		ELEVATION : 0,00 m (MTS) SHEET NO : 1															
DATE	DEPTH (m)	BORING PROFILE	STANDARD PENETRATION TEST				q _u POCKET PENETRO METER	CORE RECOVERY %	LITHOLOGIC DESCRIPTION								
			N = Number of Blows		P = Penetration (cm)												
			0	10	20	30	40	50	60	N/P	N/P	N/P	Remark				
24 Sept 17	± 0.00																
										2 / 15	2 / 15	3 / 15	N = 5				Koordinat : X = 731270 Y = 931185 Lempung lanauan, abu-abu muda Contoh : I (- 1,50 +- 2,00) m SPT : 1 (- 2,00 +- 2,45) m
										2 / 15	3 / 15	3 / 15	N = 6				Lempung lanauan, abu-abu muda Contoh : II (- 3,50 +- 4,00) m SPT : 2 (- 4,00 +- 4,45) m
										2 / 15	3 / 15	4 / 15	N = 7				Lempung lanauan, abu-abu muda Contoh : III (- 5,50 +- 6,00) m SPT : 3 (- 6,00 +- 6,45) m
										3 / 15	3 / 15	5 / 15	N = 8				Lempung lanauan, abu-abu muda SPT : 4 (- 8,00 +- 8,45) m
										3 / 15	3 / 15	4 / 15	N = 7				Lempung lanauan, abu-abu muda SPT : 5 (- 10,00 +- 10,45) m
	- 11.00																
	- 12.70									1 / 15	2 / 15	2 / 15	N = 4				Lanau, hitam SPT : 6 (- 12,00 +- 12,45) m

Appendix 1.3 Data of Sub Soil Condition

4.3. Keadaan Tanah Dasar (sub soil condition)

Dari hasil penyelidikan di lapangan Bor Dalam (Deep Boring), secara garis besar dapat disajikan sebagai berikut :

1) Pada daerah sekitar titik penyelidikan Bor : BH-28, ABT-2 (STA 7+500) JU. Sungai Sadang-2.

Ke dalaman	Perkiraan Jenis Tanah
Surface : - 0,00 m	Elevasi ($\pm 0,00$) m diambil dari Muka Tanah Setempat (MTS).
- 0,00 ÷ - 11,00 m	<p>Lapisan-1 Macam tanah : Lempung lanauan (silty Clay), abu-abu muda dgn Konsistensi : teguh (firm) s/d kaku (stiff) atau dengan Nilai N SPT : berkisar antara : N = 5 s/d 8 blows.</p> <ul style="list-style-type: none"> ▪ Contoh : I (- 1,50 ÷ - 2,00) m. SPT 1 (- 2,00 ≈ - 2,45) m, nilai N = 5 Blows, dengan Konsistensi : teguh (firm) ▪ Contoh : II (- 3,50 ÷ - 4,00) m. SPT 2 (- 4,00 ≈ - 4,45) m, nilai N = 6 Blows, dengan Konsistensi : teguh (firm) ▪ Contoh : III (- 5,50 ÷ - 6,00) m. SPT 3 (- 6,00 ÷ - 6,45) m, nilai N = 7 Blows, dengan Konsistensi : teguh (firm) ▪ SPT 4 (- 8,00 ÷ - 8,45) m, nilai N = 8 Blows, dengan Konsistensi : kaku (stiff) ▪ SPT 5 (- 10,00 ÷ - 10,45) m, nilai N = 7 Blows, dengan Konsistensi : teguh (firm)

oyek : Rencana Pembangunan Jalan Tol Lingkar Luar Jakarta-II, Ruas Cibitung-Cilincing.
kasi : Area Rencana Jl. Tol Lingkar Luar Cibitung-Cilincing, Provinsi : Jawa Barat.
r : Titik BH-28, ABT-2 (STA. 7+500), JU. Sungai Sadang-2.

- 11,00 m ÷ - 12,70 m	<p>Lapisan -2 Macam tanah : lanau (Silt), hitam dengan Konsistensi : sangat padat (very dense) atau dengan Nilai N SPT : berkisar antara : N = 4 blows.</p> <ul style="list-style-type: none"> ▪ SPT 6 (- 12,00 ÷ - 12,45) m, nilai N = 4 Blows, dengan Konsistensi : lunak (soft)
- 12,70 m ÷ - 17,30 m	<p>Lapisan -3 Macam tanah : lanau (silt) membatu, abu-abu muda dengan Konsistensi : sangat keras (very hard) atau dengan Nilai N SPT : berkisar antara : N > 60 blows.</p> <ul style="list-style-type: none"> ▪ SPT 7 (- 14,00 ÷ - 14,22) m, nilai N > 60Blows, dengan Konsistensi : sangat keras (very hard) ▪ SPT 8 (- 16,00 ÷ - 16,23) m, nilai N > 60 Blows, dengan Konsistensi : sangat keras (very hard)

Appendix 1.4 Data Specification of Geotextile Woven

UnggulTex

POLYPROPYLENE WOVEN GEOTEXTILES

TECHNICAL SPECIFICATIONS

PROPERTIES	UNIT	TEST METHOD	UW - 150	UW - 200	UW - 250
Physical Properties					
Mass	g/m ²	ASTM D 5261-92	150	200	250
Thickness	mm	ASTM D 5199-91	0.5	0.6	0.7
Colour	-	-	Black	Black	Black
Mechanical Properties					
Strip Tensile Strength (Wrab/Weft)	kN/m	ASTM D 4595-94	37/35	42/39	52/52
Elongation at Max. Load (Wrab/Weft)	%	ASTM D 4595-94	19/18	20/20	20/20
Grap Tensile Strength (Wrab/Weft)	N	ASTM D 4632-91	1210/1200	1600/1600	1750/1750
Elongation at Max. Load (Wrab/Weft)	%	ASTM D 4632-91	14/13	22/22	22/22
Trapezoidal Tear Strength (Wrab/Weft)	N	ASTM D 4533-91	615/615	700/700	800/800
Hydraulic Properties					
Pore Size O ₃₅	µm	ASTM D 4751-95	320	275	250
Water Permeability	l/m ² /sec	100 mm water head	28	16	7.5
Environmental Properties					
Effect of soil Alkalinity	-	-	nil	nil	nil
Effect of soil Acidity	-	-	nil	nil	nil
Effect of Bacteria	-	-	nil	nil	nil
Effect of U.V. Light	-	-	Stabilized	Stabilized	Stabilized
Packaging					
Roll Length	m	-	150 - 200	150 - 200	150 - 200
Roll Width	m	-	3 - 4	3 - 4	3 - 4
Roll Area	m ²	-	640 - 760	640 - 760	640 - 760
Roll Diameter (Approx)	m	-	0.4 - 0.5	0.4 - 0.5	0.4 - 0.5
Roll Weight (Approx)	kg	-	96 - 114	128 - 152	160 - 190

All information, illustration and specification are based on the latest product information available at the time of printing. The right is reserved to make changes at any time without notice.

Distributed by :


PT. TEKNINDO GEOSISTEM UNGGUL

 Wisma SIER Building, 1st Floor, J. Rungkut Industri Raya 10, Surabaya 60293
 Tel. 031-8475062 Fax. 031-8475063

الجمعية الهندسية
 البستنة الاندو